Aalto University
School of Engineering
Department of Mechanical Engineering

Pravin Luthada

Tension-Tension Fatigue Testing of Pultruded Carbon Fibre Composite Profiles

Master's Thesis
Espoo, May 30, 2016

Supervisor: Professor Heikki Remes
Instructor: Markus Wallin M.Sc. (Tech.)

Aalto University
School of Engineering

Aalto University, P.O. BOX 11000, 00076 AALTO
www.aalto.fi

Abstract of master's thesis

Author	Pravin Luthada
Title of thesis	Tension-Tension Fatigue Testing of Pultruded Carbon Fibre Composite Profiles
Degree programme	Master's Programme in Mechanical Engineering
Major/minor	Mechanical Engineering
Code	IA3027
Thesis supervisor	Professor Heikki Remes
Thesis advisor(s)	Markus Wallin
Date	30.05.2016
Number of pages	88+6
Language	English

Abstract

Carbon Fibre Reinforced Plastics (CFRP) are composite materials commonly used in advanced lightweight structures. Their anisotropic nature, combined with the high strength of carbon fibre, results in negligible degradation in strength over fatigue life. Hence, CFRP structures are increasingly used for fatigue load intensive applications. For uniaxial fatigue loading applications, unidirectional (UD) CFRP composites are commonly used. Prior to their use in a practical application, validation of fatigue performance is required through a fatigue test setup. However, fatigue testing of the UD CFRP composites is difficult, as these composites often fail under the machine grips due to high-stress concentration at the gripping area.

The main objective of this master thesis is to design an in-house test setup to evaluate the tension-tension fatigue behaviour of the UD CFRP pultruded profile of a rectangular cross-section with dimensions of 5.1×2.56 mm. The pultruded profiles comprised UD CFRP composites of fixed cross section manufactured through the pultrusion process. The testing of the pultruded UD CFRP profile is even more difficult due to a limitation in the available gripping area and low out-of-plane compressive strength.

The guidelines for the test setup was obtained from the fatigue testing standard available for UD CFRP laminate. However, the standard specimen produces high-stress concentration at the gripping area, causing failure of the specimen under the grips. Hence, to reduce the stress concentration, a new specimen design was created based on state-of-the-art research. The specimen design was further modified for the specific pultruded profile to reduce stress concentration.

The newly designed specimen was manufactured and primarily tested under static tension loading. The tension test results indicated improvement in the strength for the newly designed specimen. Further, the newly designed specimen was tested for two different load levels under tension-tension fatigue loading. Despite an initial debond between the tab and profile, 9 of the 12 specimens completed more than 10^5 cycles resulting in only minor damage to the UD CFRP profile. Based on the observed damage progression during fatigue testing, the thesis suggests that the design of the new specimen could be improved by selecting a new tab adhesive and adhesive front.

Keywords Fatigue, Pultruded profile, Carbon fibre, Stress concentration

Acknowledgements

This study is carried out as a project work concerning the tension-tension fatigue testing of carbon fibre pultruded profile. The work is supported by the Exel Composites Oyj., Finland. The work is completed at the Aalto university in the Laboratory of Lightweight Structure. I am grateful to the Exel Composites Oyj. for providing me with the opportunity to participate in this super awesome project. My grateful thanks are also extended to Antti Hassinen and Matti Suominen, for coordinating and ensuring all the support during the research work.

I would also like to express my deep gratitude to Markus Wallin, my research instructor, for his guidance during the writing process and assistance for use of laboratory equipment during the research work. I would like to extend the gratitude to Professor Heikki Remes, my research supervisors, for his patient guidance, enthusiastic encouragement and useful critiques of this research work. I would also like to extend my special thanks to Jarno Jokinen, for his advice and assistance during my analytic works and constant support during my research work. I am also grateful to my colleagues Samuli Korkiakoski, Lauri Oittinen and Ilpo for their awesome support.

Sincere thanks to Emeritus Professor Olli Saarela for offering me the opportunity to work on this project and guiding me through the initial phase of work.

Last but not the least, I would like to thank my Family, especially my Parents, who are constant source of my inspiration. I would also like to extend my thanks to my friends Rahul Kallada, Vaibhav Shah, Rahul Abhishek, Gaurav Kulkarni and others for their support and motivation.

Espoo, May 30, 2016

Pravin Luthada

Table of Contents

Abbreviations and symbols

ASTM	American Society for Testing and Materials
CF	Carbon Fibre
CFRP	Carbon fibre reinforced plastic
CoV	Coefficient of variation
DLJ	Double Lap Joint
FEM	Finite Element Method
FRP	Fibre Reinforced Plastic
FVF	Fibre Volume Fraction
GFRP	Glass Fibre Reinforced Plastic
ISO	International Standard Organization
KFRP	Kevlar Fibre Reinforced Plastic
PEEK	Polyether ether ketone
PU	Polyurethane
SCF	Stress Concentration Factor
SD	Standard deviation
STP	Standard Technical Publication
TTZ	Tab Termination Zone
UD	Unidirectional
σ_x	Stress in x-axis
σ_y	Stress in y-axis
τ_{xz}	Stress in XZ plane

1 Introduction

The composite materials are used in making structures for advanced applications such as Aerospace, Marine and Automotive. The composite materials are a combination of reinforcements and a matrix at the macroscopic scale, where the reinforcements provide strength and the matrix holds the reinforcements together. This unique nature of composites allows tailoring of properties to suit the application while keeping the structure weight light with optimal strength.

Carbon fibre reinforced plastic (CFRP) are composites material with carbon fibre reinforcement and the polymer matrix. The inherited nature of composites combined with the high strength of the carbon fibre results in superior performance of CFRP composites under fatigue loading. Due to the superior fatigue resistance, CFRP composites are replacing conventional isotropic material for fatigue intensive structure applications, such as aerospace structures, wind turbine blades, and other high-end application.

Superior fatigue resistance in composite arises due to their anisotropic and inhomogeneous nature. These natures of material are caused by different orientations of the reinforcements, presence of individual components (i.e. fibre and matrix) and interfaces between the reinforcement and matrix. Under the fatigue loading, these features provide weak spots for localised damage formation. The growth of these localised damages is deterred by the reinforcements, resulting in superior fatigue resistance of the composites. These damages deterred with the high stiffness of carbon fibre in CFRP composites, provide fibre dominant fatigue behaviour. These results in comparatively better fatigue resistance to other Fibre Reinforced Plastic (FRP) composites.

CFRP composites with all the fibres aligned in one direction are known as UD (Unidirectional) CFRP composites. UD CFRP composites are highly anisotropic and are very strong under tension along the fibre direction and are presumed to be very good under tension-tension fatigue loading. Application of UD CFRP composite structure can provide great structural durability subjected to tension-tension fatigue. However, the standard testing methods are unreliable in evaluating fatigue life under tension-tension load for UD CFRP material. The primary reason being the highly anisotropic nature of the UD CFRP material which leads to high-stress concentration near the gripping area and causing premature failure.

Hence, structural use of UD CFRP material requires experimental validation through testing. Most of the UD CFRP structural parts or profiles are manufactured using Pultrusion process. In the pultrusion process, the fibres are impregnated into a resin bath and then the wetted reinforcement is pulled through a heated die. The reinforcement is then cured and the outcome of the process is a UD pultruded profile. The profiles manufactured through this process have constant cross-section area and consistent quality.

The thesis is carried out in collaboration with Exel Composites Oyj., a leading technology company that designs, manufactures and markets composite profiles. The main purpose of this work is to

design an in-house test setup to evaluate the tension-tension fatigue behaviour of the UD CFRP pultruded profile provided by Exel Composites Oyj. The cross section of pultruded profile provided is shown in Figure 1.1 and is later referred as the Exel profile.

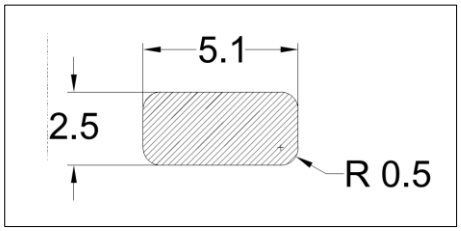

Figure 1.1 Cross section view of Exel profile

The task of developing a tension-tension fatigue test setup includes design, development and validation of the specimen for the pultruded profile without tampering with its shape. The fixed cross-section of the pultruded profile adds to the difficulty of testing an anisotropic UD CFRP material, as the load transfer to the profile is with limited surface area. Additionally, the profile has low compressive strength in the lateral direction, hence, it is more likely that the profile might fail under the machine grips due to gripping pressure.

To develop a test setup with the design of specimen for the UD CFRP pultruded profile, the work is divided into following sub-tasks.

- Understanding the fatigue behaviour of UD CFRP composites under tension-tension loading
- Reviewing and researching state of the art methods and standards for experimental evaluation of fatigue behaviour for UD CFRP material
- Creating an initial specimen design for the pultruded profile based on gathered information
- Evaluation and refinement of the initial design using finite element method (FEM) to arrive at final specimen design for the pultruded profile
- Developing manufacturing process, tooling to manufacture the designed specimen
- Experimental evaluation of failure strain with static tension test and validation through tension–tension fatigue test for the designed specimen
- Discussion of results, drawing conclusions and recommendation for future work

2 Fatigue damage mechanisms in FRP

Tension-tension fatigue behaviour of FRP composite materials has been studied extensively during recent years (1-3). Under the fatigue loading, the FRP composites develop localised damages, due to their anisotropic and inhomogeneous nature. Accumulation and formation of these damages leading to failure have been studied in great detail (4-7). Based on the reported mechanisms many fatigue life prediction models have also been proposed (8, 9). Reported damage mechanisms in FRP composite are discussed here, along with a comparison of damage mechanism in various FRP composites. Later in the chapter, detailed discussion on damage mechanism for UD CFRP composites is also presented.

2.1 FRP composites

Fatigue damage mechanism is the study of initiation and progress of distributed damages as the material is subjected to external fatigue loading. For FRP composites, damage refers to a collection of all irreversible changes such as fibre breakage, matrix cracks and fibre bridged cracking. Under the applied loading, different orientations of fibre in each layer of the FRP materials are subjected to different stresses. These stresses are transferred between fibres through the matrix at the fibre-matrix interfaces. These stresses transferring features, i.e., fibre, matrix and fibre-matrix interfaces; provide a condition for complex micro-level failure and crack development in the composites. Hence, a combined effect of inhomogeneity and anisotropy often leads to complex crack initiation and development process. The reported literature on various crack development process is known collectively as damage mechanism (5, 10). A generic damage progression in five identifiable stages for FRP composites is shown in Figure 2.1. The identified stages are

1. *Matrix cracking:* Under the fatigue loading, initiation of microcracks begins with matrix cracking. Growth and density of these cracks depend on the matrix toughness and ductility. The matrix cracks progress perpendicular or along the fibre direction in their respective laminar planes and is known as primary cracks.

2. *Crack coupling- Interfacial debonding:* The primary cracks growth stops at Characteristic Damage State (CDS), which is an indication of the upper limit for saturation state of primary matrix cracks. Subsequent loading cycle leads to initiation of in-plane transverse cracks i.e. cracks growth perpendicular to crack tip; these cracks are known as secondary cracks and are most probable cause for interfacial debonding.

3. *Delamination:* The secondary cracks are initially small and isolated in the interlaminar layers. Some of these interlaminar cracks merge into strip-like zones, leading to large scale debonding between the layers i.e. delamination.

4. *Fibre breaking:* Fibre reinforcements present in the material acts as a barrier for the stabilised primary cracks. Subsequent crack propagation has a high probability of

occurring near the tip of primary crack; this crack propagation leads to fibre cutting and causes strength reduction in the composites material.

5. *Fracture*: Final failure in the FRP composites is highly random, due to the involvement of various localised damages often resulting in sudden failure.

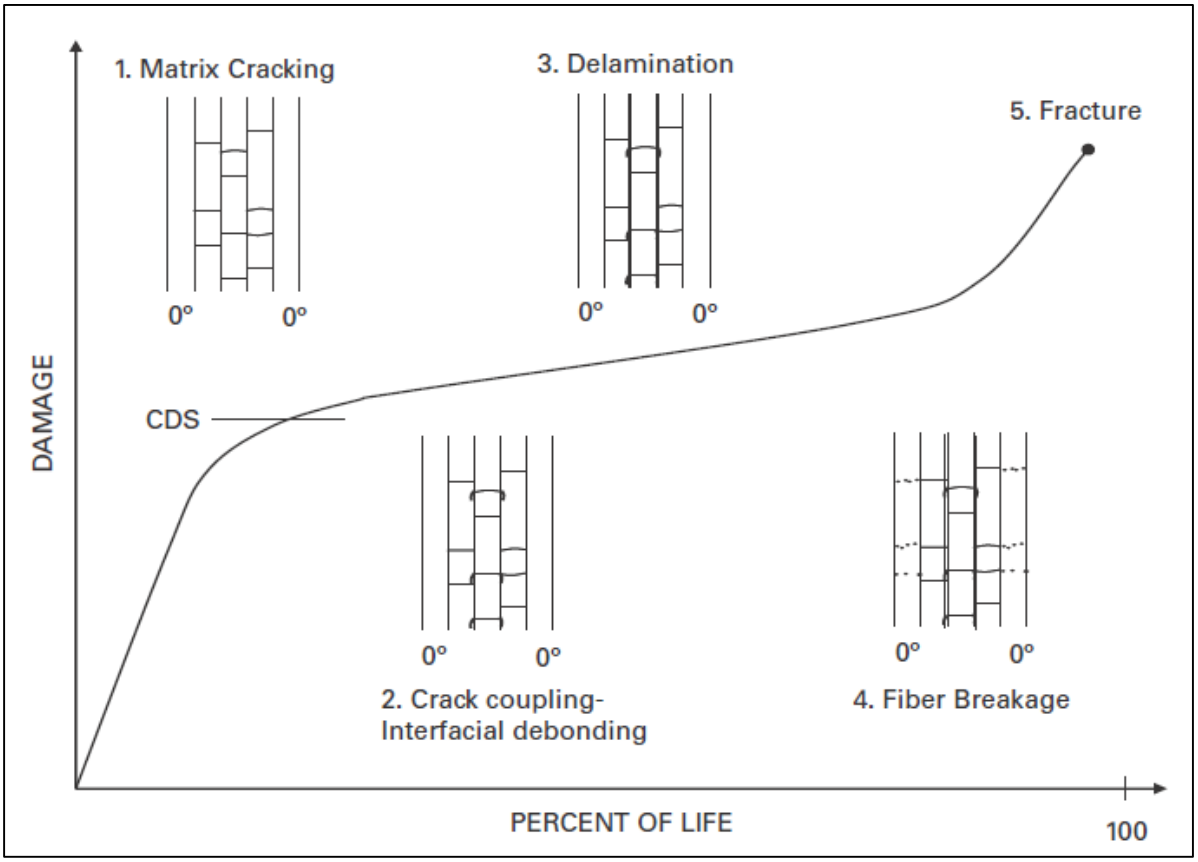

Figure 2.1 Development of damage in composite laminate (11)

Talreja et al. (10, 12) suggested that depending upon the reinforcement dominant damage mechanism in various FRP composites such as GFRP, KFRP and CFRP changes. Fatigue life diagram of these FRP composites is shown in Figure 2.2. These FRP with their respective reinforcements (i.e., glass fibre, Kevlar/aramid fibre or carbon fibre) have different stiffness thus different working stress levels as discussed in Table 2.1. These working stress levels affect the dominant damage mechanism in respective FRP composites.

Table 2.1 stress level dominant damage mechanism (11)

Stress level	**Dominant damage mechanism**
High-stress level	Fibre failure without allowing any other damage mechanism
Low-stress level	Applied cyclic loading cause slower rate fibre breakage, allowing another damage mechanism, such as matrix cracking, fibre-matrix interface debonding; to take place.
Notional endurance limit	Observing technically flat strain-log life curve, suggesting stabilised or no damage growth, also known as fatigue limit strain

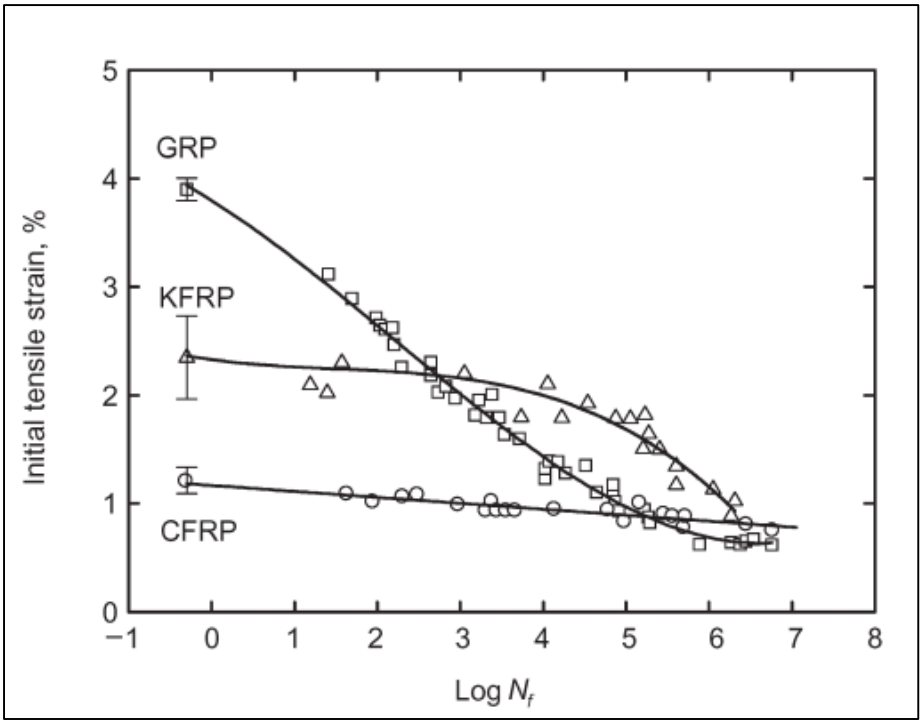

Figure 2.2 Fatigue life diagrams of GFRP, KFRP and CFRP material(13)

As shown in Figure 2.2, the fatigue behaviour of Glass Fibre Reinforced Plastic (GFRP) suggests, a very short life at high-stress level. Due to this, there is a short time for the matrix cracks to occur due to the high working strain of glass fibre. However, during the low-stress level other damage mechanisms are dominant e.g. matrix cracking and fibre-matrix interface debonding. Kevlar Fibre Reinforced Plastic (KFRP) composites have comparatively longer life in high-stress level due to stiffer fibre than glass fibre. In KFRP composites, another damage mechanism such as matrix cracking begins approximately in mid of fatigue life. However, carbon fibres have comparatively higher stiffness than glass and aramid fibres, thus, low working strain even at high stresses prevents matrix strain limits from reaching a critical stage. Therefore, the fatigue life of

CFRP composites is mostly governed by the fibre failure without allowing any other damage mechanism to occur. Almost flat strain-log life curve for CFRP composites also suggests, very less deterioration in strength under cyclic loads, making them most suitable for fatigue loading.

2.2 Damage mechanism of UD CFRP

The damage mechanism of UD CFRP composites have been extensively studied by Sturgeon et al. (14) and Gamstedt and Talreja. (7). In the study performed by Gamstedt and Talreja (7), a CFRP laminate with carbon fibre reinforcement and epoxy matrix specimen (CF/epoxy) was manufactured with dimensions of 127×12.7×0.5 mm (i.e. gage length, width, and thickness respectively). Fatigue tests were carried out with stress ratio max stress/ minimum stress (R) = 0.1 and 10 Hz loading frequency. The observed damage mechanism is presented using fatigue life diagram as shown in Figure 2.3. The damage mechanism for UD CFRP is segmented into three major regions,

1. Region I (Fibre breakage)
2. Region II (Fibre bridging)
3. Region III (Crack arrest)

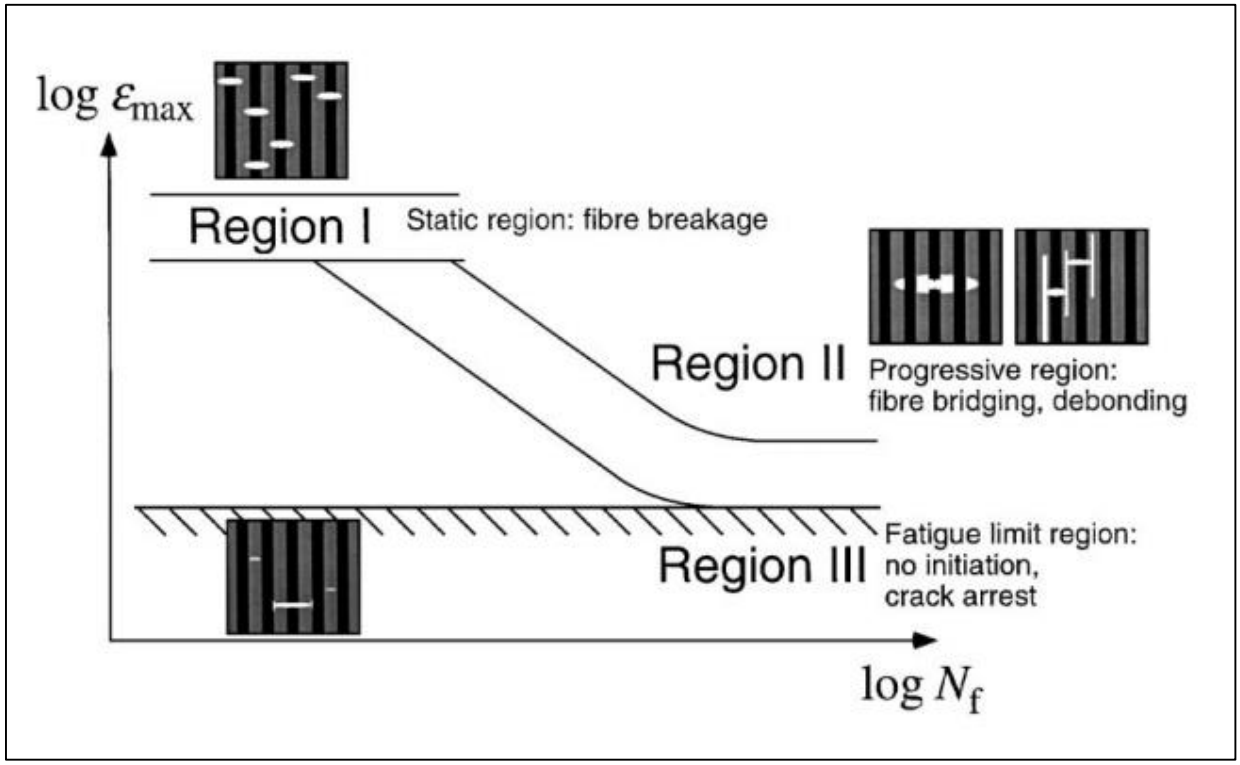

Figure 2.3 Damage mechanism in UD CFRP laminate (7)

Region I (Fibre breakage): During the cyclic loading, initial fibre breakage occurs well below static strain limit due to higher spread in fibre properties. Microscopic view of the fibre breakage is shown in Figure 2.4, beginning with a pristine laminate image, followed by fibre breakage after the first cycle. From these fibre breakages, as further cyclic loading is applied, matrix cracks

originate at the broken fibre tips. Continuing with further load cycles, theses cracks progresses perpendicular to the fibre direction.

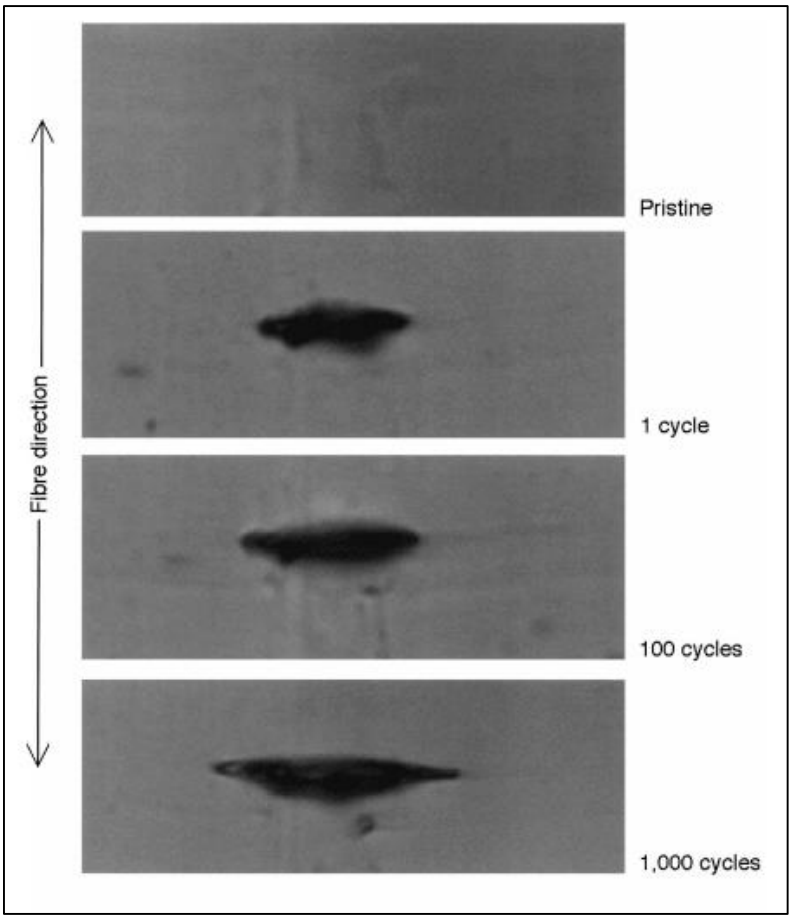

Figure 2.4 Microscopic view of UD CFRP laminate indicating crack initiation and progress (7)

Region II (Fibre bridging): Progressing matrix cracks are encountered by adjacent fibre as shown in Figure 2.5. This fibre reinforcement act as a barrier bridge, deterring the matrix cracks from propagating further, this phenomenon is known as fibre bridging.

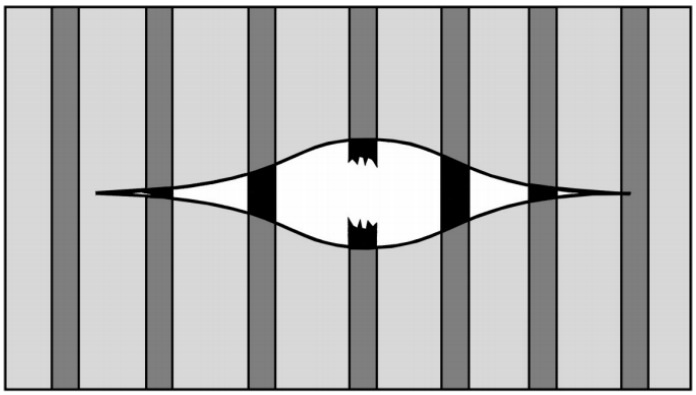

Figure 2.5 Crack bridging by fibre reinforcements (7)

Region III (Crack arrest): As the third region arrives after few million cycles, the matrix cracks approaches neighbouring fibres (Figure 2.6). The fibre act as a barrier to the crack growth, giving rise to two competing mechanisms; (a.) the growth of the fibre bridged crack that is suppressed by debonding along the fibre and, (b.) the effective crack growth is deterred by blunting the crack tip along the fibre. It is highly probable that these cracks would lead to successive breakage of fibre in the nearby region causing sudden failure.

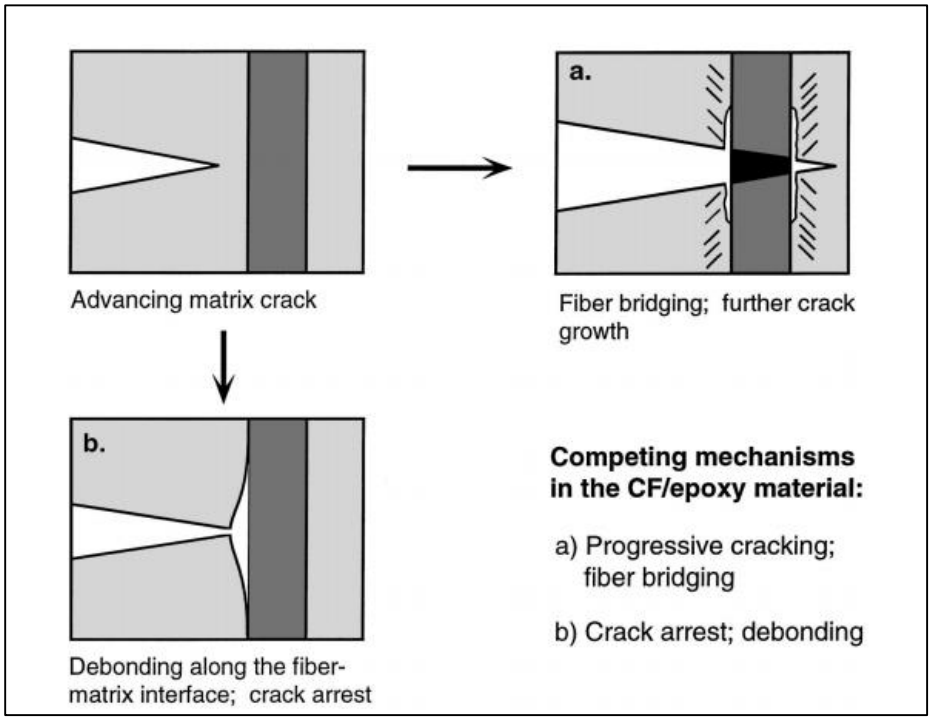

Figure 2.6 Crack progressing to adjacent fibres causing (a) fibre bridged cracks growth and/or (b) fibre-matrix interface debond by blunting crack tip (7)

Based on the damage mechanism described above, the UD CFRP composites have a fibre dominant damage mechanism. Thus, high stiffness of carbon fibre plays a very important role as it deters most the damages to occur in the matrix. To understand the holistic behaviour of the UD CFRP composites, fatigue-life diagram provides an overall picture. The fatigue-life diagram is created between maximum initial strain and log of a number of fatigue cycles. The fatigue-life diagram with strain below the fatigue strain limit (Figure 2.7) displays no fatigue degradation; this was first suggested by Sturgeon et al (14). As the strain increased above the fatigue strain limit, other regions of fatigue-life diagram become evident (Figure 2.8).

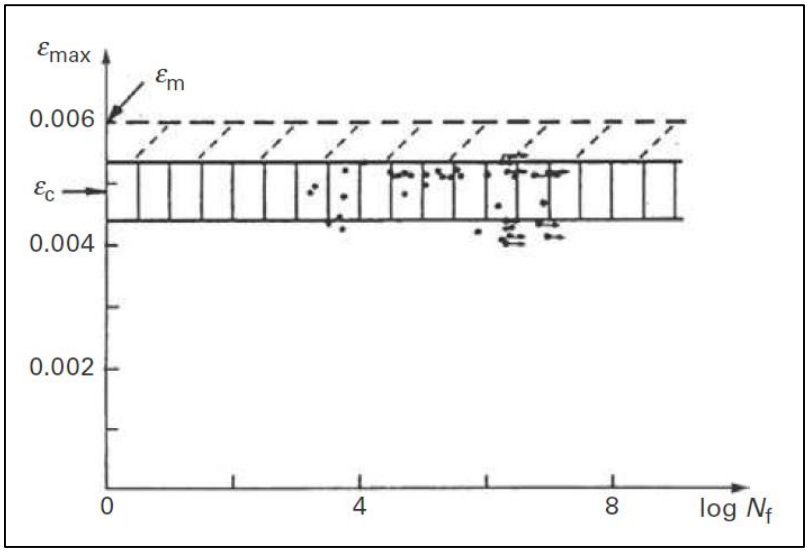

Figure 2.7 Fatigue-life diagram for UD CFRP laminate with lower strain than fatigue limit strain(14)

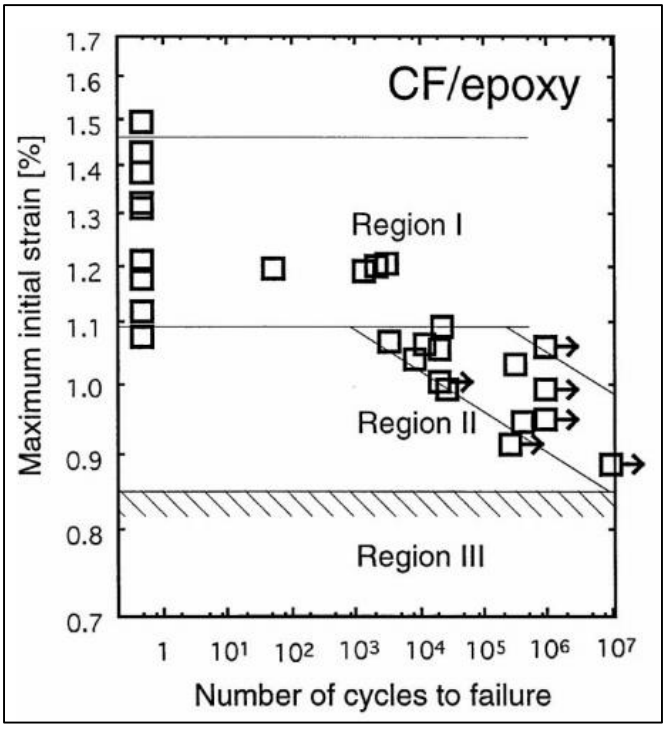

Figure 2.8 Fatigue life diagram for UD CFRP laminate with higher strain than fatigue limit strain (7)

The large spread in the fatigue life of UD CFRP is quite evident and is presumed largely due to brittle nature of carbon fibres. However, the fibre dominant failure of these materials displays no degradation of properties over fatigue life. This unique behaviour of UD CFRP composites makes them most suitable for fatigue application in structures.

3 State of the art of UD CFRP fatigue specimens

3.1 Testing Standards

The Exel profiles are UD CFRP composites of fixed cross section. Hence, to arrive at the initial testing procedure for the Exel profiles, testing standards for UD CFRP is utilised. The ASTM and ISO standards provide guidelines for evaluating fatigue properties of the UD CFRP laminate.

3.1.1 ASTM Standards

Following ASTM standards are used for tension-tension fatigue testing UD CFRP laminates.

- ASTM D3479/3497M (15) "Standard Test Method for Tension-Tension Fatigue of Polymer Matrix Composite Materials" for fatigue test parameters.
- ASTM E122 (16) "Standard Practice for Calculating Sample Size to Estimate, With Specified Precision, the Average for a Characteristic of a Lot or Process" for sample size estimation.
- ASTM D 3039/D 3039M (17) "Standard Test Method for Tensile Properties of Polymer Matrix Composite Materials" for specimen geometry.

The information from the ASTM standards is summarised in Table 3.1. ASTM D3479/3497M provide elaborated guidelines for testing, with two main test control parameter as load and strain in procedure A and B, respectively. The ASTM standard recommends experimental measurement using static tension test of failure strain, sequentially evaluating maximum load levels with a statically significant sampling lot size as per the ASTM E122. In the standard, typical specimen configuration (Figure 3.1) is referred from ASTM D3039/D3039M. A specimen configuration includes geometrical as well as the material parameters of the specimen. The geometrical parameters include width and thickness of the gage section along with other tabbing parameters such as tab length, tab taper angle, and tab overhang. The ASTM standards also define the probable failure modes of the specimen (Figure 3.2).

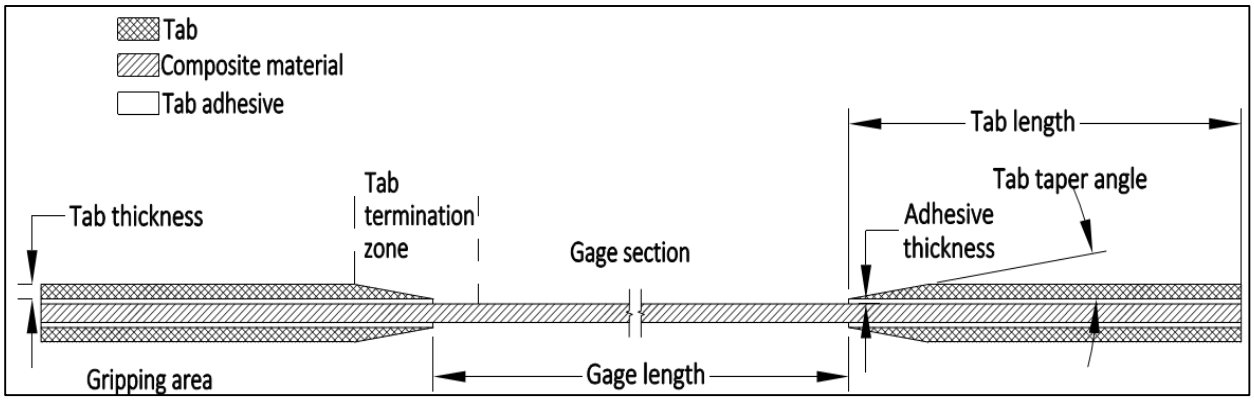

Figure 3.1 Typical specimen configuration with terminologies

Table 3.1 Summary of ASTM standards for tension-tension fatigue testing of FRP composite

Feature	**ASTM D 3479/D 3479M (15)**
Test control parameter	Load (procedure A) and strain (Procedure B)
Procedure A	Load monitoring
Procedure B	Strain monitoring
Load/Strain levels for S-N curve	Minimum three
Number of tests	As per ASTM E122 (16), minimum 5 specimen per load/strain level
Specimen failure	Specimen fracture or user specified degrees of failure
Specimen geometry as per ASTM D 3039/D 3039M (17)	
Tab material	GFRP (±45°), Al or same as material to be tested
Tab length	56 mm
Tab taper angle	7-10 ° or 90°
Tab overhang	10- 15 mm
Tab thickness	1.5 mm
Gripping pressure	To avoid slippage or crushing
Width (gage)	15 mm
Thickness (gage)	1 mm
Gage length	138 mm
Specimen shape	Straight sided specimen

ASTM D3479/3497M (15) recommends special guidelines regarding tab failure as "premature failure of the specimen in the tab region is common in tension-tension fatigue testing as a result of stress concentrations in the vicinity of tab region. A set of preliminary fatigue tests is recommended to find the combination of tab material, tab length, and adhesive that minimises tab failures. Using an optical microscope to view the edge of the specimen, it can be determined if similar states of damage occur in the tab region and the gage region".

Tab failure has been studied extensively with a major focus on reducing stress concentration by choosing optimal tabbing and gripping parameters. The tabbing and gripping parameters are a set of a geometrical and material parameter associated with tab for the specimen and jaw gripping while mounting specimen in the testing machine. The tabbing and gripping parameters are discussed in detail later.

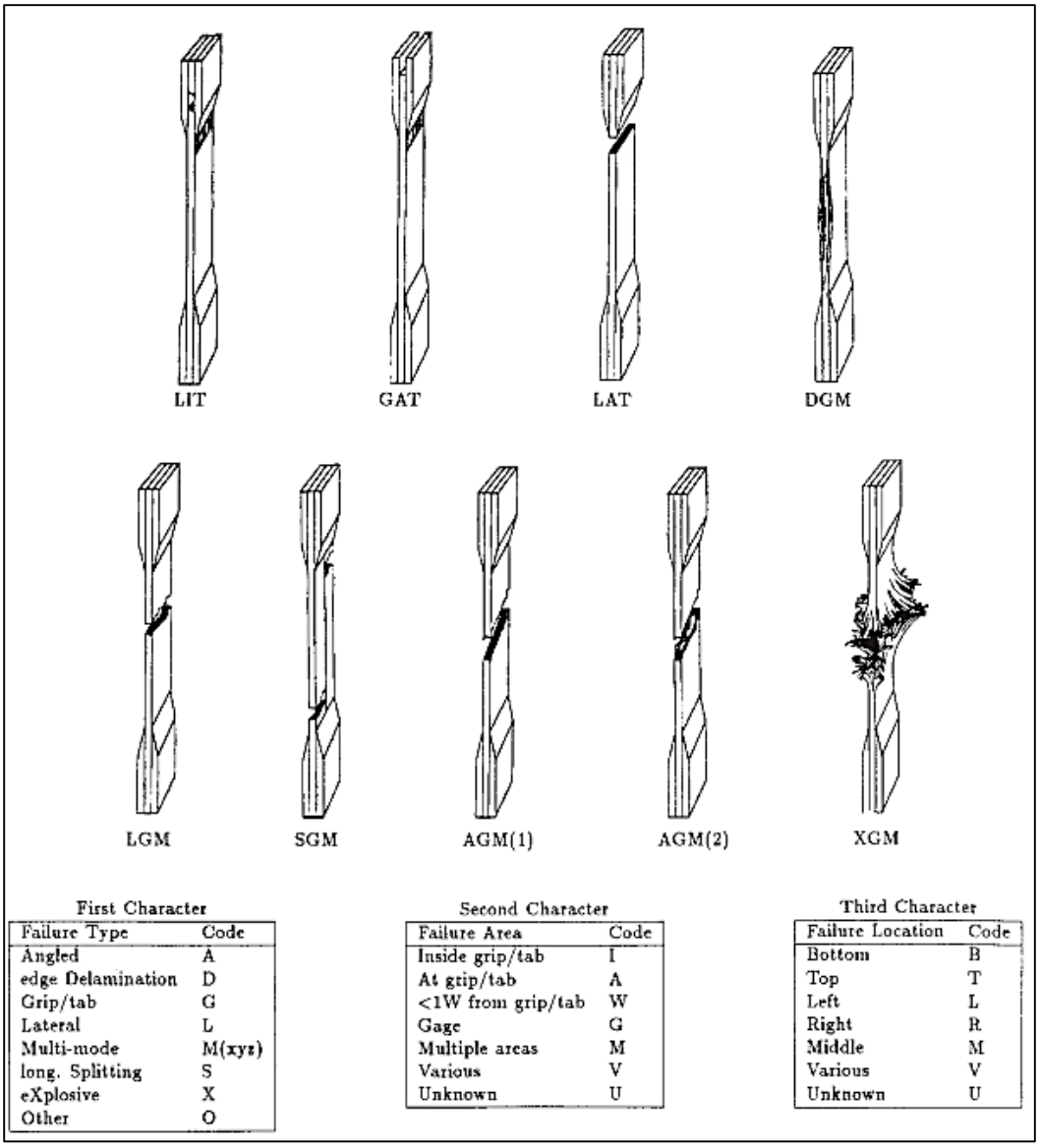

First Character

Failure Type	Code
Angled	A
edge Delamination	D
Grip/tab	G
Lateral	L
Multi-mode	M(xyz)
long. Splitting	S
eXplosive	X
Other	O

Second Character

Failure Area	Code
Inside grip/tab	I
At grip/tab	A
<1W from grip/tab	W
Gage	G
Multiple areas	M
Various	V
Unknown	U

Third Character

Failure Location	Code
Bottom	B
Top	T
Left	L
Right	R
Middle	M
Various	V
Unknown	U

Figure 3.2 Tensile Test Failure Codes/Typical Modes(17)

3.1.2 ISO Standards

Following ISO standards are used for tension-tension fatigue testing UD CFRP laminates.

- ISO 13003:2003 (18) "Fibre-reinforced plastics — Determination of fatigue properties under cyclic loading conditions"
- ISO 527-5 (19) "Part 5: Test conditions for unidirectional fibre reinforced plastic composites"

A summary of the ISO standards is provided in Table 3.2. The ISO 13003:2003 standards cover the fatigue testing procedure; suggesting a stress or strain controlled loading with minimum five specimens for each stress/strain level. However, the ISO standard does not provide detailed guideline regarding gripping of the specimen. The standard refers to specimen configuration from ISO 527-5 (19) and the suggested specimen geometry is shown in Figure 3.3. The specimen

geometry is with a taper angle of 90° and a gage length of 50 mm. The specimen mounting in the jaws is overarching above tab by 7 mm.

Table 3.2 Summary of ISO standards for tension-tension fatigue testing of FRP composite

Feature	**ISO 13003:2003 (18)**
Test control parameter	Stress or strain
Number of tests	5 specimen for each stress or strain level
Load/Strain levels for S-N curve	Minimum four
Gripping	-
Specimen failure	Break or loss of stiffness
Specimen geometry as per ISO 527-5 (19)	
Tab material	GFRP (±45°)
Tab length	50 mm
Tab taper angle	90°
Tab overhang	-
Tab thickness	0.5 - 2 mm
Gripping pressure	-
Width (gage)	15 mm
Thickness (gage)	1 mm
Gage length	50
Specimen shape	Straight sided specimen

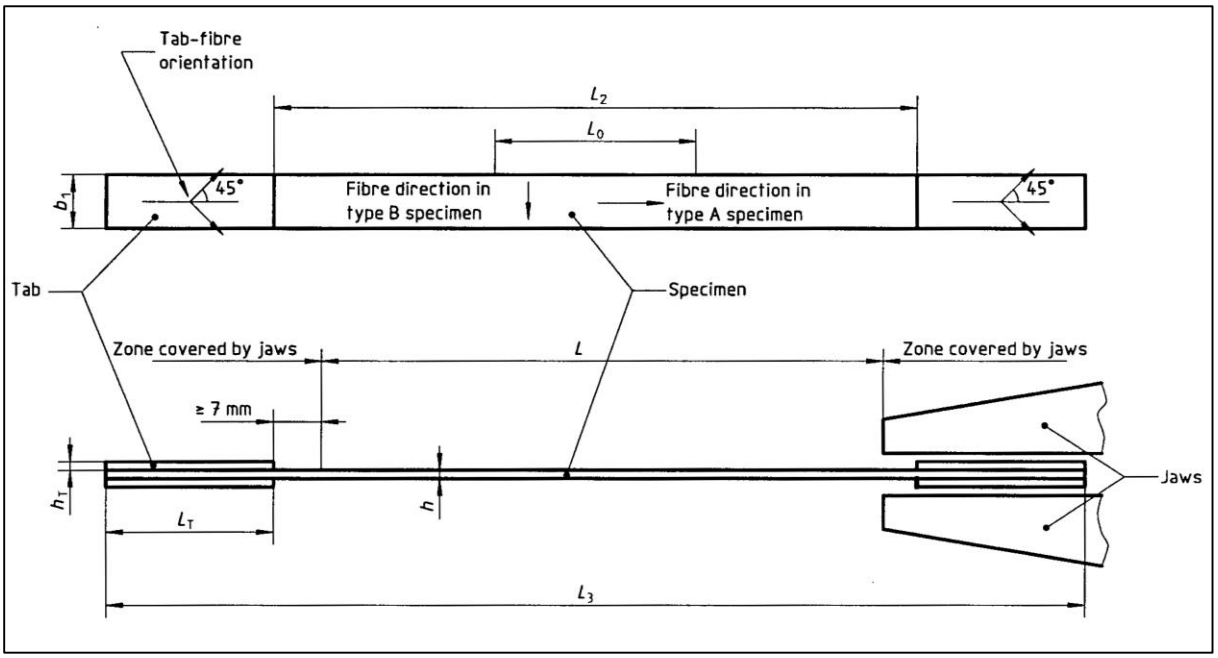

Figure 3.3 Specimen configuration as per the ISO standard (19)

3.1.3 Selection of standard

The ASTM and ISO Standards can be used for fatigue testing of UD CFRP specimen. However, the ASTM standards described specimen design is more detailed, i.e., tab failure and specimen failure modes. Regarding the tab failure, the ASTM standards provide an experimental guideline for selection of tabbing parameters. Additionally, the ASTM standard defines failure mode for the specimen and provide selection guideline for tab adhesive. Thus, the ASTM standards are chosen for carrying out testing as well as for initial specimen configuration.

The Exel profile can be tested as per the ASTM standard testing procedure and parameters. However, The specimen shape suggested by the ASTM standard, i.e., width and thickness of the gage section cannot be achieved due to shape restriction of the Exel profile (Figure 3.4). As the Exel profile has t/w (thickness/width) ≅ 1/2, which is very high compared to the ASTM standard UD laminate specimen t/w ≅ 1/15 (17). Assuming same gripping pressure for both t/w, increases the gripping forces on the Exel profile, this might cause crushing of the Exel profile. Additionally, reduced width reduces the effective tab bonding area by 2/3. Thus, a new specimen design is required for the Exel profile.

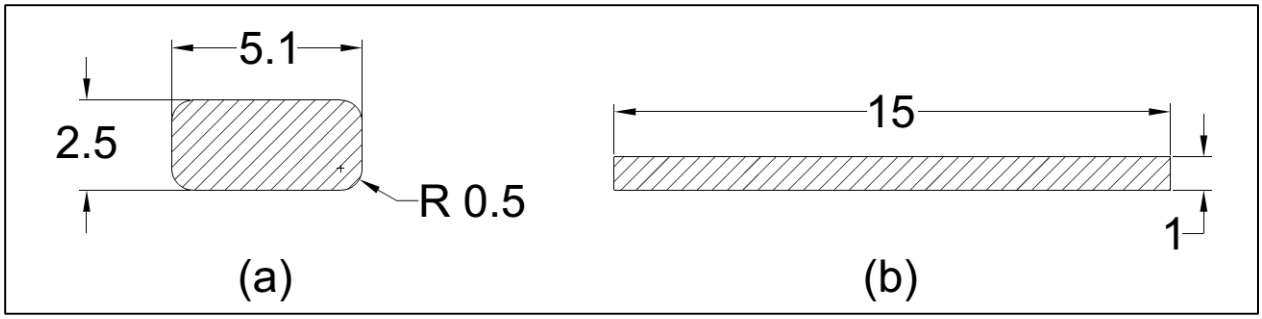

Figure 3.4 Cross-section of the Exel profile (a) and the ASTM standard UD CFRP test specimen (b)

An initial design for the specimen means, selecting tabbing and gripping parameters which increase the tab bond length and additional support for the profile to prevent crushing. However, before making these changes, an initial tabbing and gripping parameters needs to be finalised. The initial tabbing and gripping for the Exel profile specimen can be reached based on the guidelines from the ASTM standards.

As per the ASTM standards, premature failure of the specimen is very common during tension-tension fatigue testing in the tabbing area due to high stress concentration.(15) The major reason being stress concentration in the vicinity of Tab Termination Zone (TTZ). The stress concentration is quantified as Stress Concentration Factor (SCF) and is evaluated using Equation 3.1.

$$SCF = \frac{\sigma_x^{max}}{\sigma_x} \qquad \ldots\ldots \{3.1\}$$

Where
σ_x^{max}, is the maximum stress observed in principle loading direction, i.e., along x-axis direction and σ_x is the nominal stress in principle loading direction in middle the of the gage section.

To reduce SCF in the tabbing area, the ASTM standard recommends a set of preliminary fatigue tests to find the combination of tabbing and gripping parameters. However, a preliminary testing without prior understanding of the effect these parameters on SCF would require a lot of resources and time. Hence, a review of reported studies is carried out to understand the effect of tabbing and gripping parameters on SCF in the UD CFRP specimen. In the process, selecting a primary set of parameters which affect SCF in the specimen.

3.2 Literature review of UD CFRP specimens

In this section, reported literature on specimen configuration of UD CFRP laminate and effect of the tabbing and gripping parameter on SCF for their testing under static tension loading or tension-tension fatigue is reviewed. Earlier investigation in fatigue test specimen configuration of UD CFRP laminates started by Sturgeon et al.(14, 20) and Curtis et al.(21, 22) Initial experimental studies probed into the geometrical aspect of the specimen by comparing waisted and plain rectangular specimens. These studies concluded that the rectangular specimen gave comparatively high fatigue life, although, the failure observed was mostly near the gripping area suggesting high-stress concentration.

Later with the plain rectangular specimen, a detailed analytical and experimental study to optimise the tabbing parameter for testing UD CFRP tensile testing was carried out by Cunningham et al. (23). This study provided a comprehensive understanding of stress distribution in the tabbing area and recommended necessary parameters to have minimal SCF in the tabbing area. Despite the analytical finding, most of the specimen tested failed prematurely. In mid-1990, a new approach for providing tabbing by stepped laminate was proposed by Wisnome et al. for evaluating tensile strength of UD CFRP laminate. The experimental measurement showed 14% higher tensile strength compared to un-tabbed specimen (24).

In early 2000 Kulakov et al.(25), Portnov et al. (26-28) and Adams et al. (29) conducted studies for UD CFRP laminate tension testing, with a broader range of material and tabbing parameters, with the aim of providing tabbing and gripping parameter guidelines for a UD CFRP specimen. An analytical study by Adams et al. provided comprehensive guidelines for UD CFRP laminate testing. In addition to tabbing and gripping parameters, Following studies by Kulakov et al.(25) and Portnov et al. (26-28) was aimed at reducing SCF drastically with novel configuration for tabbing for UD CFRP laminate. Later, Bare et al. (30) conducted series of experimental and analytical studies to arrive at the best combination of tab material, tab adhesive and surface preparation for bonding for tension testing of cross-ply CFRP specimen. Baere et al. (31) also carried out trials for finding out optimum gripping pressure with optimum tab overhang in the specimen.

Based on these reported studies, critical tabbing and gripping parameters are enlisted in Table 3.3. The reported research also highlighted some novel specimen configurations for UD CFRP specimen and those are enlisted in the table under novel shape configuration.

Table 3.3 Critical parameters

Tabbing and gripping parameter	**Novel shape configuration**
• Tab thickness • Tab length • Tab material • Tab taper angle • Tab adhesive • Tab adhesive thickness • Gripping pressure	• Dog-bone • Stepped laminate tapper • Inverted tabs configuration

3.3 Specimen configuration parameters

3.3.1 Tab thickness

Effect of tab thickness on the SCF in the specimen has been first studied by Cunningham et al. in 1985, based on the evaluated reduction in SCF, tab thickness was not considered for specimen design. Corroborating the result further, Adams et al.(29) and Kulakov et al.(25) carried out similar studies in early 2000, displaying the effect of tab thickness on SCF. The result of an analytical study by Kulakov et al.(25) is presented in Table 3.4, where the SCF is proportional to σ_x^{max} assuming constant σ_x at the mid of gage section. Increasing thickness (h_{tab}) from 0.5 mm to 2.0 mm, increases SCF very marginally by 0.7%, thus the ASTM standard recommended tab thickness of 2 mm is suggested for the UD CFRP specimen.

Table 3.4 Effect of tab thickness on stresses occurring in CFRP and Tab (25)

h_{tab}, mm	σ_x^{max}	σ_z^{max}	τ_{xz}^{max}
	MPa		
	CFRP		
0.5	2221.7	43.8/–47.8	80.0
1.0	2231.3	86.9/–50.3	84.5
1.5	2237.2	110.6/–44.9	83.7
2.0	2238.2	125.0/–37.8	81.3
	Tab		
0.5	240.0	–70.5	53.0
1.0	185.4	–69.2	52.5
1.5	153.3	–67.9	49.1
2.0	132.3	–59.8	45.1

3.3.2 Tab length

Tab length (l^{tab}) can be defined as the bond line length of adhesive between the tab and the specimen. The tab length can be calculated analytically considering load transfer of forces through tabs to specimen via shear. Ives De Baere et al.(31) suggested analytical formulation for evaluating tab length; though using suggested formulation for a typical UD CFRP laminate of 1 mm thickness with typical epoxy adhesive, evaluated tab length is well below 50 mm.

In order to understand the effect of l^{tab} on the SCF in the UD CFRP specimen, there have been studies by Kulakov et al.(25) and Adams et al. (29) Analytical studies from Adams et al. (29) displaying plot between normalized principle stresses σ_x and Tab length is shown in Figure 3.5, where the SCF is proportional to normalized principle stresses σ_x. The study indicates almost no effect of tab length on SCF as a change of tab length from 40- 80 mm reduced the SCF by meagre 0.2%. Hence, the ASTM standard recommended tab length of 56 mm can be taken for the UD CFRP specimen.

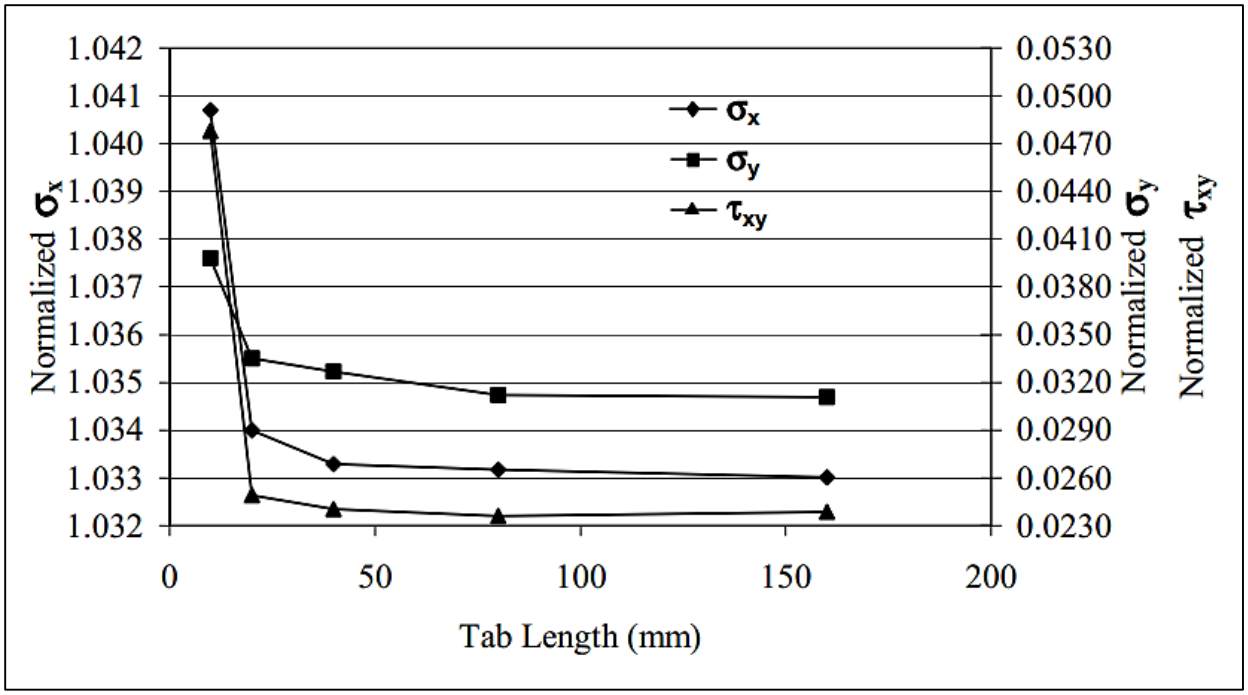

Figure 3.5 Tab length vs. normalised principle stresses σ_x , normalized in-plane transverse stress σ_y and normalized tangential stress τ_{xy}.(29)

3.3.3 Tab material

The selection of tab material depends on the SCF it generates at the TTZ. In addition to this, the conductivity of tab material can be critical parameters for heat dissipation, which is typically generated during the fatigue loading. The heat is generated in the tabbing area, due to viscous or frictional heating under fatigue loading (32).

There have been analytical and experimental studies by Cunningham et al.(23), Adams et al.(29) and Kulakov et al.(25) on the effect of tab material causing SCF in TTZ for static tension loading. Results from these analytical studies suggest that 2D woven GFRP tab provides optimal SCF. Analytical study data from Kulakov et al. (25) presented in Table 3.5. Where the SCF in specimen is proportional to σ_x^{max} in CFRP assuming constant σ_x at the mid of gage section

The study compared four different tabbing materials

- 2D woven CFRP
- Aluminium
- 2D woven GFRP
- 3D GFRP

Achieving least SCF for 3D GFRP, however, the cost and labour of manufacturing 3D preform for making 3D GFRP tab far exceed the benefits compared to 2D woven GFRP. Thus, Kulakov et al. suggested the 2D woven GFRP, i.e. GFRP 2D woven cross-ply with 45°orientations, and here onwards referred as GFRP ±45°.

Table 3.5 Effect of tab material on SCF in the specimen Longitudinal stress (σ_x),In-plane transverse stress (σ_z) and tangential stress (τ_{xz}).(25)

Tab material	σ_x^{max}, MPa	σ_z^{max}, MPa	τ_{xz}^{max}, MPa
		CFRP	
2D woven CFRP	2593.1	179.7/–71.0	296.6
Aluminum	2511.7	204.2/–73.6	257.4
2D woven GFRP	2237.2	110.6/–44.9	83.7
3D GFRP	2225.7	59.5/–14.3	85.2
		Tab	
2D woven CFRP	322.1	–207.9	160.6
Aluminum	266.1	–52.6	148.8
2D woven GFRP	153.3	–67.9	49.1
3D GFRP	109.3	–17.0	54.7

Fatigue testing is very time and resource consuming and high loading frequency can help to speed up of such test, which is necessary for optimum resource utilisation. But as the specimen is subjected to high-frequency loading, it leads to localised heating due to intrinsic friction (viscous heating, internal friction between newly created surfaces e.g. micro-cracks, delamination), extrinsic friction (e.g. with the grips) or through the temperature increase of the hydraulic system itself (33). The temperature rises due to heat generated can be mitigated by dissipating heat quickly by conduction through tabs. Above chosen tab material i.e. GFRP is not very good heat conductor compared to CFRP or Aluminium, consequently hindering the heat flow and giving rise to a temperature in the tabbing zone.

The high temperature in the tabbing zone can lead to property deterioration of bonding adhesive in the gripping area. Bailey et al.(34) carried out thermographic measurement on an E-glass GFRP specimen with different tabbing material as shown in Figure 3.6. The frequency of fatigue loading was kept at 5 Hz. As the thermographic image suggests the 2D woven GFRP tab produces 2°C rise in temperature. And as per THE ASTM D3479/D 3479M (15) an upper limit of temperature to 30°C is acceptable, assuming the testing temperature of 20°C. thus, 2D woven GFRP can be taken as tab material with a noted condition of choosing frequency that keeps the temperature rise under the aforementioned limit.

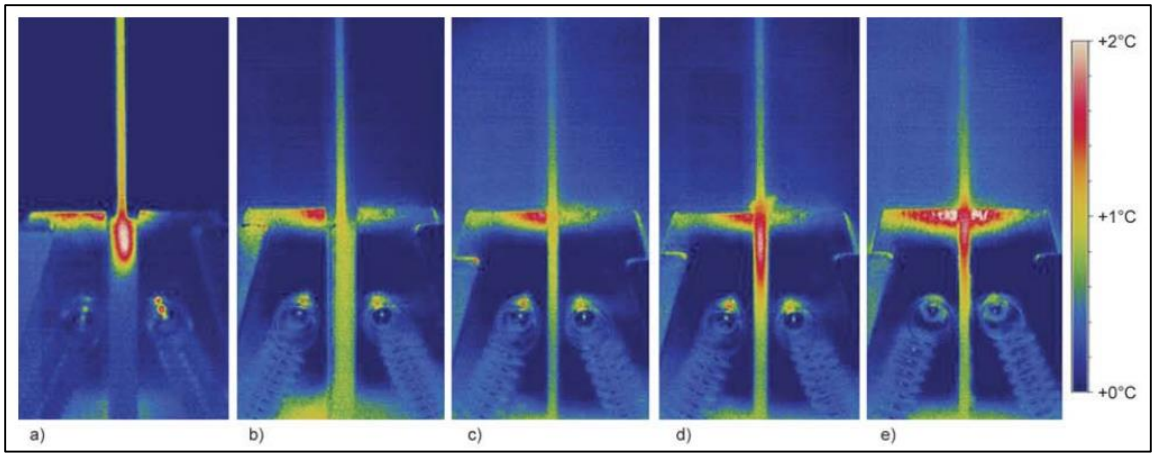

Figure 3.6 Thermal images of the specimen edge after cyclic loading. (a) GFRP tab; (b) Aluminium tab; (c) Tab-less; (d) Tab-less with abrasive cloth; (e) Tab-less in SiC fused jaws(34)

3.3.4 Tab taper angle

Adding tabs to the specimen changes the cross section of the specimen from tabbed to un-tabbed region abruptly causing high SCF in TTZ. Thus, the tabs are provided with tab taper angle, resulting in gradual transition in TTZ and helps in achieving lower stress concentration. However, gradual transition with really low tab angle is difficult to manufacture. The lower value of tab taper angle can also result in high tensile normal stress (peel off stress) and shear stresses in the adhesive (29) .The analytical and experimental studies on the effect of tab taper angle on SCF is conducted by Cunningham et al.(23) Adams et al.(29) and Kulakov et al.(25) Analytical study data from Adams et al.(29) is presented as plot in Figure 3.7, between normalised principle stresses σ_x and tab taper length where the SCF is proportional to normalized principle stresses σ_x. The plot indicates lower SCF and other stresses for lower tab angle of 5°.

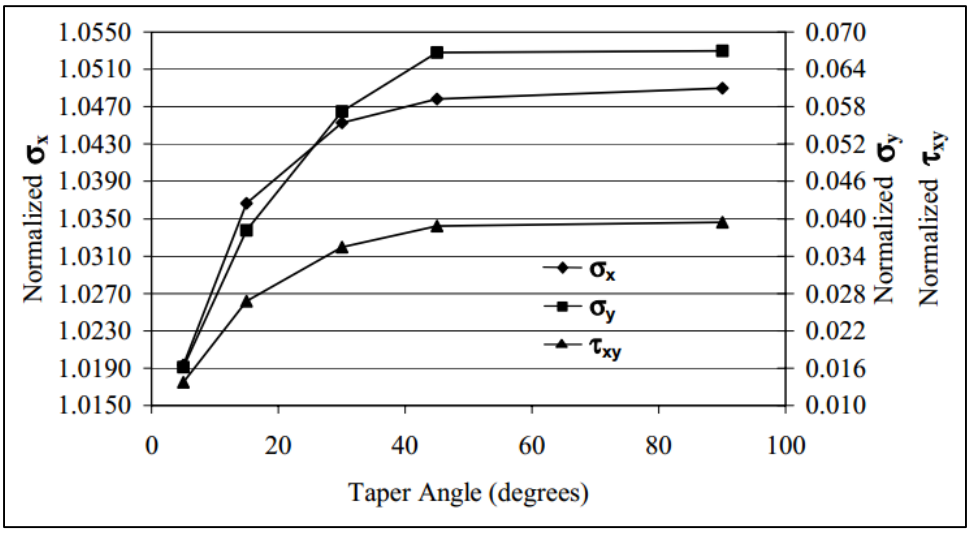

Figure 3.7 Tab taper angle vs. normalised principle stresses σ_x, normalized in-plane transverse stress (σ_y) and normalized tangential stress (τ_{xy}).(29)

Other criteria for tab taper angle evaluation were the peel off and shear stresses in tab adhesive. The plot from the similar study is presented below demonstrate the effect of tab taper angle on peel off stress and shear stress. The Figure 3.8 top and bottom indicate an approximate drop of 50% in the normalized and peel off stresses respectively as the tab taper angle reduces from 15° to 5° at the tab tip. A minimally tapered angle is desired to minimise the SCF in the specimen. A minimum angle of 10° was suggested by studies, considering ease of manufacturing for UD CFRP laminate specimen.

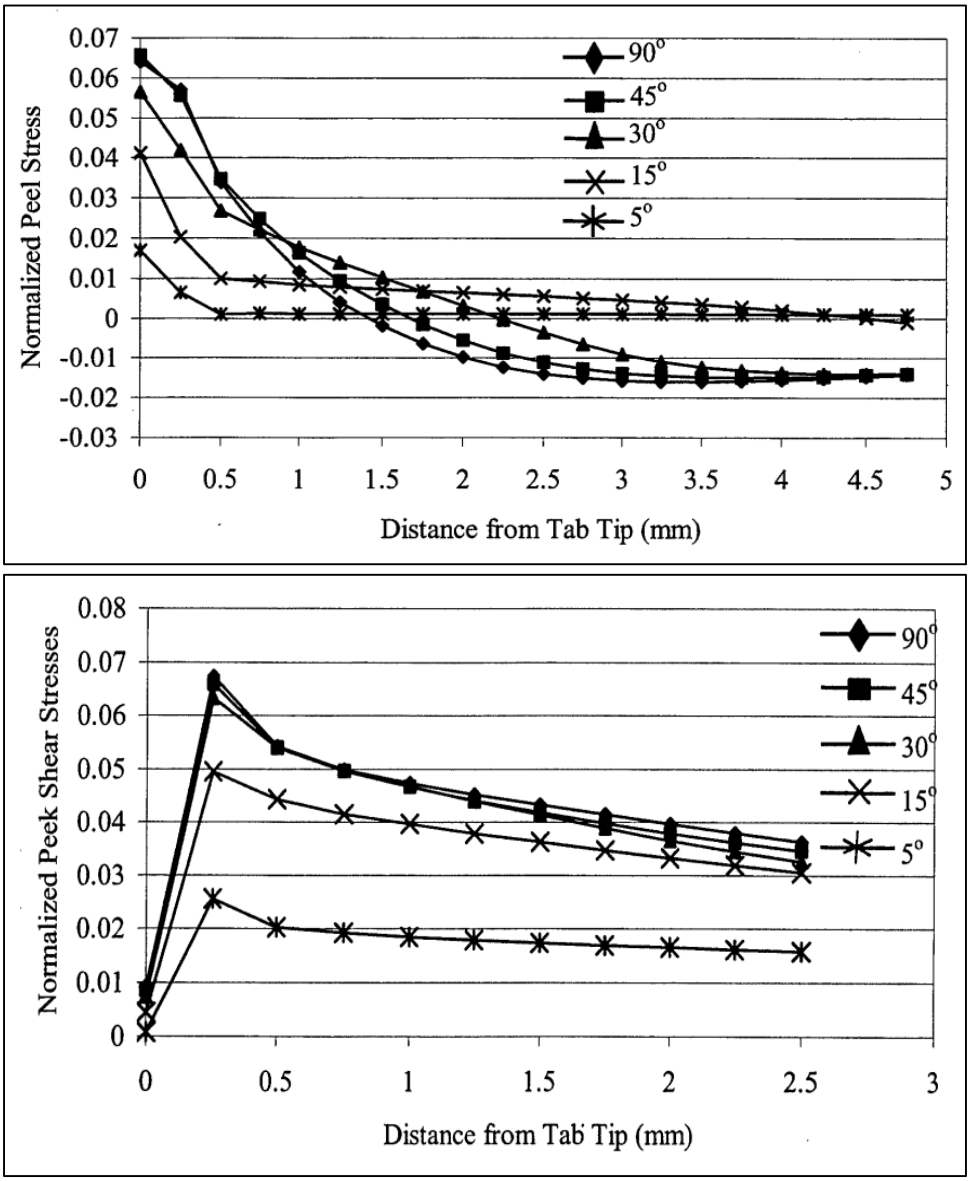

Figure 3.8 Effect of tab angle on normalised peel off stress (top) and normalised shear stress in the tab adhesive (bottom).(29)

3.3.5 Tab adhesive material

The tab adhesive is used to bond the tab to the UD CFRP material. The adhesive material selected based on achieving lower SCF and its ability to withstand fatigue loading.

There have been analytical studies for evaluating the effect of the adhesive material on SCF in the specimen by Adams et al.(29) and Kulakov et al.(25) The studies by Kulakov et al.(25) included typical adhesive materials Epoxy (Young's modulus E = 3.7 GPa) and polyurethane (E=0.3 GPa) and a case without adhesive. The results from the study displayed in the Table 3.6, where SCF is proportional to σ_x^{max} assuming constant σ_x at the mid of gage section. The results indicate lower SCF for polyurethane i.e. the adhesive with lower modulus.

Table 3.6 Effect of Adhesive Material on Maximum Stresses

Adhesive material	σ_x^{max}, MPa	σ_z^{max}, MPa	τ_{xz}^{max}, MPa
	CFRP		
Without adhesive	2237.2	110.6/–449	83.7
Epoxy resin	2192.7	112.1/–46.8	88.7
Polyurethane	2123.0	24.1/–40.6	35.8
	Tab		
Without adhesive	153.3	–61.1	49.0
Epoxy resin	142.3	–48.2	60.8
Polyurethane	118.8	–30.5	41.1
	Adhesive		
Epoxy resin	94.1	115.4/–44.8	92.4
Polyurethane	10.2	12.9/–30.8	38.8

Continuing the evaluation with second selection criteria i.e. the adhesive should also be able to withstand fatigue loading. The aforementioned reason for tab heating usually causes a temperature rise in the tabbing zone, thus weakening the adhesive strength (32, 35). Frédéric Lani (36)studied the effect of fatigue life on epoxy adhesive material subjected to different temperature and humidity (Figure 3.9). Based on provided plots, utilising the plot with 23°C and 50% Relative humidity (RH), a loss in stiffness of 2.6% due to presumed temperature rise of 5°C - 6°C is deduced. That suggests the loss in stiffness is negligible for the epoxy adhesive material for a given temperature rise (36). Thus, a tab adhesive with lower Young's modulus to achieve lower SCF and better performance under fatigue loading is suggested.

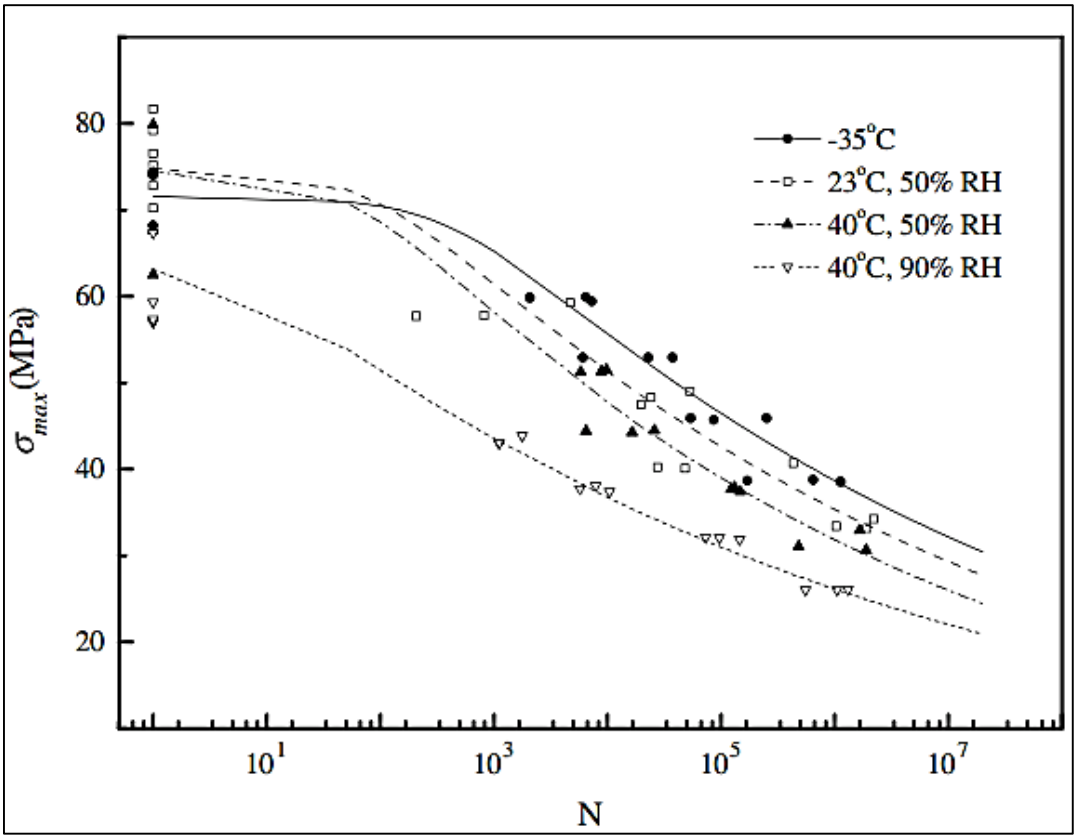

Figure 3.9 Two-component epoxy system derived S-N curves for examined fatigue datasets (36)

3.3.6 Tab adhesive thickness

The thickness of adhesive bond line between tab and specimen material is tab adhesive thickness. Effect of tab adhesive thickness on SCF occurring in UD CFRP specimen has been studied by Adams et al.(29) and Cunningham et al(23). The result of the study by Adams et al.(29) with varying adhesive thickness from 0.5mm to 2 mm is shown in Figure 3.10. The plot is drawn between tab adhesive thickness and normalised principle stresses σ_x,where the SCF is proportional to normalized principle stresses σ_x.

The plot indicates 0.13 % reduction in SCF by increase in adhesive thickness from 0.26 mm to 1.3 mm. However, the ASTM standard recommended a minimum adhesive thickness for good bond strength (17), hence a value 0.2 mm by is selected for the initial specimen configuration.

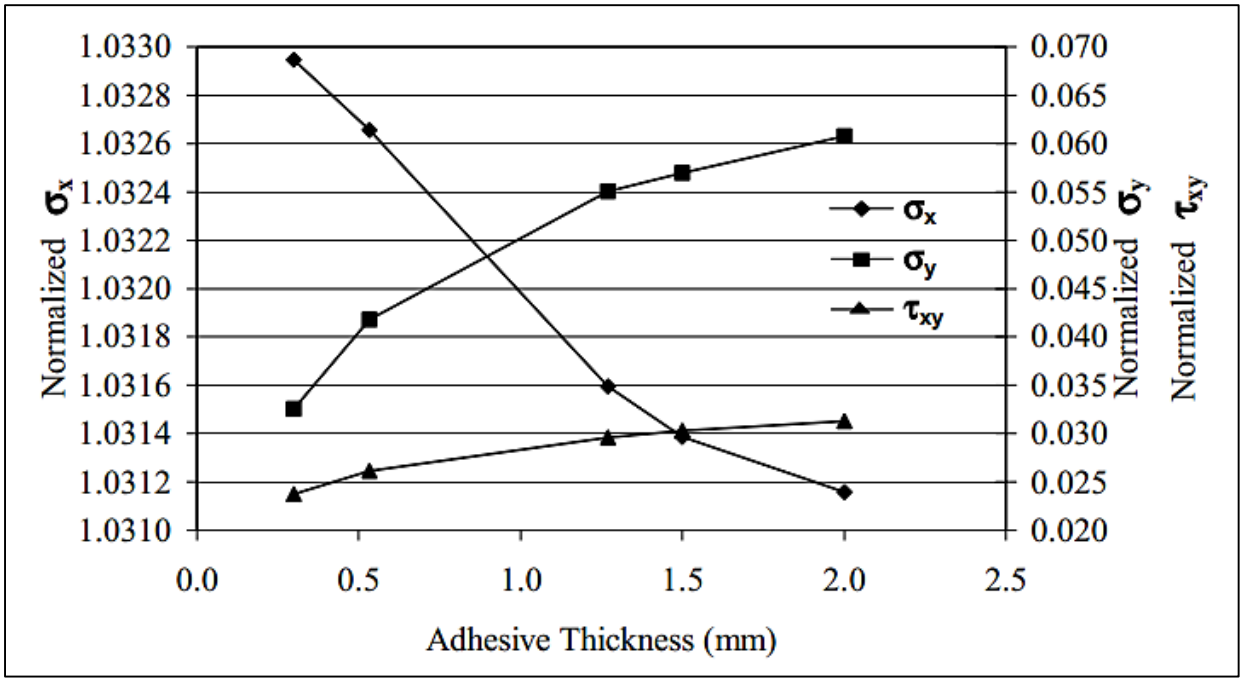

Figure 3.10 Adhesive thickness vs. normalised principle stresses σ_x, normalized in-plane transverse stress (σ_y) and normalized tangential stress (τ_{xy}).(29)

3.3.7 Tab overhang

Tab overhang is the distance between tab termination point and front of the gripping jaw (Figure 3.11). Bare et al. (31) and Kulakov et al. (25) carried out studies on the effect of tab overhang on SCF in the specimen. The studies suggested that the tab overhang of 10 mm helps in reducing the SCF.

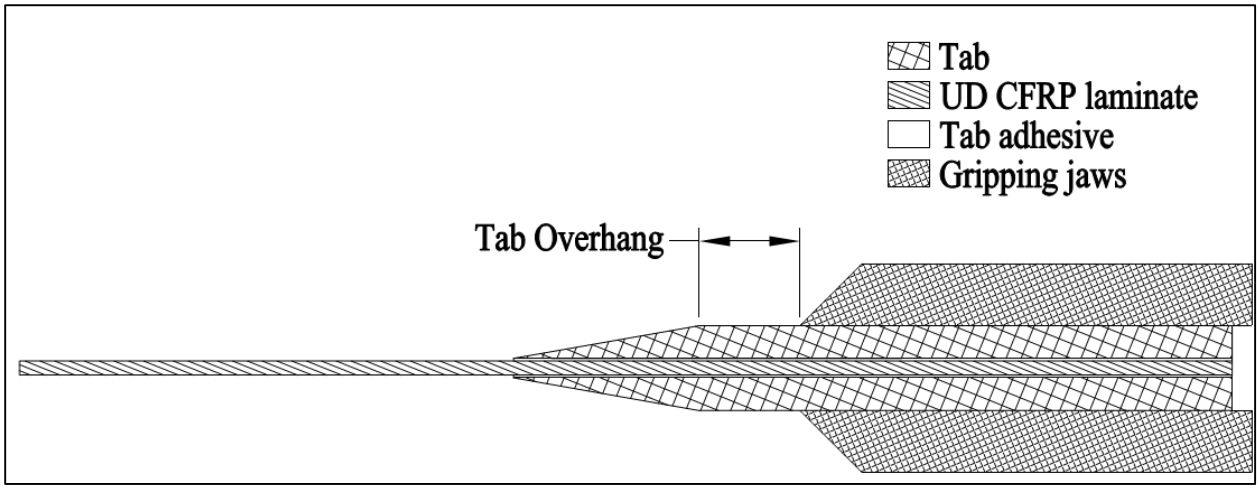

Figure 3.11 Tab overhang in the specimen

3.3.8 Tab cut-off thickness

At the tab tip, where tab taper ends, the sharp edge of the tab is cut short at the TTZ, leaving a step of the tab as shown in Figure 3.12, the thickness of the step is called tab cut-off thickness. Effect of tab cut-off thickness on stress concentration has been studied by Cunningham et al. (23). The study indicated the cut-off thickness increased from 0.00 to 0.254 produced a 6% increase in the SCF. A minimal tab cut-off thickness as possible by manufacturing can be suggested for UD CFRP specimen.

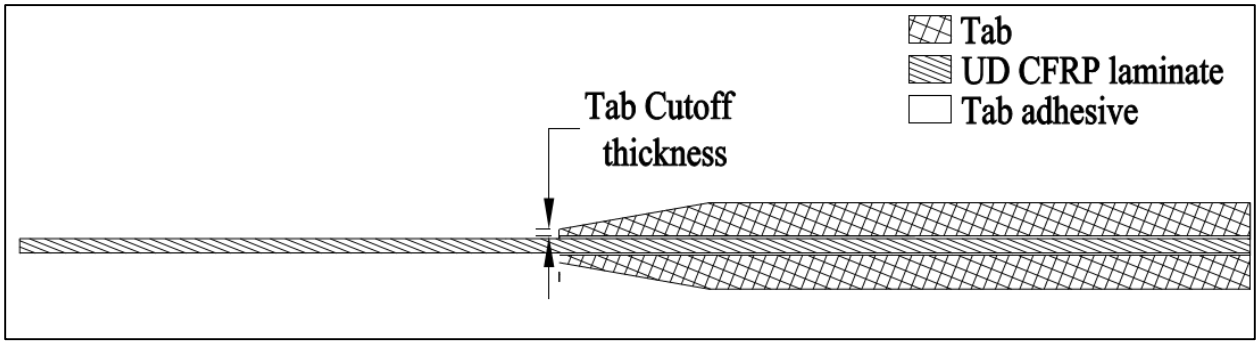

Figure 3.12 Tab cut-off thickness

3.3.9 Gripping pressure

The pressure applied in the grips for holding the specimen while loading is known as gripping pressure. The gripping pressure is a function of the type of grips, wedge of grips and the hydraulic pressure. There have not been any studies on the effect of pressure on SCF of specimen however the excessive gripping forces may lead to heating in tabbing zone. Experimental studies conducted by Bare et al. (31) suggested that most of the CFRP cross-ply specimen with end tab of CFRP (0/90) tab angle 13.5°, failed due to frictional heating in the tab zone. Gripping pressure based on trial and error to avoid slippage can be selected for primary testing, although, during testing the temperature monitoring is recommended.

3.3.10 Novel specimen shape

The UD CFRP test specimen can be designed based on the study for all the aforementioned critical parameters. However, there have been few new approaches to reduce SCF in the gripping area which might be helpful in gaining more insight about specimen design. The new approaches for specimen design opted were: new gage profiles, novel tab design and stepped laminate as a tab. A summary of research carried out novel design is presented here.

The experimental studies were carried out by Curtis et al.(22) in 1983 for three different gage profiles of the specimen, i.e. waisted, parallel sided and notched. The specimen of UD CFRP laminate was subjected to tension-tension fatigue loading. The studies concluded that the rectangular specimen performed best among the three specimens tested (Figure 3.13). However most of the time the specimen failed near the grips.

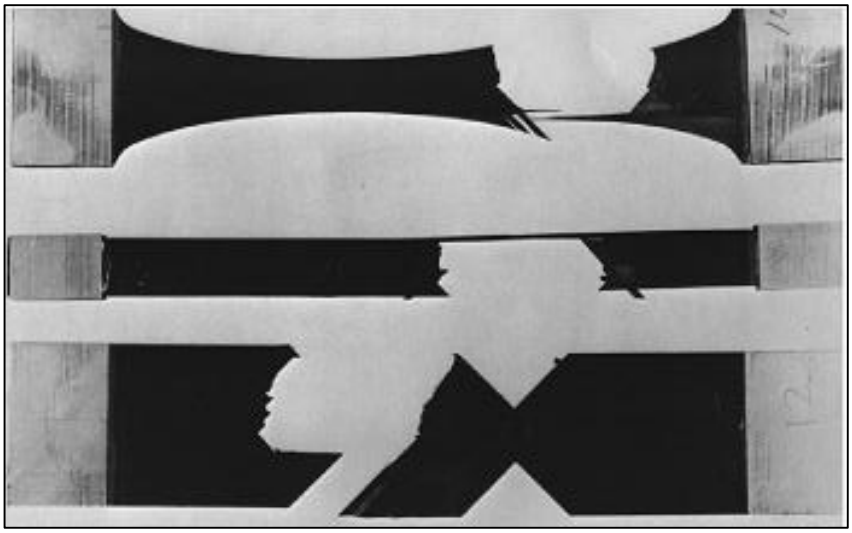

Figure 3.13 Coupons with varying gauge profiles under tension-tension fatigue loading (22)

Subsequently in 1995, Wisnome & Maheri (24, 37) created a stepped laminate of UD CFRP creating a taper angle of 0.7° on all four sides (Figure 3.14). Further cutting it in the ASTM standard specimen shape, stepped specimen were manufactured. The experimental data from the study suggests an increase of 14% in tensile strength compared 90° tabbed specimen. Although, the idea of stepped taper required specialised tooling and was not perused further.

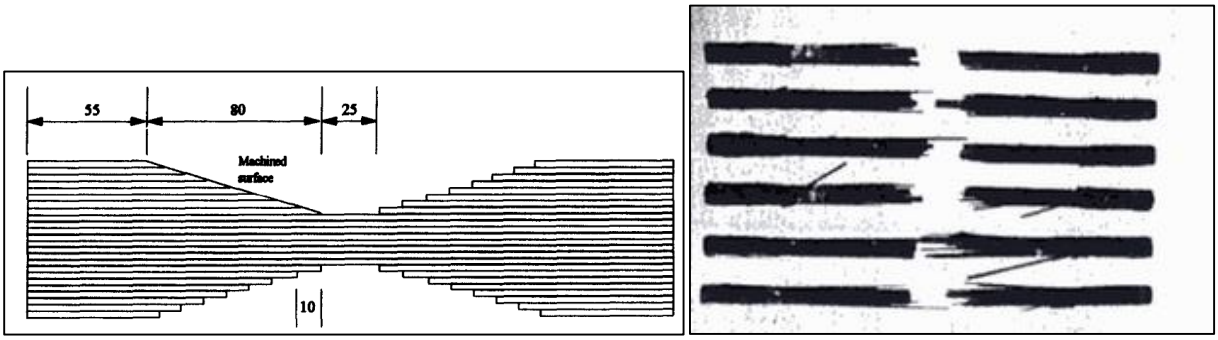

Figure 3.14 Specimen with stepped tabs of CFRP with taper angle 0.7° (37) (left) and failed specimen in gage section (right) (24)

Later in 2006, a study for novel tab design was carried out by Portnov et al. (27) In the ASTM standard uniaxial tension tests of flat composite specimens, it is technically impossible to avoid SCF in a near-surface layer close to the grips of a testing machine. In an attempt to reduce the SCF Portnov et al. carried out the analytical study with six different configurations of end geometry as shown in Table 3.7. In the process, they discovered that configuration 6 shifts the effect of stress concentration from termination edge of the tab to the back of the tab achieving SCF ≅ 1.02. Where SCF is evaluated from ratio provided in column $\sigma_x^{max}(x_1)$.

Table 3.7 End geometry of CFRP Specimens of various configurations where x1, x2, and x3 are near termination edge of tab and x4 is near back edge of tab (26)

Configuration of a specimen	$\sigma_x^{max}(x_1)$	$\sigma_z^{max}(x_2)$	$\tau_{zx}^{max}(x_3)$	$\tau_{zx}^{max}(x_4)$
1 	3389.3 (99.875) 3230.2 (99.875)	115.0 (100.0) 48.0 (100.0)	101.4 (101.250) 55.6 (101.375)	47.5 (149.875) 54.3 (149.875)
2 	3472.3 (100.0) 3291.6 (100.0)	73.1 (100.0) 100.4 (100.0)	89.9 (100.5) 54.7 (100.5)	63.2 (149.875) 68.4 (149.875)
3 	3375.3 (101.5) 3195.8 (101.5)	49.0 (101.5) 22.4 (101.5)	118.6 (102.50) 57.5 (102.75)	35.8 (149.875) 46.0 (149.750)
4 	3202.5 (99.875) 3096.5 (99.875)	75.5 (100.0) 59.4 (100.0)	106.4 (102.375) 55.9 (102.625)	49.1 (149.875) 55.5 (149.875)
5 	3291.6 (99.625) 3201.9 (99.625)	63.3 (99.875) 40.8 (99.875)	87.1 (101.0625) 57.7 (101.50)	50.4 (149.875) 61.0 (149.875)
6 	3082.8 (98.125) 3025.3 (98.125)	16.6 (98.625) 14.9 (98.375)	63.3 (101.375) 33.5 (101.125)	49.1 (149.875) 55.3 (149.875)

3.4 Summary of the specimen configuration

Based on the literature, a summary of the parameters recommended for UD CFRP laminate is shown in Table 3.8. As indicated in the table, the tab length does not affect the SCF, so THE ASTM standard suggested the value of 56 mm or above is suggested. Tab material with lower stiffness provides lower SCF, thus 2D woven GFRP is selected as tab material. Tab material conductivity also affects the temperature rise in the gripping area, thus a loading frequency to avoid excessive heating is suggested.

Tab taper angle is the most influential parameter affecting SCF in the specimen, a suggested value of 10° is selected, although, if possible to manufacture lower angle are permitted. Tab adhesive stiffness is a direct correlation with SCF evaluated, thus, an adhesive with lower stiffness and better fatigue performance is suggested. Effect of thickness of tab adhesive bond-line on SCF was not very evident thus a value close to recommended values of 0.4 mm is selected. Tab cut off should be avoided to minimise SCF, allowing the tab to end smoothly, although, very difficult to manufacture in practice. Tab overhang helps in reducing the SCF and a value of 10 mm is recommended. All the above parameters lead to specimen configuration for UD CFRP laminate as shown in Figure 3.15.

Table 3.8 Summary of UD CFRP laminates specimen configuration

Feature	**Recommended value/property**
Tab length	Analytical value (above 50 mm)
Tab material	GFRP (±45°)
Loading frequency	Selected to avoid heat rise above 26°
Tab thickness	2 mm
Tab angle	10°
Tab adhesive	Epoxy with load carrying capability and better fatigue performance
Tab adhesive thickness	0.2 mm
Tab cut-off thickness	Sharp tab tip i.e. zero cut-off thickness
Tab overhang	10 mm(min)
Gripping pressure	-
Specimen shape	Rectangular plane
Thickness	1 mm
Width	15 mm

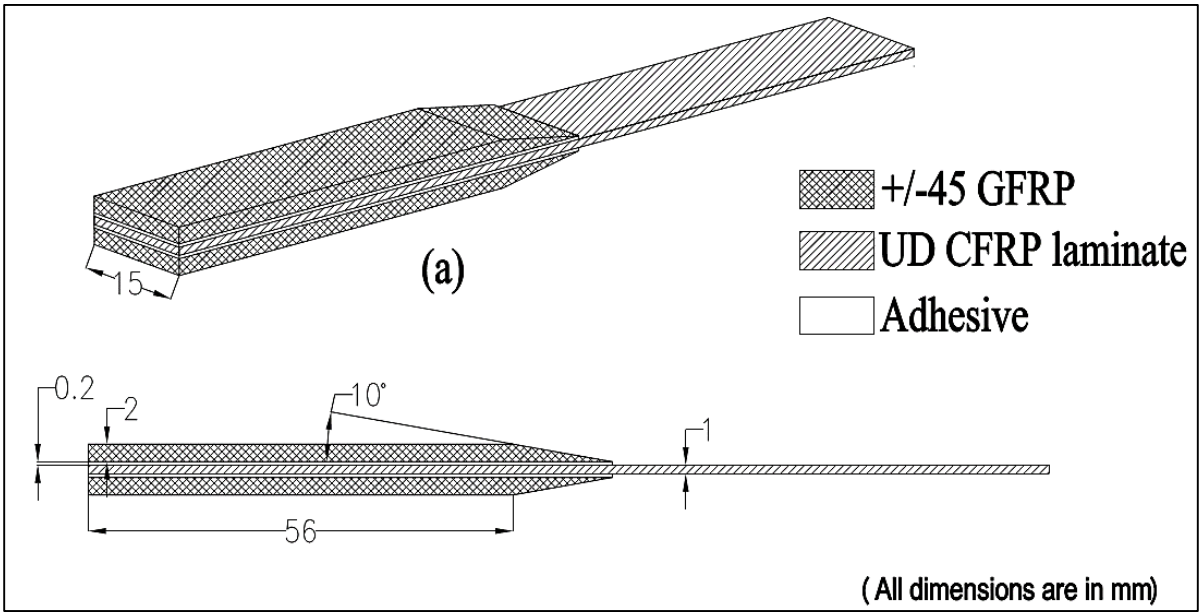

Figure 3.15 UD CFRP laminate specimen configuration

4 Specimen design for pultruded profile

4.1 Preliminary specimen design

The specimen design in the previous chapter was focused on the UD CFRP laminate. Now, the recommended suggestions for the UD CFRP laminate specimen are implemented on to the Exel profile, the outcome specimen design is shown in Figure 4.1. Unfortunately, the shape of the profile reduces the width of the tab to 5.1 mm while increasing the thickness to 2.56 mm, thus reducing the load transfer area i.e. the gripping area on the tab. The load to be transferred through tabs and adhesive is increased, due to increasing gage section thickness. Consequently, higher load transfer will require high gripping pressure increasing the risk of crushing the Exel profile. Thus, changes in the design for the Exel profile specimen is needed to address the aforementioned issues.

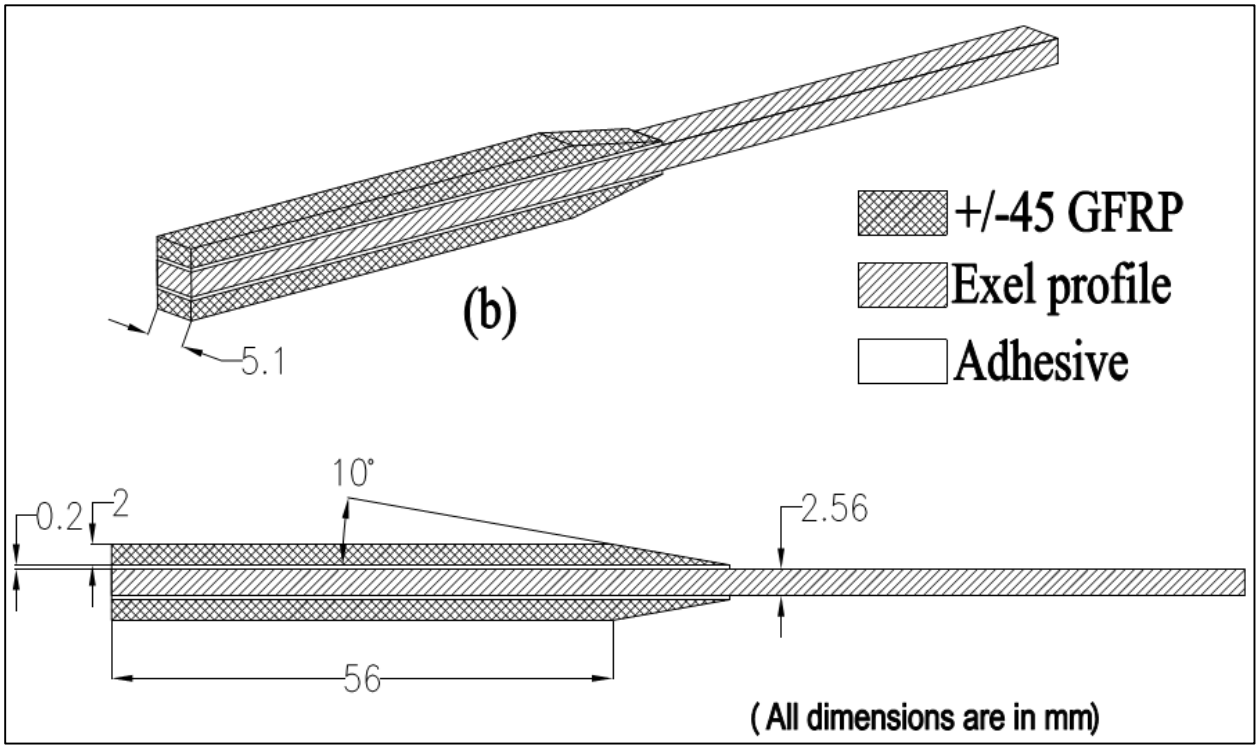

Figure 4.1 Preliminary specimen design D1 for Exel profile based on the literature

A new design for the Exel profile specimen called D1 specimen design is suggested and is shown in Figure 4.2. The recommended D1 design utilises all the mid-section parameters recommended by the ASTM standards and literature. In addition, the design extends the tabs in the lateral direction to the profile, providing higher gripping area. The gripping area is modified to take full advantage of the grips available at a testing facility of the lab i.e. 40 × 60 mm, hence distributing the pressure over a larger area. To support the extended tabs, support profiles (Exel profiles of length equal to tab length) are provided. The support profiles are placed parallel to main profile at a distance of 3 mm for now. The gap between the main profile and support profiles are filled with adhesive, increasing the adhesive bond line between the Exel profile and the tab.

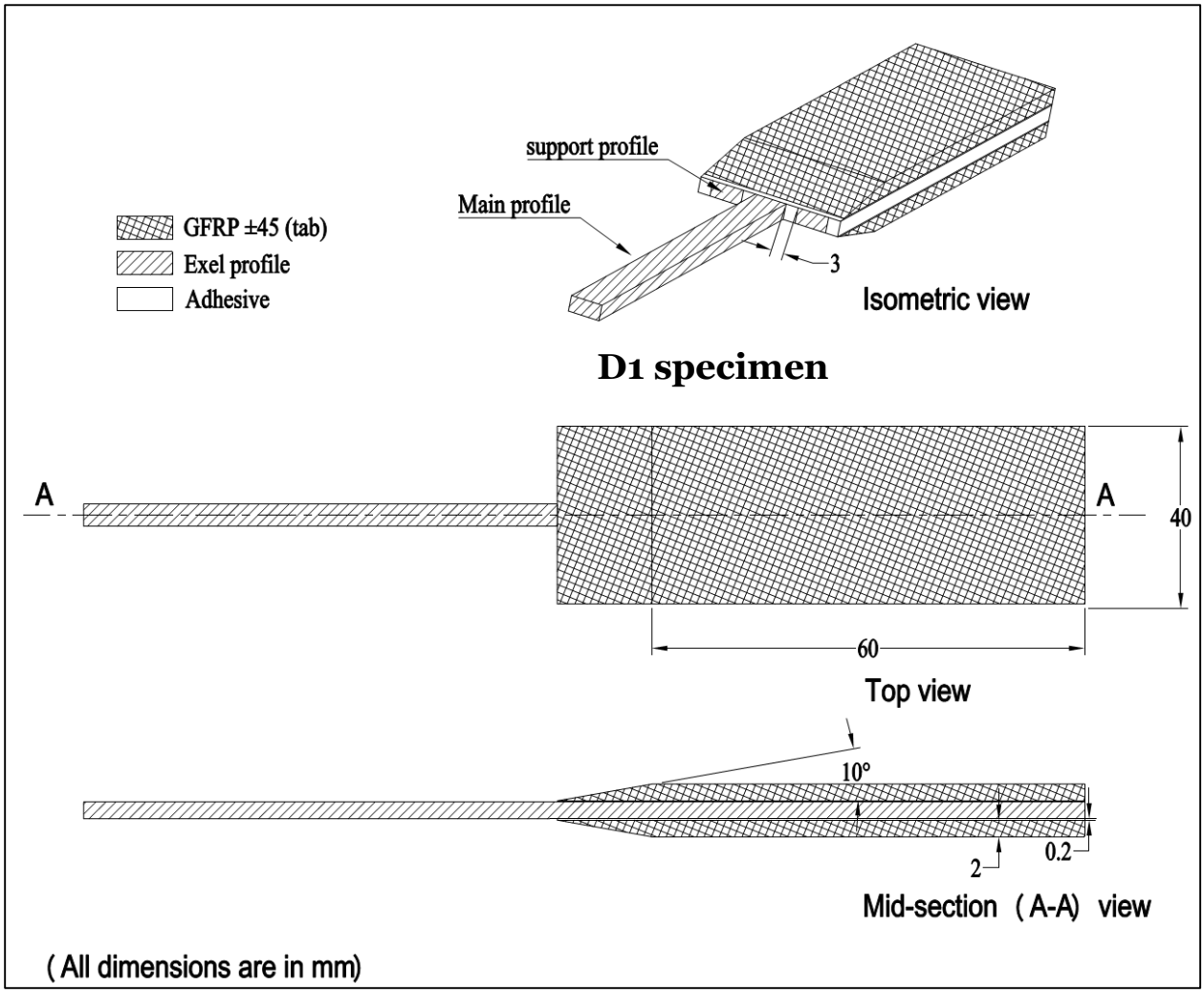

Figure 4.2 Half specimen displaying new specimen design D1 for the Exel profile

4.2 Design approach

D1 specimen design for the Exel profile is proposed based on many assumptions made for UD CFRP laminate, which may or may not be affecting the Exel profile in the similar fashion. Hence, The D1 specimen design meaning tabbing parameters (Figure 4.3), along with other tab extension and support profile needs to be evaluated.

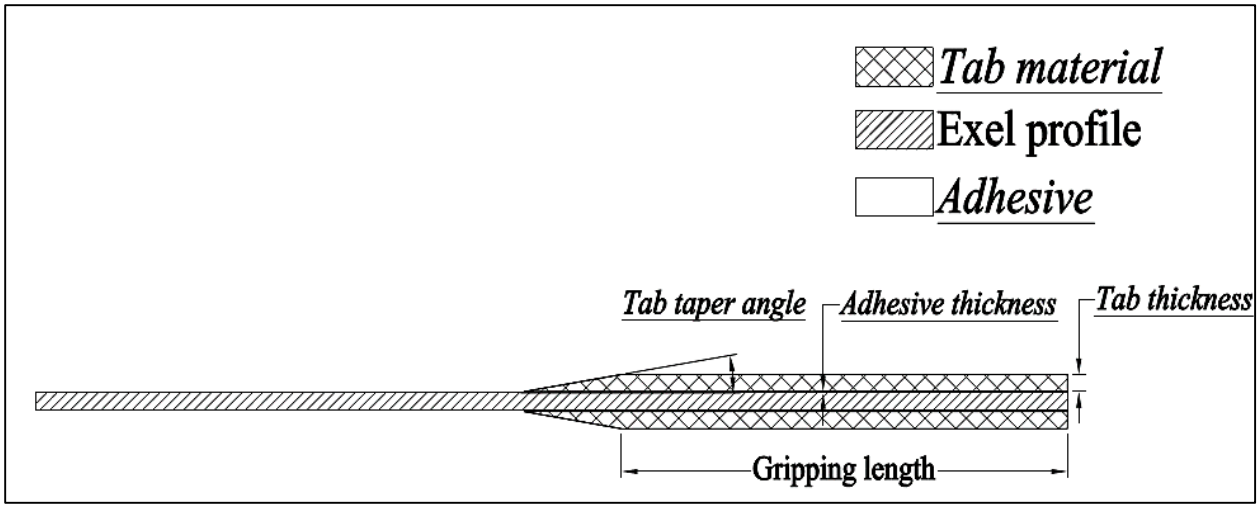

Figure 4.3 Critical mid-section parameters to finalise specimen design D1

To finalise these parameters, the major criterion is to lower the stress concentration occurring in the tab termination zone. To evaluate the stress concentration, a finite element model is created. By varying each of these parameters within the specified range with certain step sizes (Table 4.1), SCF for each step can be evaluated. Evaluated SCF is plotted against each parameter in graphs; the parameter value suggesting lower SCF with manufacturability is selected for the final specimen design.

Table 4.1 Critical parameters: initial value, range and step size

Tabbing and gripping parameter	**Initial parameter**	**Range of parameter**	**Step size**
Tab length	Controlled by testing machine grip length (60 mm)		
Tab thickness	2 mm	1 - 4 mm	0.5 mm
Tab taper angle (in degree)	10°	2°-14°, 30°-90°	2°, 15°
Tab material	GFRP ±45	Aluminium, GFRP (±45), GFRP UD	-
Adhesive thickness	0.2	0.2- 1.4	0.2
Adhesive material	Hysol 907	Hysol 907, 3M AF163-2K, film adhesive	-

The numerical analysis is carried out using Finite Element Method (FEM). In this thesis work, ABAQUS V 6.14 analysis software is used for finite element modelling and analysis. The FEA carried out in two stages: 1) A 2-dimensional (2D) FE model simulating mid-section of the specimen 2) A 3-dimensional FE model simulating 3D specimen.

4.3 2D Finite element model

2D FEA is carried out for tabbing and gripping parameters which are displayed in Table 4.1. The main objective of 2D analysis is to arrive at mid-section parameters for the specimen design D1. A 2D FE model of the specimen with the initial geometrical and material parameters for mid-section is created and is shown in Figure 4.4.

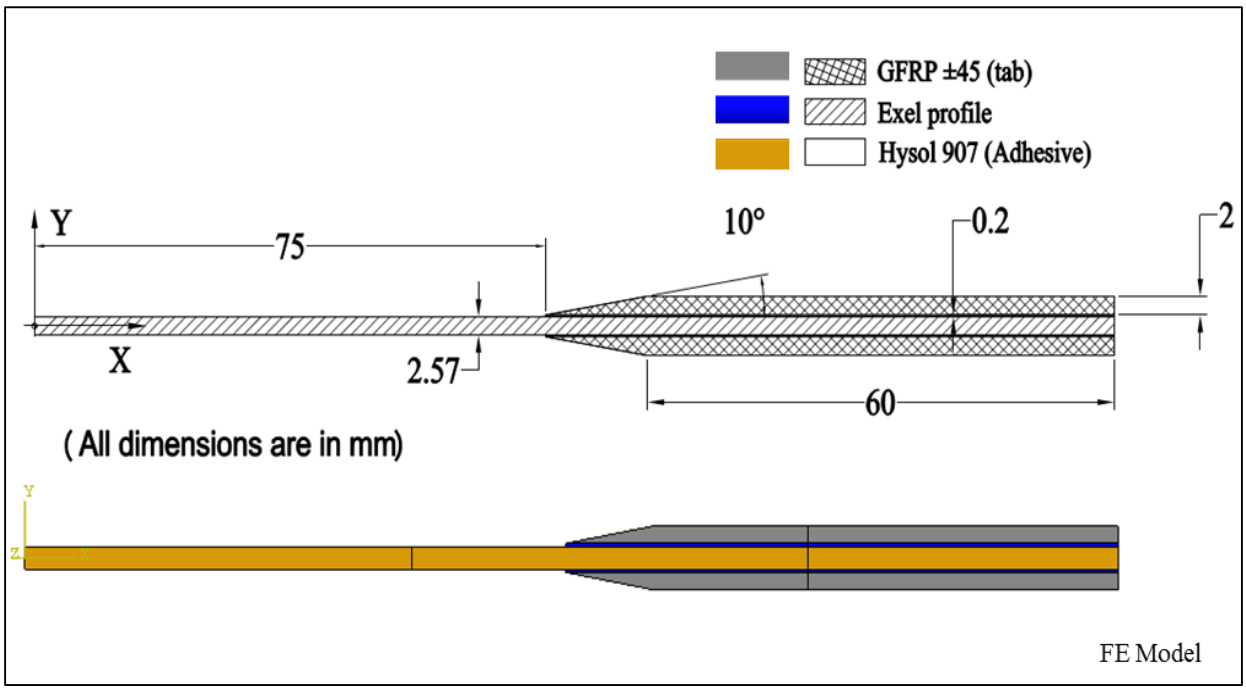

Figure 4.4 2D FE model, initial parameters i.e. dimensions and material

The range of material selection for tab and tab-adhesive are taken based on their prior use found in the literature for analytical or experimental evaluation (25, 29). The material properties utilised for FEA modelling is given in Table 4.2. UD CFRP, ±45 GFRP, and UD GFRP being anisotropic materials, the material property orientation for each of them is assigned as per the datum orientation is shown in Figure 4.4. The material properties for UD CFRP, ±45 GFRP, and UD GFRP are referred from a material database of ESAComp software, whereas, adhesive material property are taken from the respective material datasheet.

Table 4.2 Material Properties used for finite element modelling (38)

Property	**UD CFRP**	**±45 GFRP**	**UD GFRP**	**Aluminium(39)**	**Hysol 907**	**3M AF163-2K**
E (GPa)				70	1.6	1.1
v				0.3	0.31	0.34
E_x (GPa)	169	13.3	24.8			
E_y (GPa)	10	10	24.8			
E_z (GPa)	10	13.3	10			
v_{xy}	0.3	0.516	0.1			
v_{yz}	0.3	0.35	0.35			
v_{zx}	0.3	0.35	0.35			
G_{xy} (GPa)	5	11.3	4.4			
G_{yz} (GPa)	5	4	4			
G_{zx} (GPa)	5	4	4			

In order to simulate the mid-section plane, i.e., X-Y plane of the specimen, it is assumed that all loading and deformation are restricted to this plane and out-of-plane normal and shear strains are negligible. Hence, for modelling a plain strain element (CPE8R, i.e., 8-node quadratic, reduced integration element) is used. Evaluated stresses are very sensitivity to the mesh size, hence, to select a correct mesh size, the mesh is first evaluated for mesh sensitivity. Based on the mesh sensitivity study, a range of 0.1-0.3 mm arrives with a stress variance <=0.1%. Thus, the model is meshed (Figure 4.5) with 0.1 mm in TTZ zone (shown in zoomed view), as the stress in this area is of prime importance, and rest of the model is meshed with a coarse mesh of 0.5 mm.

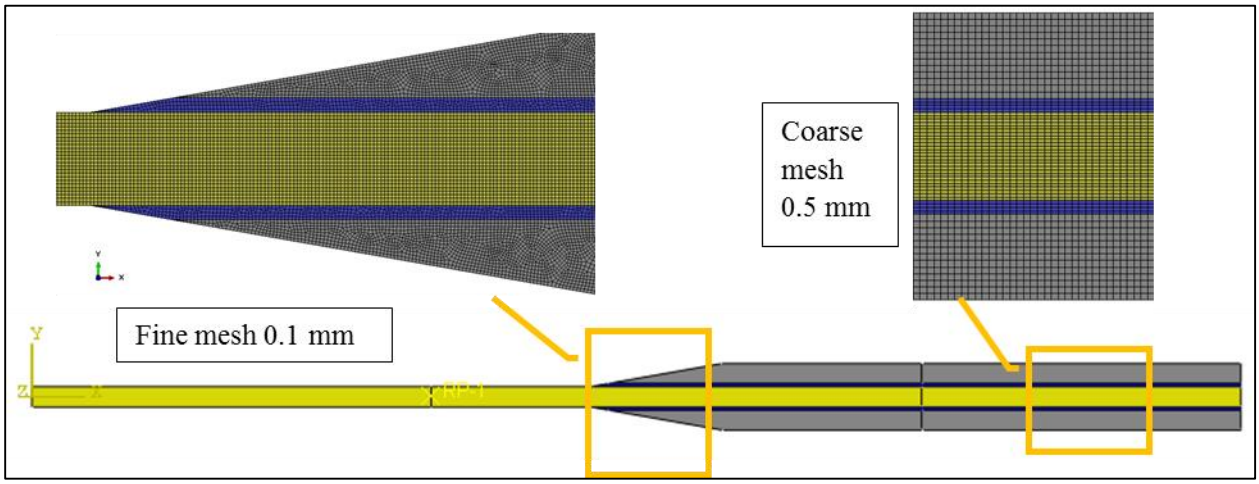

Figure 4.5 Meshed specimen: Fine mesh (0.1 mm) & coarse mesh (0.5 mm)

The specimen under tension loading in machine grips is shown in Figure 4.6. The specimen is held under machine grips by applying gripping pressure. To apply the load in the

direction X-axis, the machine grips on the right moves by Ux, while the machine grips on the left are kept stationary i.e. Ux =0.

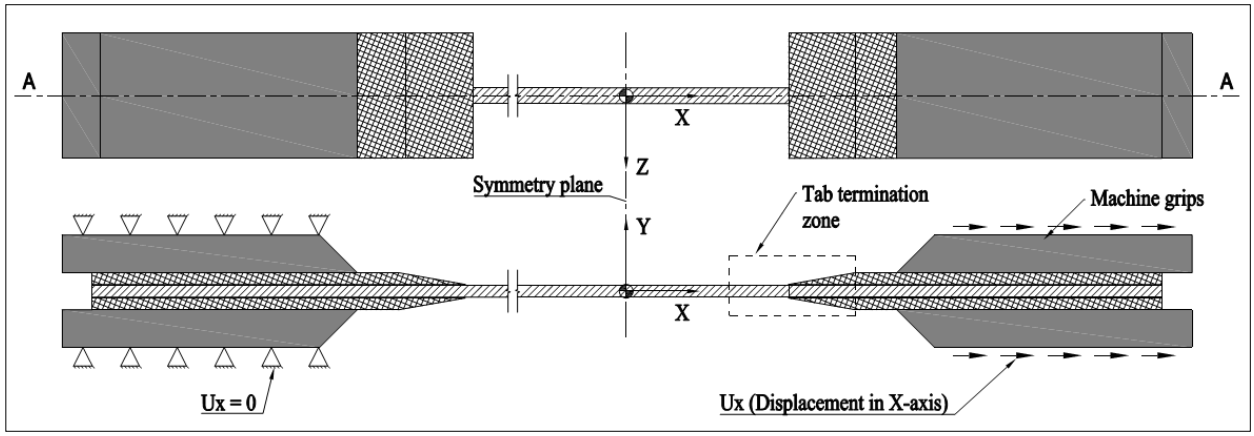

Figure 4.6 Specimen under tension loading in machine grips

This displacement induces elongation in the specimen, except at the symmetry plane (plane Y-Z). By utilising the symmetry of the specimen about Y-Z plane, only right half of the specimen is modelled, consequently reducing CPU runtime. Boundary conditions Ux =Uy =0 is provided at the symmetry planes to simulate no displacement (Figure 4.7). Gripping of tabs in test machine grip is simulated by applying gripping pressure of 50MPa. Tension loading in the specimen is simulated by providing displacement in the direction of X-axis (Ux) of 0.65 mm i.e. ≅ 1% strain in the specimen. The FE model with all the boundary conditions applied is also displayed.

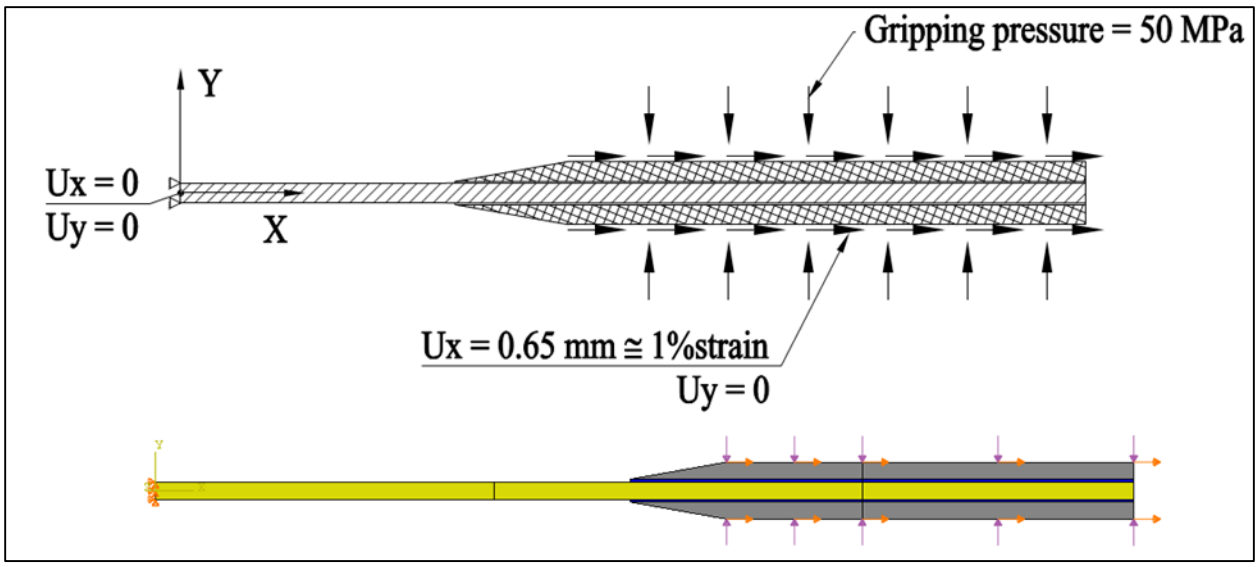

Figure 4.7 Boundary conditions for 2D FEA (material code similar to Figure 4.8)

After finalising the FE model, simulations were run for the 2D FE model. In this section, plots of evaluated SCF against the corresponding parameter are presented. The SCF has been evaluated in principle loading direction using the Equation 3.1. The stresses (X-axis principle stresses in

Exel profile) used for SCF calculations is picked from identified focus zone i.e. 10 mm on each side of the tab ending as shown in Figure 4.8.

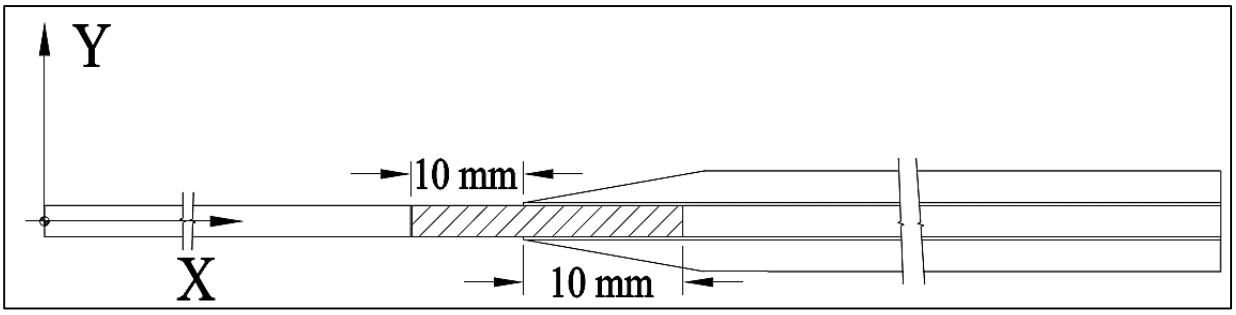

Figure 4.8 Focus zone for SCF evaluation

4.3.1 Tab thickness

The tab material should be compliant to get sufficient gripping from metallic grips and should have enough strength to transfer the load. The FEA simulation results are plotted (Figure 4.9) for different tab thickness for different tab materials (±45 GFRP, UD GFRP, and Aluminium). Each point in the graph indicates evaluated SCF for corresponding tab thickness. It is evident from the plot that the tab thickness inversely correlates to the SCF occurring in the specimen and does not seem to affect significantly after the thickness of 2.5 mm.

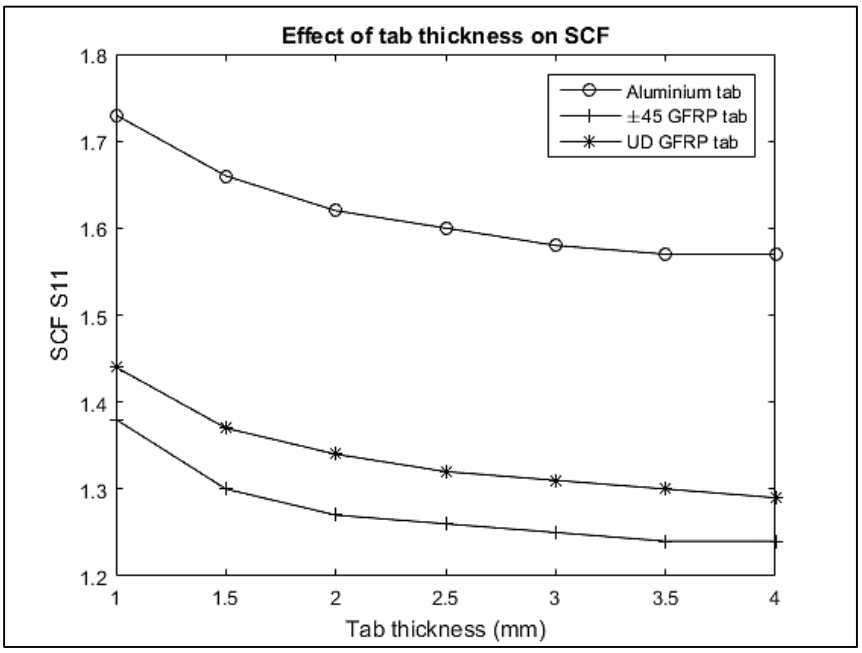

Figure 4.9 Effect of Tab thickness on SCF

4.3.2 Tab taper angle

Tab taper is provided for the smoother transition from the gage section to the tabbing area. Tab taper angle is the most sensitive parameter to SCF. The changes in tab taper angle are plotted against corresponding the SCF. The FEA simulation results are plotted (Figure 4.10) for different tab taper angle (2°-90°) for different tab materials (+/-45 GFRP, UD GFRP, and Aluminium). The minimal tab taper angle gives the least SCF, suggesting smoother transition. Although lower tab taper angle leads to very long unsupported tab (i.e. tapered tab area). in addition, The manufacturing of smaller tab angles than 10° are time-consuming and requires special zig. The tab angle is studied further detail in the 3D FEA section, for now, it is kept at 10°.

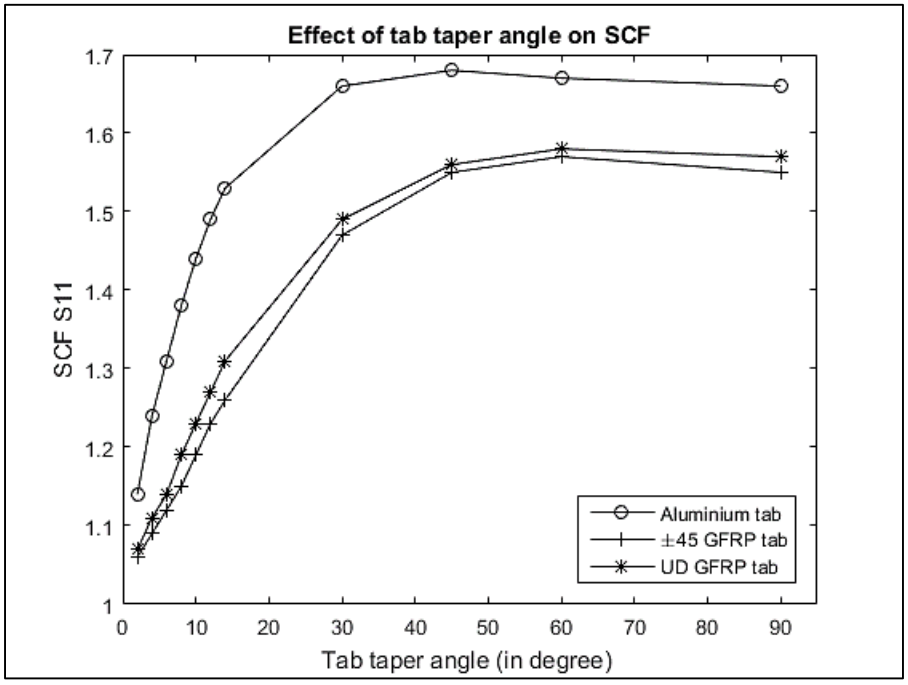

Figure 4.10 Effect of tab taper angle on SCF

4.3.3 Adhesive thickness

High adhesive thickness is providing softer tab adhesive interface whereas lower thickness provides higher strengths to the joints. Using Hysol adhesive, and three different type of tab material (±45 GFRP, UD GFRP, and Aluminium), the SCF results are plotted in Figure 4.11. The plot adhesive thickness against SCF in specimen suggests lower adhesive bond thickness gives lower SCF in the specimen. The trend in the result is contrary to the result achieved by Adams et al. (29) To understand the result better further analytical modelling with tapered adhesive boundary is presented in adhesive boundary discontinuity section later.

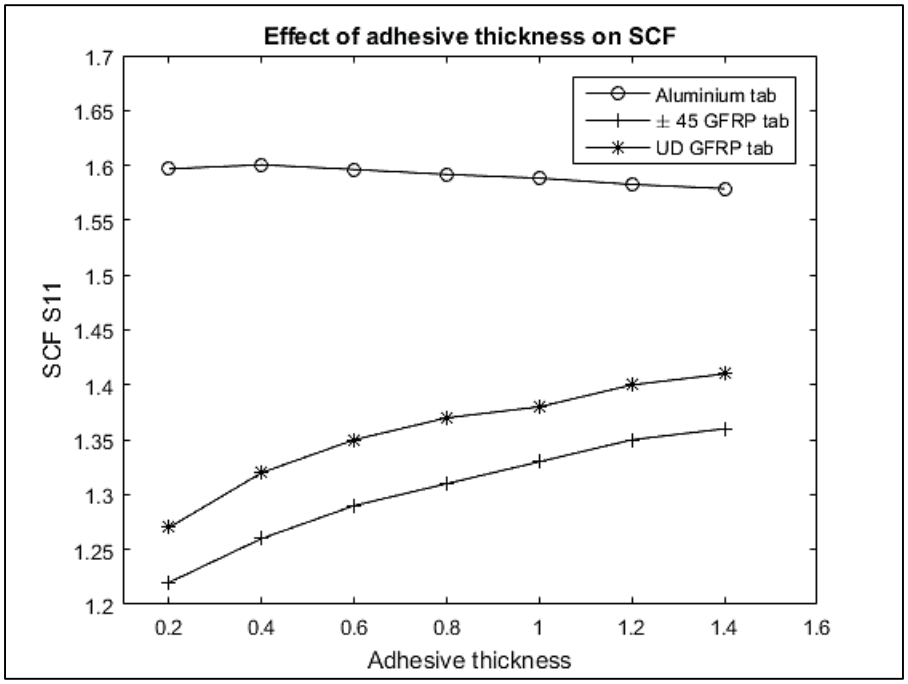

Figure 4.11 Effect of adhesive thickness on SCF

4.3.4 Effect of tab material

Tab material to be provided should be strong enough to transfer the load from the machine grips to the specimen. In addition, it should also provide a softer interface, thus resulting in lower stress concentration. Three different tab materials, i.e. ±45 GFRP (E_x =13.3 GPa), UD GFRP(E_x =24.8 GPa) and Aluminium(E_x =70 GPa); have been used for evaluating the effect of tab thickness, tab taper angle and adhesive thickness on SCF in the specimen (Figures 4.9, 4.10 and 4.11 respectively). All the plots indicate minimal SCF for ±45 GFRP material, due to comparatively lower E (Young's modulus). Hence ±45 GFRP laminate is selected as tab material for the final specimen.

4.3.5 Adhesive material

The adhesive material used mainly for bonding the tab to the profile. More compliant adhesive acts as a cushion for the gripping force. The effect of three different adhesive material, i.e., Film adhesive, E =2.5GPa; Hysol 907, E =1.6 GPa; and 3M AF163-2K, E =1.1 GPa; is plotted against evaluated SCF with ±45 GFRP tab (Figure 4.12). The plot suggests higher SCF for high adhesive modulus. Thus adhesive for testing would be an adhesive with lower modulus and superior fatigue property. Recent findings from Korkiakoski et al (40) suggests that the 3M DP190 adhesive (E=0.8 GPa) performed well under tension-tension fatigue for UD GFRP. Hence, considering the lower modulus and successful use as tab adhesive under tension-tension fatigue, 3M DP190 is selected.

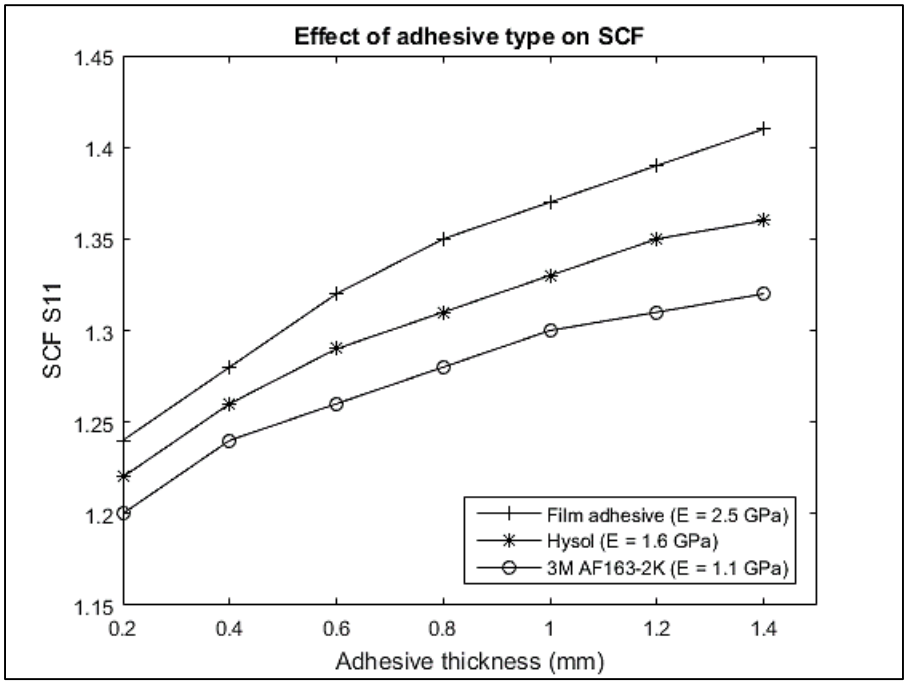

Figure 4.12 Effect of tab adhesive material on SCF

4.3.6 Effect of adhesive boundary discontinuity

The anomaly in the adhesive thickness vs SCF trend can be seen by comparing Figure 4.11 and Figure 3.10. In order to understand the anomaly in the trend for the adhesive thickness at the TTZ, new 2D FE model with tapered adhesive boundary is modelled. To make a one-to-one comparison all other tabbing parameters are kept constant. The plots before deformation for the vertical adhesive boundary (a) and tapered adhesive boundary (b) is presented in the Figure 4.13.

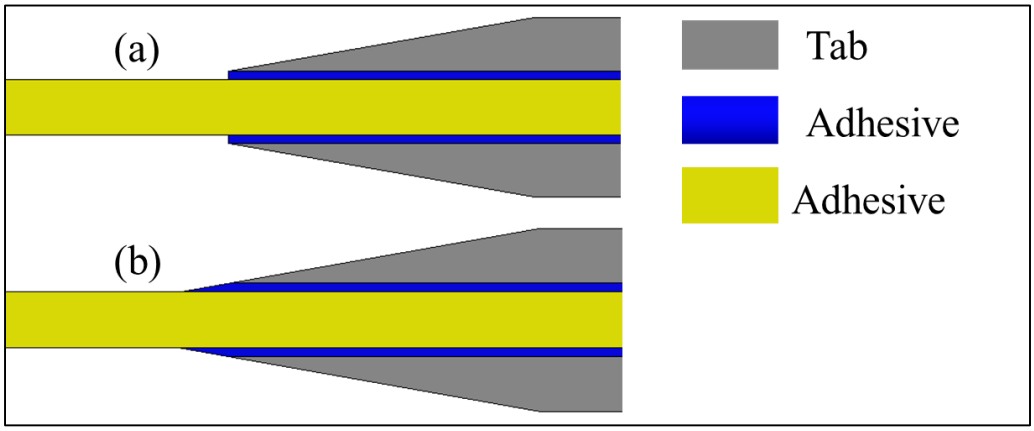

Figure 4.13 a) Vertical adhesive boundary; b) Tapered adhesive boundary.

As the loads are applied, Ux displacement plot for both the boundary condition (a & b) is plotted in Figure 4.14. The vertical ending for the adhesive causes higher peel off deformation at TTZ (b), whereas tapered adhesive boundary shows negligible peel off deformation (a).

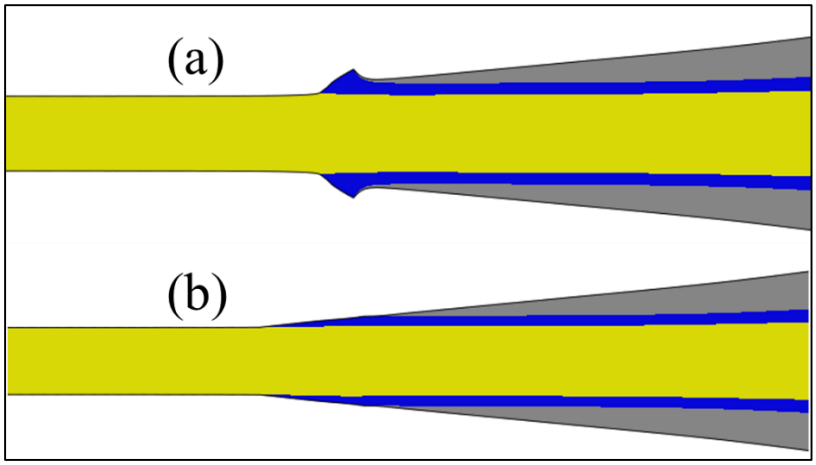

Figure 4.14 Ux deformation plot (deformation scale 50x) for the vertical (a) and tapered (b) adhesive boundary

The effect of adhesive thickness is re-evaluated for the tapered adhesive tip (a) of the specimen using Hysol adhesive, and ±45 GFRP tab. The SCF results for different adhesive thickness are plotted in Figure 4.15. The plot indicates increasing adhesive thickness from 0.4 to 0.8 mm marginal reduction of SCF by 1%. Thus, 0.4 mm adhesive thickness is selected for the final design.

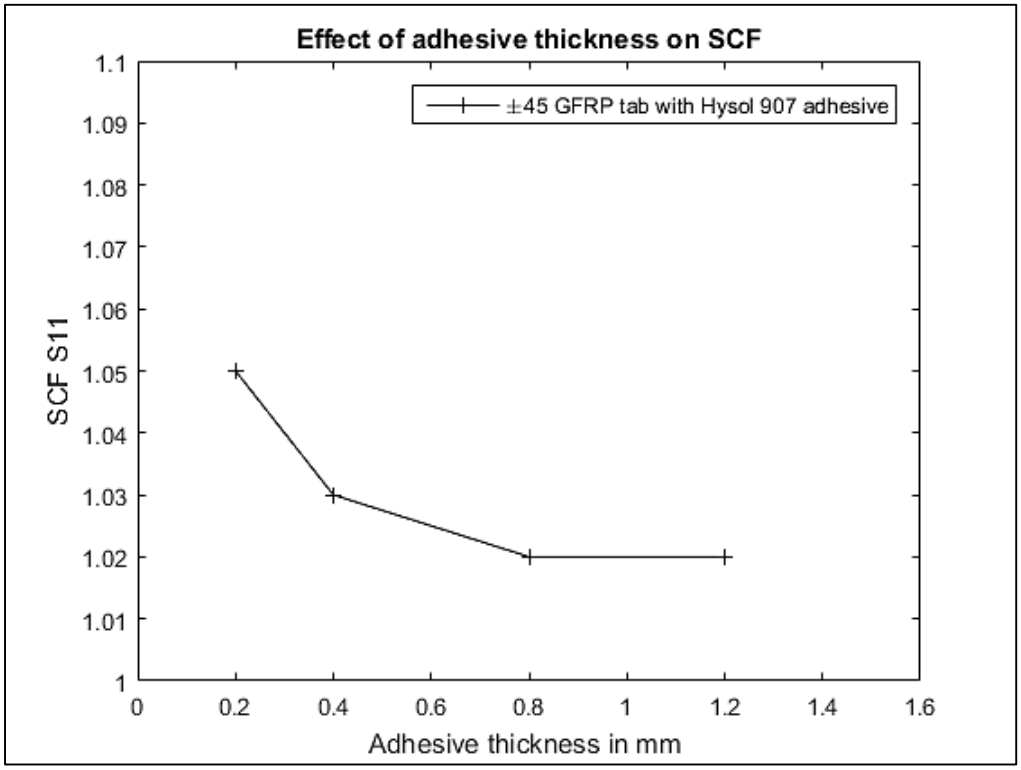

Figure 4.15 Effect of adhesive thickness (tapered end adhesive)

To see the effect of the tapered adhesive boundary on the SCF on the tab taper angle and tab thickness are re-evaluated using ±45 GFRP Tab (figure 4.16). The plots indicate lower SCF value compared to vertical adhesive boundary because the tapered adhesive boundary results in a

smoother transition. However, the evaluated trends remain similar leaving finalised parameters for tab taper angle and tab thickness unchanged.

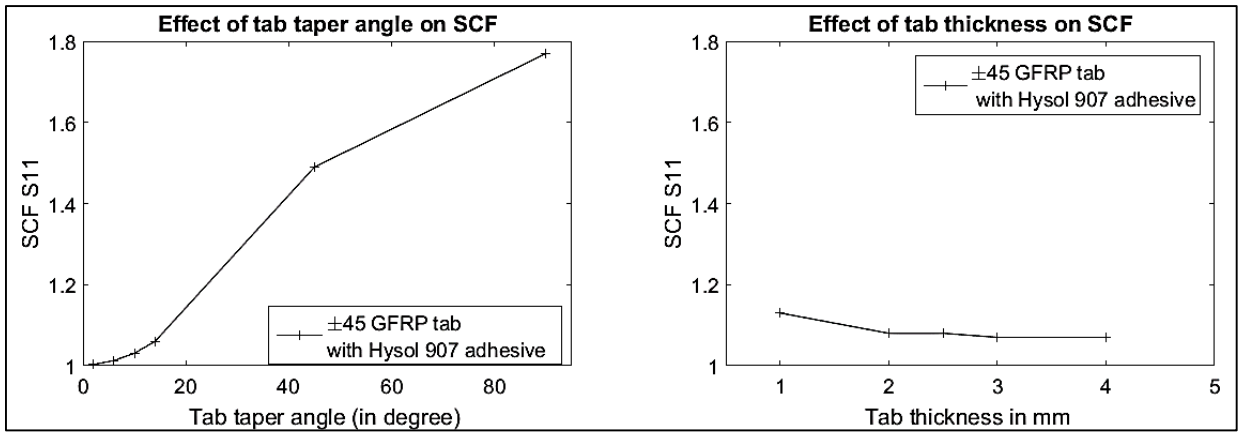

Figure 4.16 Effect of tab taper angle (left) and tab thickness (right) for tapered adhesive boundary

4.3.7 Testing different TTZ front

The smoother transition in TTZ (Tab termination Zone) is usually achieved by choosing optimal aforementioned parameters. Despite not being a parameter the tab termination shape of the specimen is a configurational choice that affects the SCF significantly (26). Based on the literature studies and subject know how three different TTZ front are selected for evaluation. The specimen configuration chosen for 2D FE modelling are presented in Table 4.3.

The configuration (a) represent the typical specimen configuration for UD CFRP laminate testing. The configuration (b) was first suggested by Portnov et al.(26) (Table 3.7) and is claimed to be the configuration with least SCF to author's knowledge. The configuration (c) is a variation of (b) and was analysed for gaining more understanding the effect of the adhesive front on SCF of the specimen.

The FEA model for (a) has already optimised for achieving minimal SCF of 1.031. The FE modelling parameters for (b) and (c) are kept almost similar except for tab taper angle. The tab taper for (b) and (c) are kept at 45° as suggested by Portnov et al.(26) The evaluated SCF for all three configurations is also shown in Table 4.3.

Table 4.3 SCF for different TTZ configuration

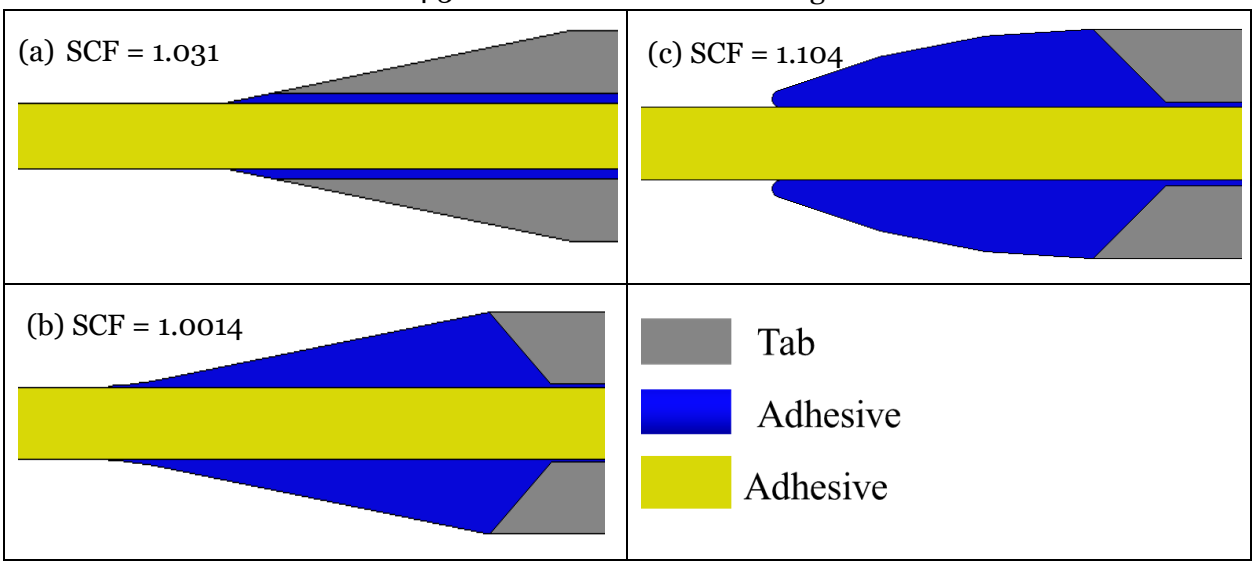

Based on the SCF evaluated for (a), (b) and (c), the configuration, b) has minimum stress concentration. Whereas (c) has highest SCF due to negative adhesive angle and (a) has an SCF slightly higher than (b). In an ideal condition, the failure or breakage should occur in the gage section. If configuration (b) is selected, then the failure is likely to happen inside the tabs due to higher stresses occurring inside the tabbing area (Figure 4.17). Additionally, the manufacturing of configuration (b) is difficult, as it requires a specialised mould to contain the adhesive during manufacturing. Compared to the configuration (b), configuration (a) has high stresses occurring just outside the tabbing area and is easier to manufacture. Hence, considering all considering the practicality of manufacturing and likely failure mode, configuration (a) is selected for further evaluation

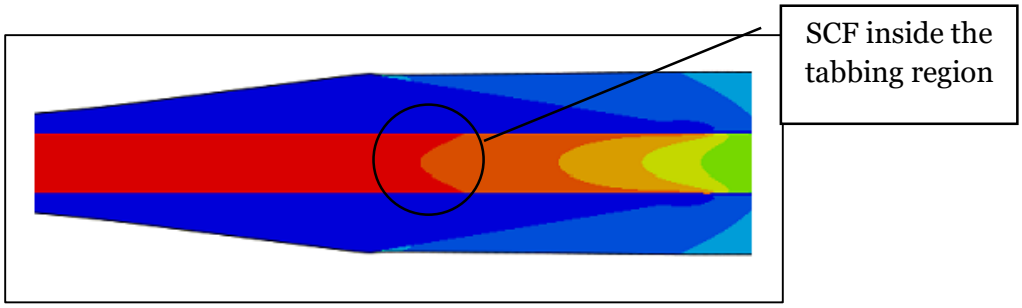

Figure 4.17 Stress plot σ_x for configuration b), highlighting point of stress concentration

4.3.8 2D FEA specimen configuration

Based on the finding from 2D FEA, finalised tabbing and gripping parameters are enlisted in Table 4.4. Compared to initial values from Table 4.1, there are two main changes in the tabbing and gripping parameters i.e. tab thickness is increased from 2 mm to 2.5 mm and the tab adhesive is changed to 3M DP190. The major finding from the 2D FEA was tapering adhesive tab tip to reduce stress concentration. After 2D FEA, the finalised mid-section parameters for D1 specimen design is shown in Figure 4.18.

Table 4.4 Tabbing and gripping parameters and SCF after 2D FEA

Tab thickness	2.5 mm
Tab taper angle(in degree)	10°
Tab material	GFRP ±45
Adhesive thickness	0.4
Adhesive material	3M DP190
SCF	1.033

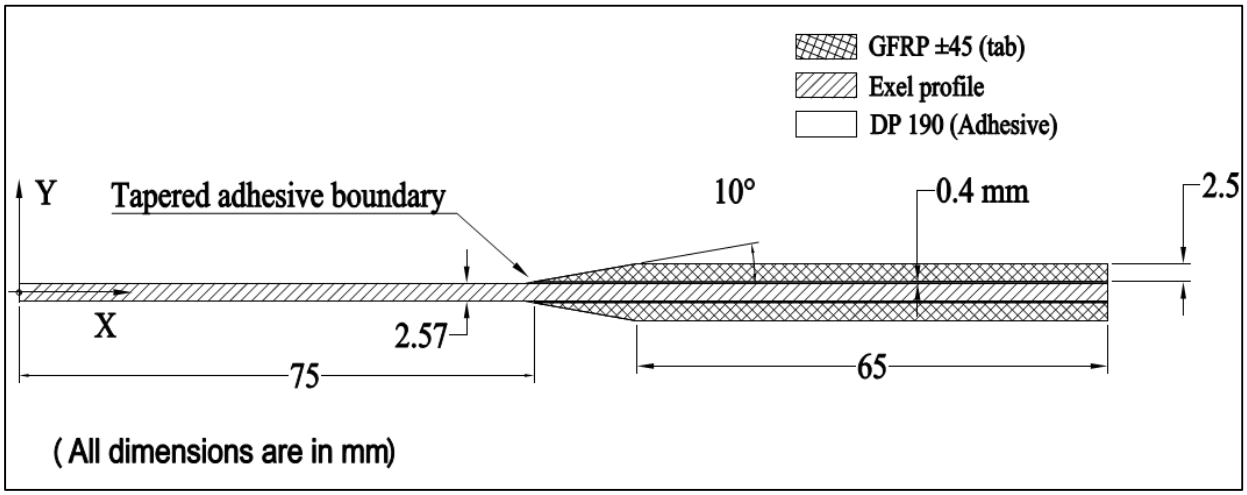

Figure 4.18 Mid-section parameters for D1 specimen design after 2D FEA

4.3.9 3D finite element model

Mid-section parameters for the Exel profile specimen design are concluded in the previous section. However, it is difficult to simulate the extended tab with support profiles in 2D FE modelling. Hence, a 3D finite element model of the specimen is created. First to maintain continuity of the results, a continuity 3D model replicating 2D FE model is created to finalise 3D modelling parameters. After confirming the continuity, a 3D model of the D1 specimen will be created and analysed.

3D FE model is an extension of 2D FE model carried out in the previous section. Thus, an initial 3D model with mid-section parameters from Table 4.4 is created. To simulate the thickness of the specimen, The continuity 3D model is given a thickness of 5.1 mm (i.e. width of the Exel profile) (Figure 4.19).

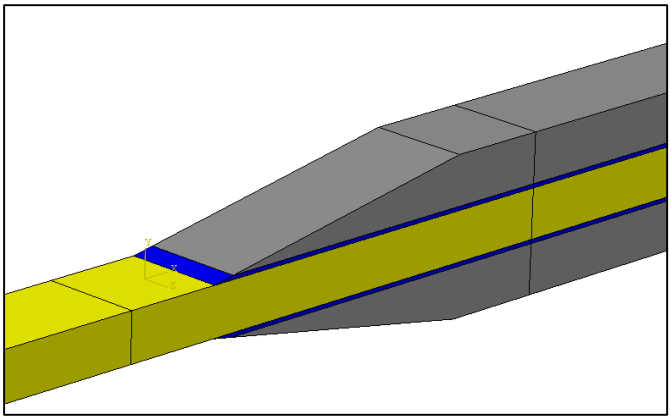

Figure 4.19 Continuity 3D model, extruded by 5.1 mm

This continuity 3D model is given with same boundary condition as for 2D counterpart. The model is meshed using 3D stress element (C3D8R, i.e., 8 nodes, a linear brick element with reduced integration) with mesh size 0.2 mm in TTZ and 0.5 mm elsewhere (Figure 4.20).

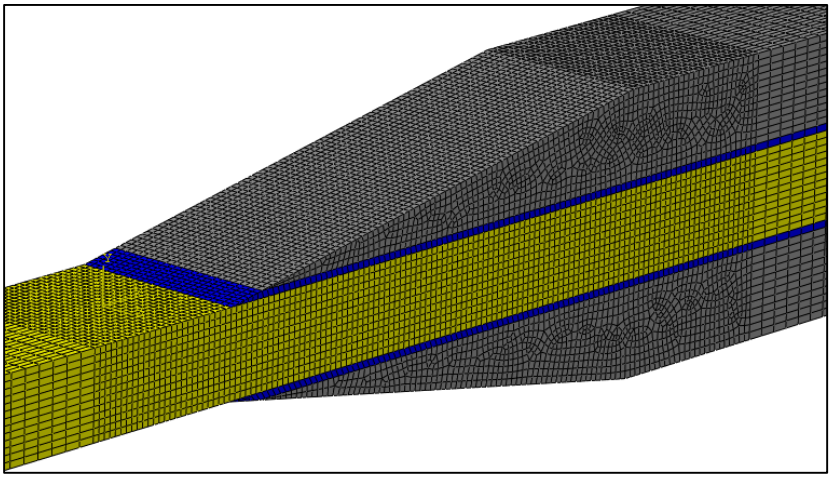

Figure 4.20 3D mesh with fine mesh (0.2 mm) in TTZ and coarse mesh (0.5 mm) elsewhere

The SCF of 1.044 is evaluated for the 3D model, which is close to 1.031 SCF evaluated for 2D FEA. The difference in the SCF can be attributed to two main factors. 1) Use of linear element within 3D FEA compared to a quadratic element in 2D FEA. 2) the coarser mesh (i.e., 0.2mm in 2D FEA) is used compared to finer mesh (i.e., 0.1 mm) for 2D FEA. A coarser mesh is used while meshing using 3D elements, to keep the CPU run-time and software licence limitation.

The stress plot for principle stresses in X-direction (σ_x) for 3D model of main profile suggests negligible free edge effect in the 3D model (Figure 4.21). The free-edge effect is characterized by the concentrated occurrence of three-dimensional and singular stress fields at the free edges in the interfaces between two layers of composite laminates (41).

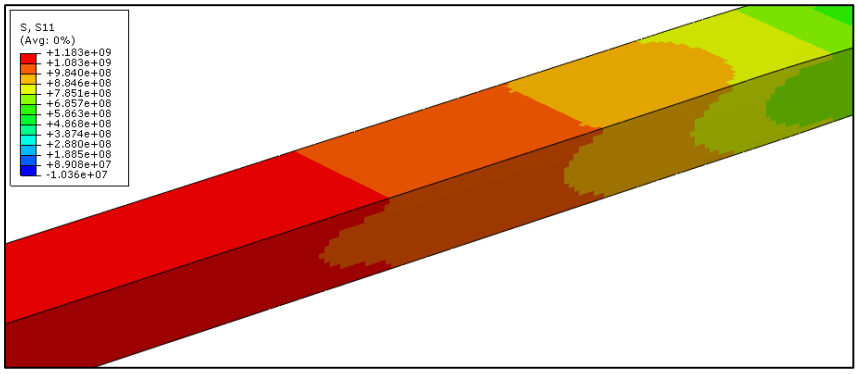

Figure 4.21 Stress distribution (σ_x) in Exel profile; constant stress along the width

4.3.10 3D FEA D1 specimen

Using similar modelling parameters as used in the continuity model i.e. material properties, meshing and boundary conditions, an FE model for the D1 specimen is created (Figure 4.22). After the simulation run, an SCF of 1.244 is evaluated. The higher SCF encountered due to the vertical adhesive on the sides of the specimen, creating a higher stress, as indicated by red colour in Figure 4.23.

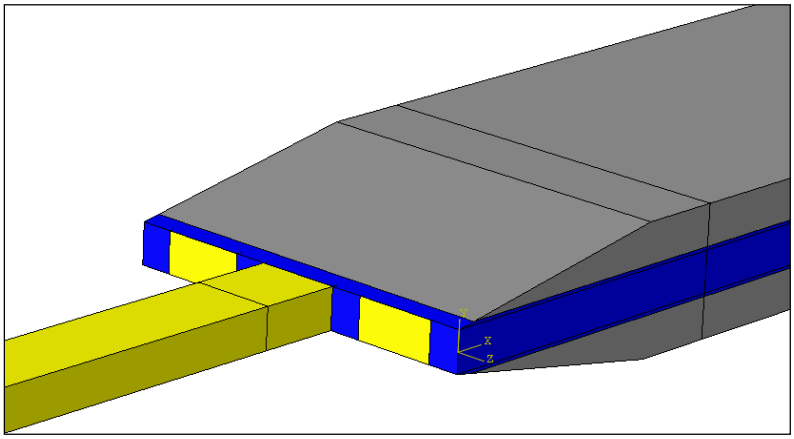

Figure 4.22 3D FE model of D1 specimen configuration

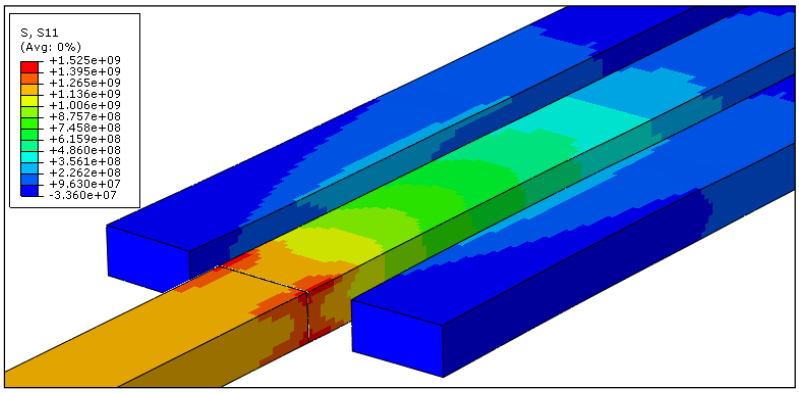

Figure 4.23 3D FE stress plot (σ_x) of D1 specimen configuration

4.3.11 3D FEA alternative D2 specimen

In order to reduce the higher stresses occurring at the side edge of the specimen, a second taper is provided. To differentiate between different tapers, new terminologies of the planar angle and the side angle are suggested as shown Figure 4.24. The earlier called tab taper angle is now Side angle and the planar angle is the tapering that needs to be provided to reduce the above-indicated stress jump.

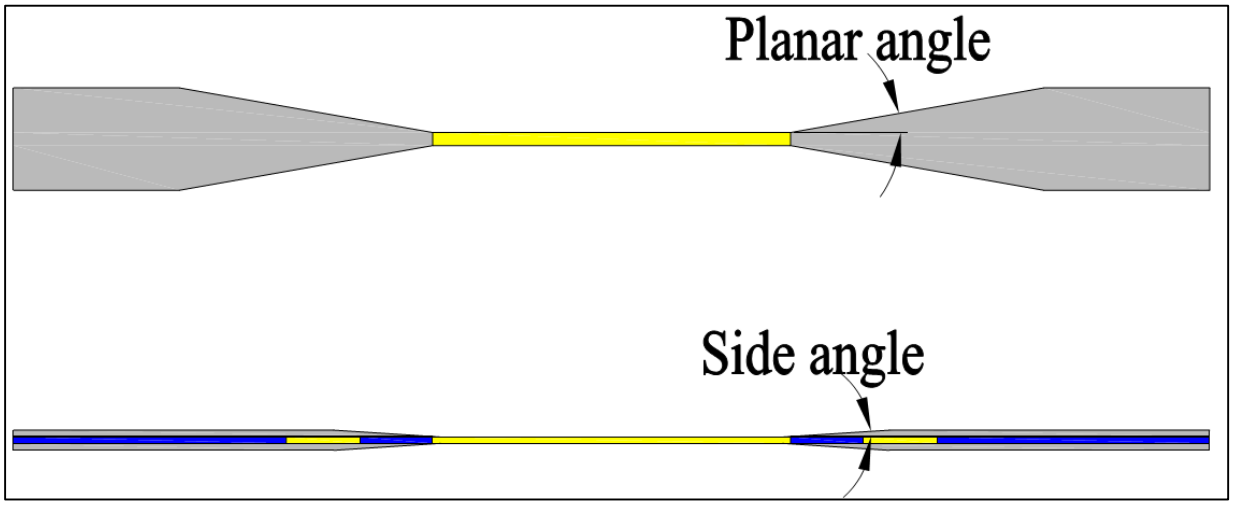

Figure 4.24 Specimen terminology for new taper angles

Four new configurations (a, b, c and d) with a variation of planar angle and side angle (a & b) along with some novel configurations (c & d) are suggested in Table 4.5. Configuration (a) is created by providing the planar angle 10°, side angle 3.7°. Whereas configuration (b) is created with same planar angle 10° but with different side angle of 1.6°. Some novel configuration for TTZ as proposed during 2D FEA are also included. In these configurations, (c) is created by providing the planar radius of 1.4 metres, side angle 3.7° simulating a dog-bone shape of the specimen. Next configuration originates from the idea of a round tab which can enclose the profile. Configuration (d) is created by providing round tab with the conical taper of 10° in the front and in addition, an adhesive front to ease the stress concentration is provided.

Table 4.5 3D FE model for D2 specimen configurations

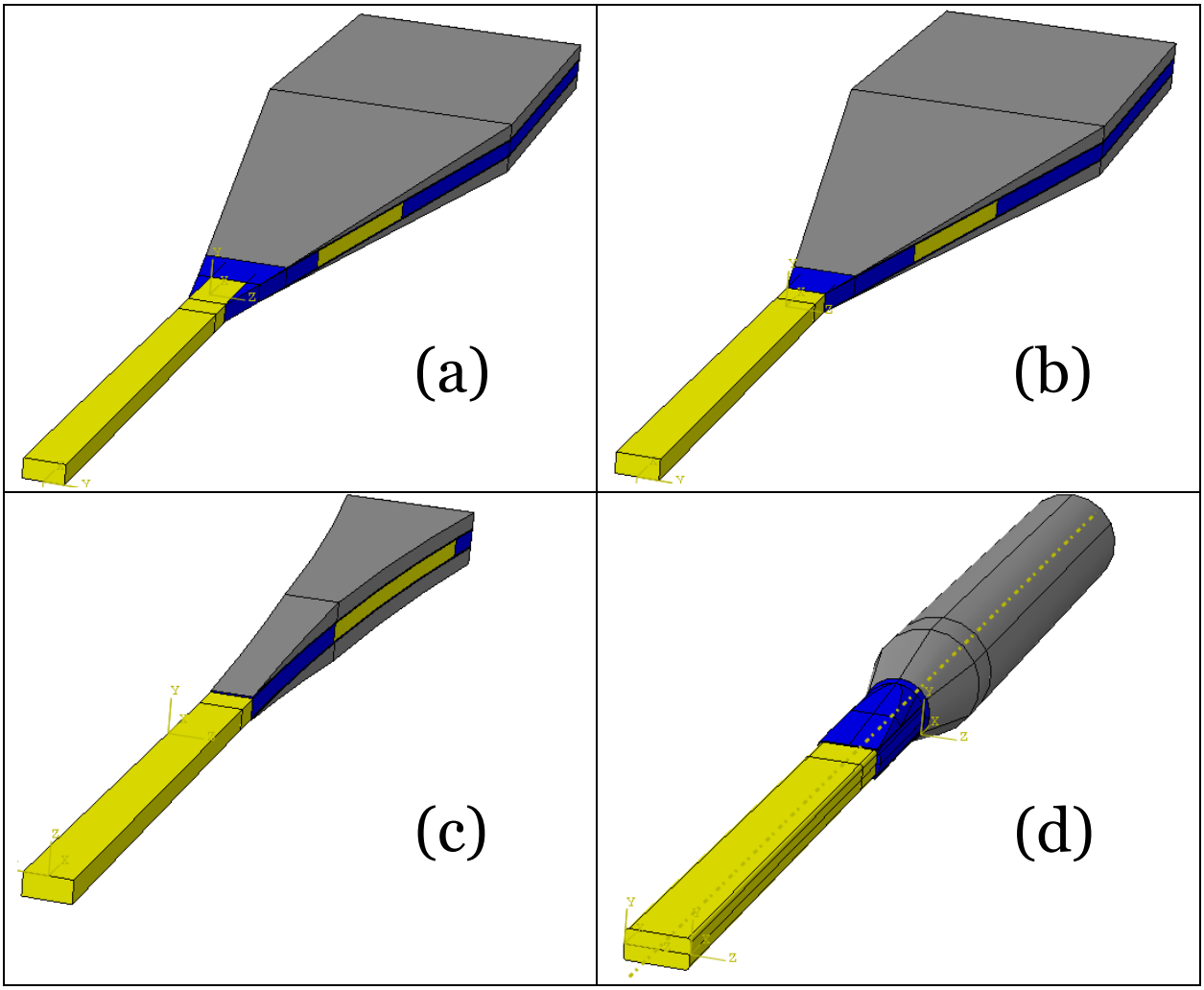

The SCF evaluated for above mentioned configuration is presented in Table 4.6. The results suggest that configuration (b) provides the minimal SCF of 1.02. Thus, configuration (b) is selected for further evaluation.

Table 4.6 3D FE stress distribution (σ_x) for Exel profile in respective specimen configurations

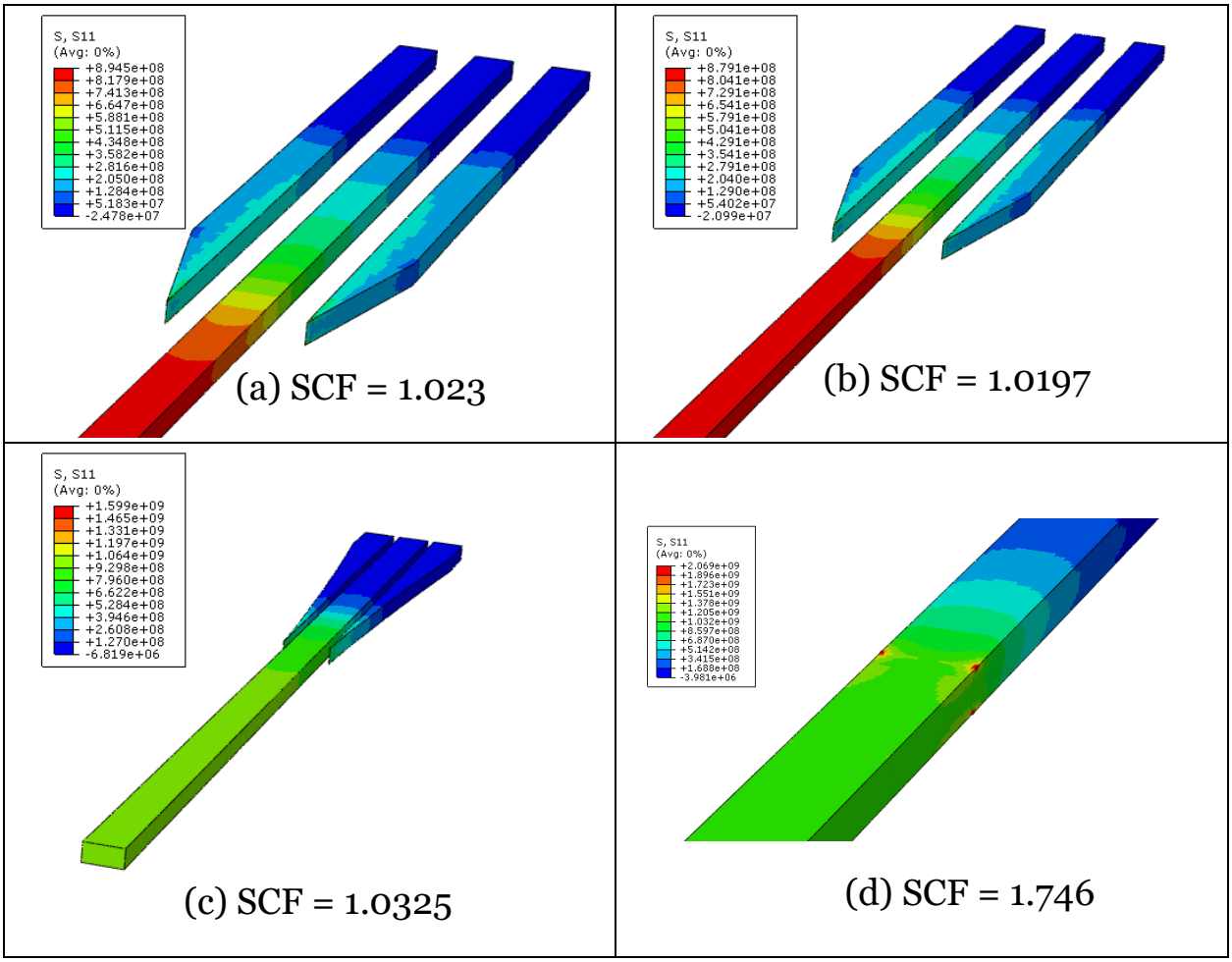

4.3.12 Spacing of support profile

The gap between the support profile and the main profile was chosen to be 3 mm randomly and need to be re-evaluated for its effect on SCF. Configuration (b) is taken and the gap between the profiles was varied to 1, 3 and 5 mm and SCF evaluated are 1.019719, 1.019715 and 1.019706. The effect of support profile spacing is negligible. Thus, considering the support profile would be able to support the tab well with higher spacing, hence, a spacing of 5mm gap is taken for the final configuration.

4.4 Final D2 specimen configuration

Based on 3D FEA analysis, the finalised specimen configuration is shown in Figure 4.25 & 4.26. The specimen configuration has an adhesive front tapering from both the sides. The gage section length of the specimen is selected to be 100 mm. summary of the parameters for the final specimen configuration is given in Table 4.7.

Table 4.7 Final D2 specimen configuration

Feature	**Recommended value/property**
Tab length	65 mm
Tab material	GFRP (±45°)
Loading frequency	Selected to avoid heat rise above 26°
Tab thickness	2.5 mm
Side tab angle	1.6°
Planar tab angle	10°
Tab adhesive	3M DP 190, E =0.8 GPa
Tab adhesive thickness	0.4 mm
Tab cut-off thickness	smooth transition
Tab overhang	Planar taper of 1.6° moved the grips 60 mm from the tab edge, thus need not provided.
Specimen shape	Suggested design (shown in Figure 4.25 & 4.26)
Gage section Thickness	2.57 mm
Gage section Width	5.1 mm

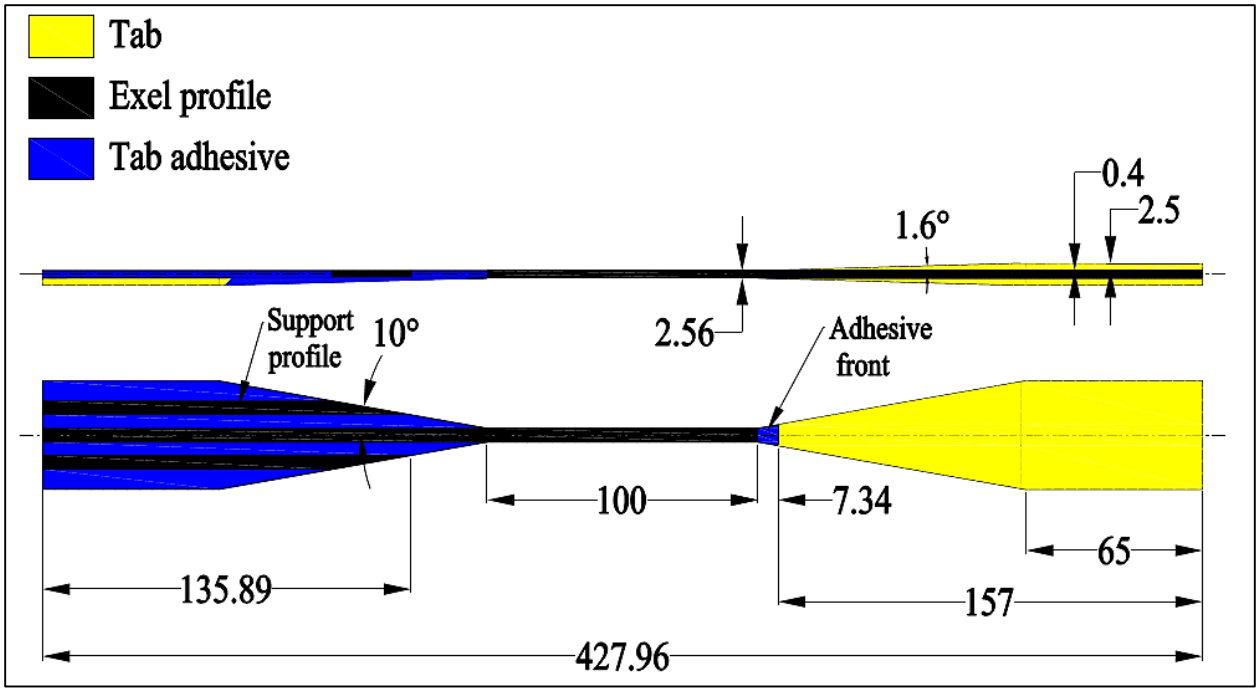

Figure 4.25 D2 specimen configuration (All dimensions in mm)

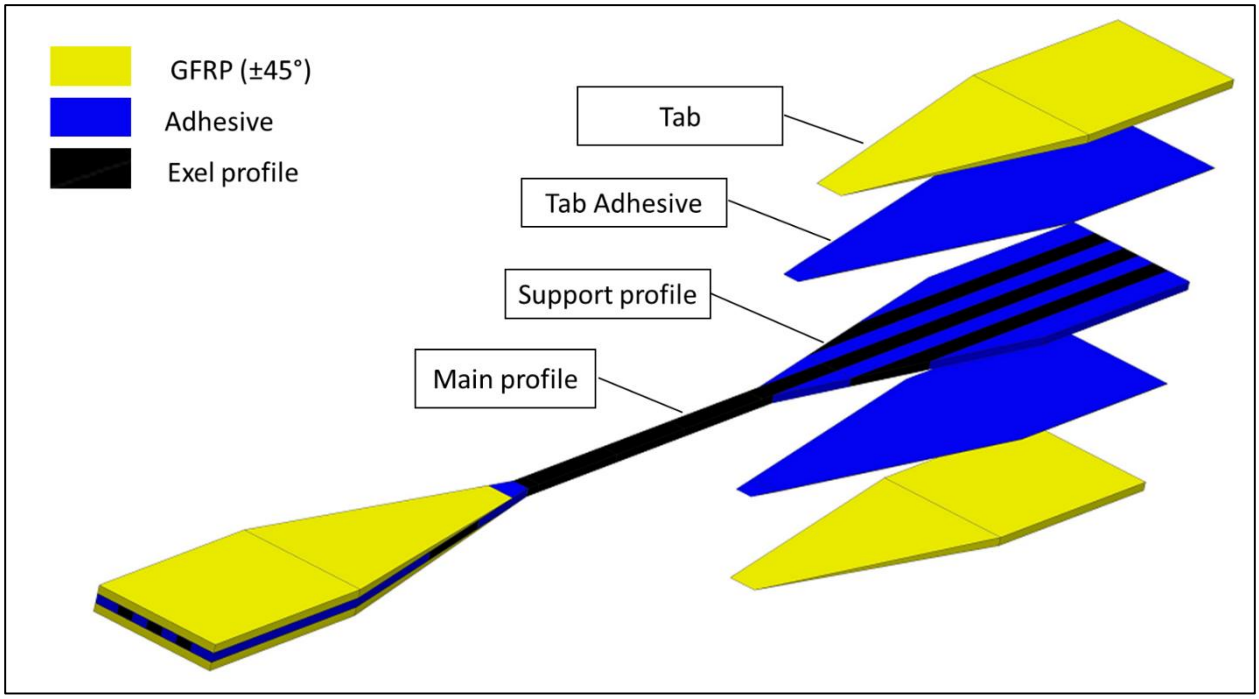

Figure 4.26 D2 specimen configuration (Exploded view)

5 Manufacturing

5.1 Manufacturing approach

The manufacturing process of the D2 specimen is divided into three main stages as shown in Figure 5.1

- *Component preparation and process planning:* Individual component of the specimen such as tab, Exel profile, and other tooling are prepared for bonding.
- *Assembly bonding and curing:* The prepared components are assembled using the designed tools and adhesive is applied, creating a bonded assembly. The assembly is then cured to harden the bond.
- *Machining and finishing:* Cured specimen are machined to form external features (i.e. planar and side taper angles) and final finishing of the specimen.

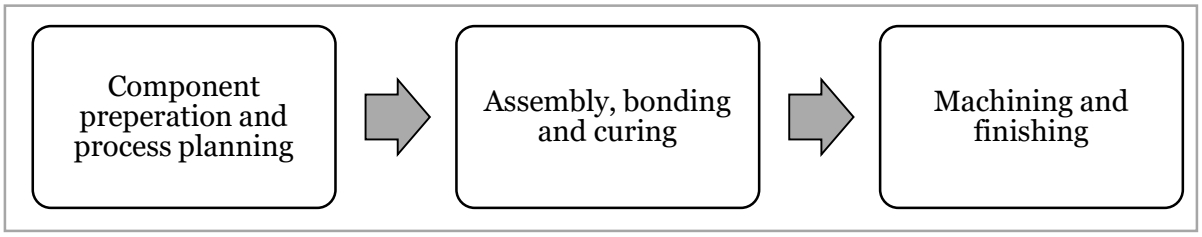

Figure 5.1 Manufacturing approach

5.2 Component preparation and process planning

5.2.1 Process planning and tool design

The specimen consists of a main Exel profile extending from one end to another end of the specimen. Using the same profile material, 4 support profiles, two at each end of the specimen is provided. Either side of these support profile is filled with adhesive. Four Tabs of GFRP (±45°) laminate, are provided on either side of the specimen and each of them is bonded with the thin tab adhesive layer. The specimen model is shown in the exploded view in Figure 4.26, highlighting its constituent materials and the inventory list for the D2 specimen component is enlisted in Table 5.1.

Table 5.1 Individual components and materials in D2 specimen

Feature	**Material**	**Quantity**
Main profile	Exel profile	1
Support profile	Exel profile	4
Tab	GFRP (±45°)	4
Adhesive	3M DP 190	Approx. 100 ml

In addition to the above-highlighted materials, the shape of the specimen is shown in Figure 5.2, highlighting critical dimensions. The total specimen length is 428 mm and is also equal to the length of the main profile. Support profiles and tabs have specific side taper angle of 10°, in addition to this, tabs are also provided with a planar taper of 1.6°. These tapers are extended beyond the tabs, to an adhesive front, smoothly merging into the main profile.

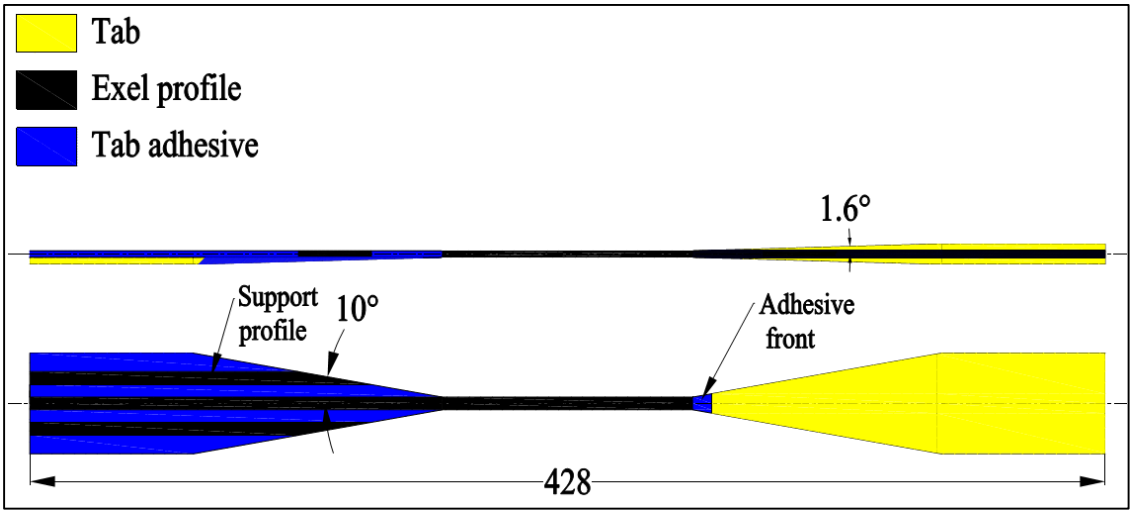

Figure 5.2 External geometrical feature to be machined later

For the ease of manufacturing, the tapers on the tabs and support profile are machined later, tooling and the machining process of the tapers are explained later in machining subchapter. This approach simplifies the geometry of the tabs and supports profiles to a rectangular shape (Figure 5.3).

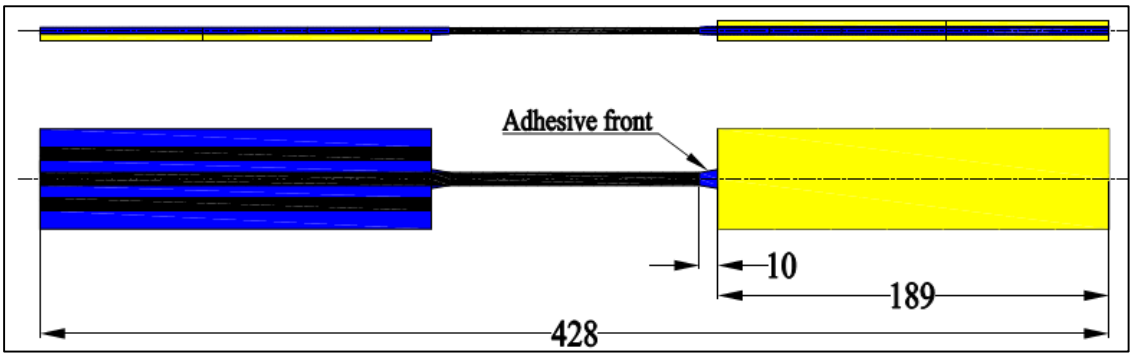

Figure 5.3 Simplified specimen geometry (without planar and side taper)

Despite the simplification, the precise placement of the main profile with respect to support profile and with tabs requires specific tooling while assembling. In addition to placement, the tooling should also incorporate the adhesive front shaped cavity for casting adhesive front taper.

Hence, three different tools are designed for profile placement and adhesive front casting for bonding the specimen; these tooling is here onwards referred to as bonding-fixture A, B and

C. Bonding-fixture A (Figure 5.4 left) ensures the specified gage length and provides alignment and support for Fixture-B.

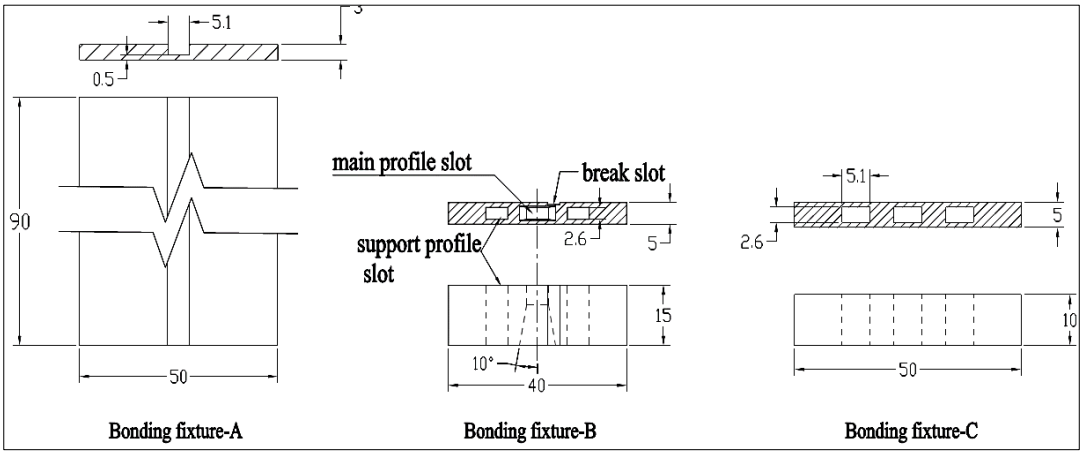

Figure 5.4 Bonding Fixture-A (left), Fixture-B (middle) and Fixture-C (right)

Bonding-fixture B (Figure 5.4 middle) is provided on either side of fixture-A and it incorporates 3 slots. Two support profile slots are provided for placement and 5 mm spacing of the support profile. In addition, the main profile slot incorporates a cavity for the adhesive front casting. The adhesive front cavity is provided with two tapering i.e. planar tapering of 10° and side tapering of 1.6° (not shown in the figure). Third tooling, Bonding-Fixture-C (Figure 5.4 right) is provided at either end of the specimen; Fixture-C is provided with three slots in a similar fashion as Fixture-B, i.e., a middle slot for main profile and side slots for support profiles ensuring the gap of 5 mm. Due to the inclusion of these fixtures, the length of the profile is increased by 10mm; thus for the single specimen assembly, required an inventory of components is mentioned in Table 5.2, where L &W are length and width, respectively.

Table 5.2 Inventory list for single specimen assembly components

Part	**Dimensions**	**Quantity**
Main profile (Exel profile)	L 448 mm	1
Support profile (Exel profile)	L 189 mm	4
Tab laminate (GFRP ±45°)	L189 × W 40 mm	4
Fixture-A	As per Figure 5.4	1
Fixture-B		2
Fixture-C		2

Assembly process of these components is planned in five major steps (a-e) as shown in Figure 5.5. Starting with the main profile of specific length (step a), Fixture-A is placed in the middle of the main profile (step b) securing the gage section in the profile. In the next step, 2 number of Fixture-B are inserted one from each side of the profile (step c) ensuring the cavity for the adhesive front on the correct side. Placement of Fixture-B provides 4 support profile slots available for positioning 4 support profile of specified length in those slots (step d). Following this, 2 number of Fixture-C are inserted, one from each side of the profile (step e), this provide continuity in the gap between the profiles.

After achieving the correct placement of the profiles and before placement of tabs, filling of the adhesive need to be planned. The adhesive filling process is planned in three steps (f-h) as shown in Figure 5.5. Two tab laminates of specific length and width are placed on one side at both ends of the profile assembly (f). Although in practice, a thin layer of adhesive is applied to tab before placement, the process is explained in bonding section later. In the next step (g), the adhesive is filled in the formed cavities between main and support profile and later on the sides. To avoid adhesive spill from the sides, in practice support walls with Teflon layer can be placed. In the final step (h), remaining 2 tabs are placed on either side. To ensure good bonding, pressure can be applied on both sides of the assembly compressing tabs.

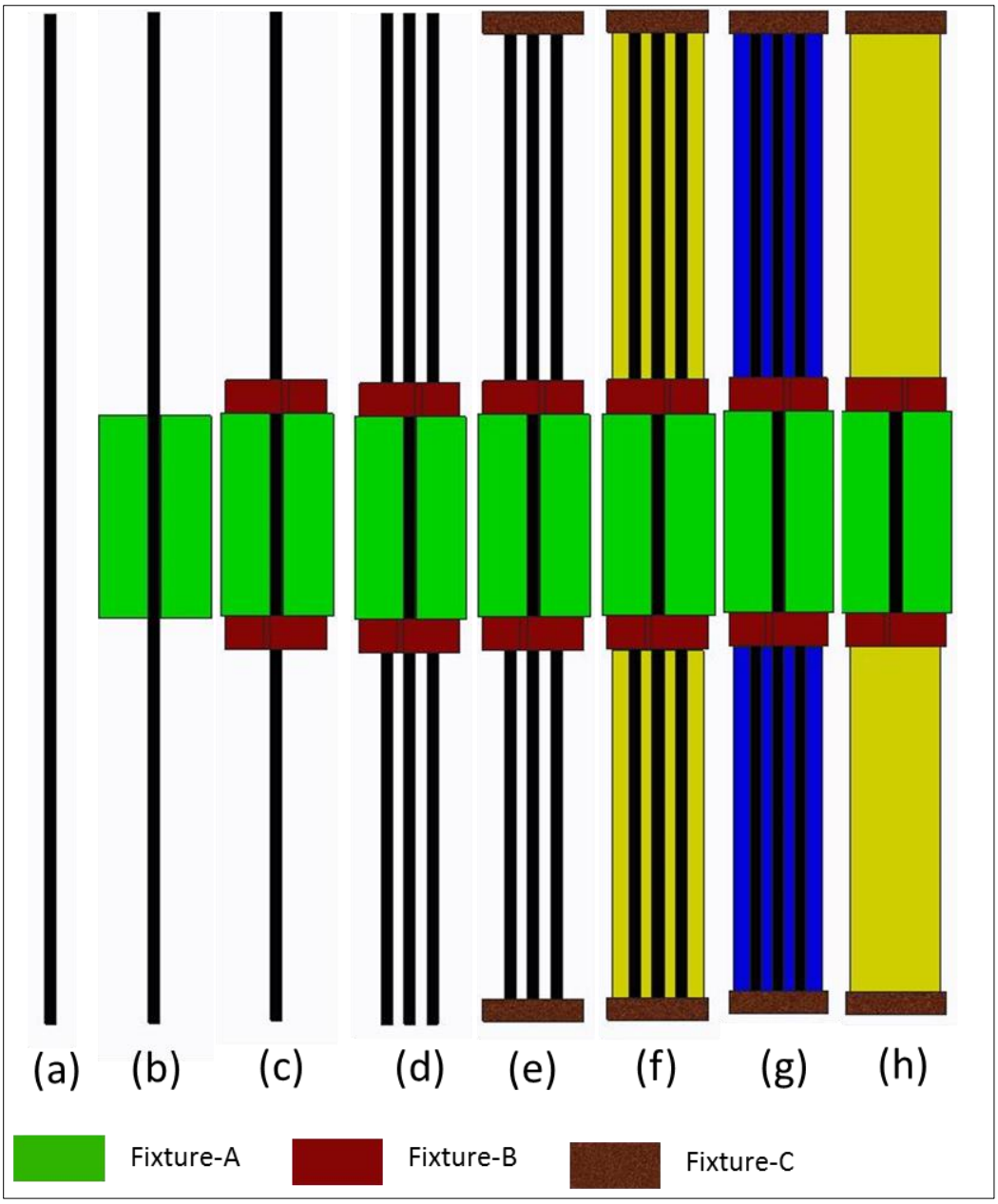

Figure 5.5 Assembly process design

In order to speed up the process, six specimens are processed at the same time. Primary task before beginning the process is to prepare required inventory for 6 specimens in Table 5.3. Preparation for each component is described in detail in following sub-sections

Table 5.3 Required inventory for assembly and bonding of 6 specimen

Entity	**Size**	**Quantity**
Tab laminate	300 X 189 mm	4
Main profile	L 448 mm	6
Support profile	L 189 mm	24
Adhesive	600 ml (approx.)	-
Scream cloth	300 X 189 mm(approx.)	4

5.2.2 Tab Laminate

The 2D woven GFRP tab laminate is manufactured using vacuum infusion method. In this method, layers of reinforcement in desired order is placed under a vacuum bag, then the binder resin is introduced into the bag on one end and a vacuum pressure is applied on the other end, thus forcing the resin through the reinforcement. This process infuses the resin into the reinforcement and is called as vacuum infusion.

First, reinforcement layer (i.e. Hexforce 1202uniform twill weave glass fibre) are cut in 900 × 900 mm sizes. To achieve a laminate close to desired thickness of 2.5 mm, 9 layers of the reinforcement is used. these layers are laid over on another forming a stack of 9 layers of in sequence of [0,90,0,90,0,90,0,90,0]. Consequently, a vacuum bag is applied around the formed stack while keeping passage for resin infusion and vacuum application. The stack is then infused with resin/hardener (i.e. Araldite/Aradur 5052 epoxy) by introducing the vacuum pressure of 0.5 bars.

For Room Temperature (RT) curing, the resin infused laminate is kept under vacuum pressure for 24 hours at room temperature. After RT curing, the vacuum bag is removed, and the laminate is post-cured at 50°C for 15 hours inside an oven. The cured laminate has a fibre orientation of (0/90), to get a ±45° orientation, required the size of the laminate is cut at 45° angle to the edge of laminate, resulting in GFRP ±45° laminate. The cutting of the laminate is accomplished using circular diamond coated blade in a table saw. Before bonding the tab, the bonding surface is roughened using Al_2O_3 grit blasted in the grit blasting chamber. After grit blasting the tabs are thoroughly cleaned with ethanol and is now ready for assembly and bonding procedure (Figure 5.6).

Figure 5.6 GFRP±45°-tab laminate

5.2.3 Main and support profile

Six main and twenty-four support profiles (Figure 5.7) are cut to specified sizes as per Table 5.3. The Exel profiles are flat and smooth, thus, it does not provide very good adhesion surface. Hence, the bonding area on the profile needs to be roughened, in a similar way as it is done for the tab. Support profiles are going to be bonded from all sides thus its entire surface needs to be roughened. However, the main profiles are only applied with adhesive only on the sides and the gage section needs to be kept as it is.

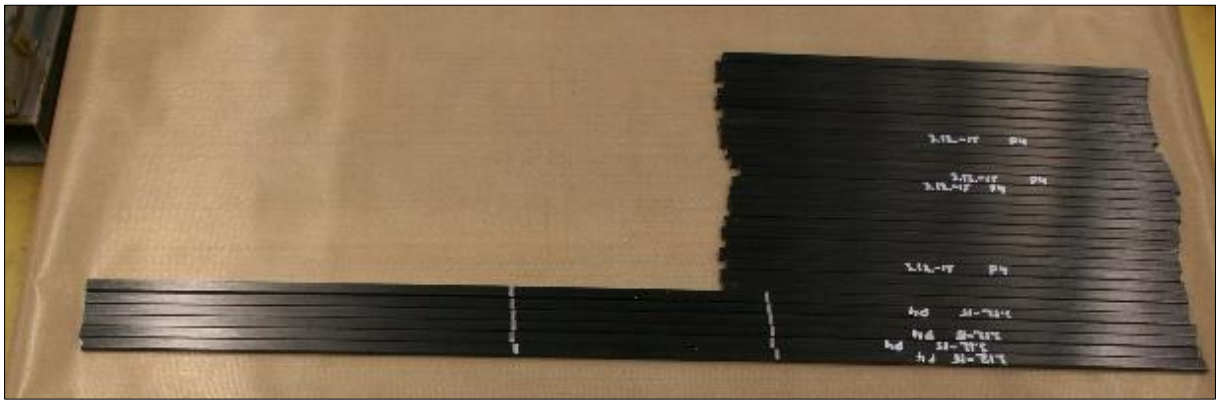

Figure 5.7 Main (6) and support (24) profiles

Therefore, the main profile is masked in the gage section using thick Aluminium tape (Figure 5.8). The grit blasting process is controlled by monitoring the colour of the Exel profile as it changes from dark black to grey during grit blasting. Caution to be taken to avoid excessive grit blasting as it might peel off the surface fibres.

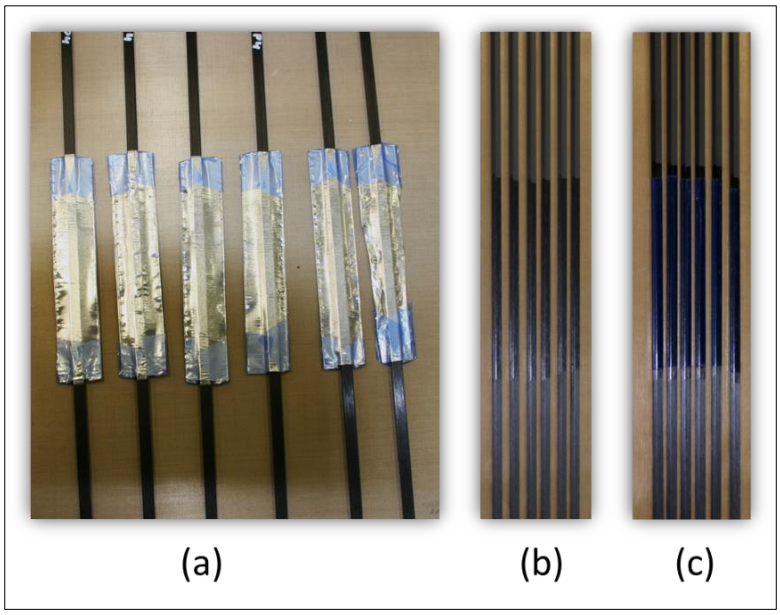

Figure 5.8 Main profile (a) Al tape Masked gage section (b) after grit blasting indicating colour difference from black to grey (c) Plastic tape for gage section protection during processing

After the blasting, the mask is removed and a plastic tape is applied to secure the gage section from any adhesive spill over. The blasted areas are cleaned using acetone and are now ready for bonding.

5.2.4 Fixture preparation

The bonding fixtures-A, B, and C are manufactured by Acrylonitrile Butadiene Styrene (ABS) material using plastic additive manufacturing (Figure 5.9). The additive manufacturing is carried out using Ultimaker 3D printer. The internal and external dimensions of the fixtures are corrected by 0.2 mm, for the 3D printer nozzle diameter of 0.4, to achieve accurate dimensions on printed parts.

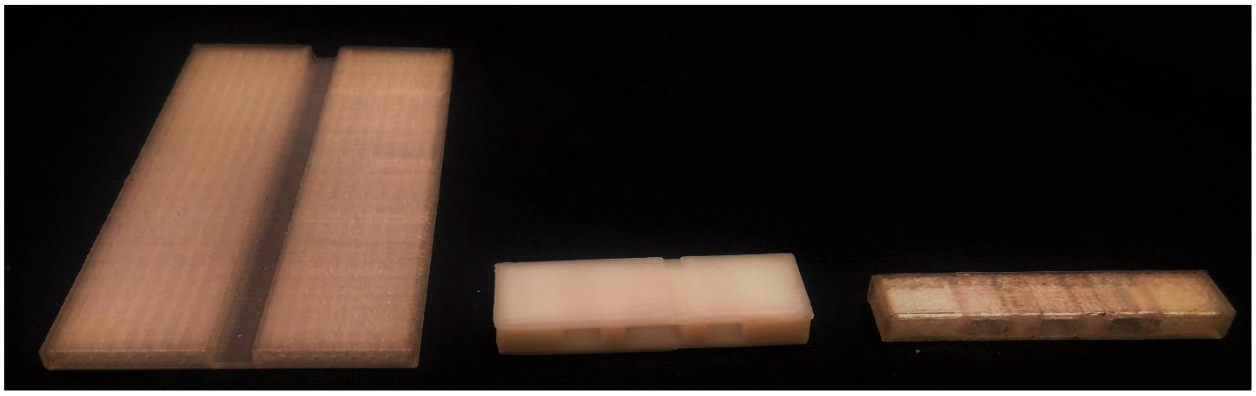

Figure 5.9 Fixture-A (left), Fixture-B (middle) and Fixture-C (right)

5.2.5 Adhesive

The bonding adhesive i.e. 3M Scotch-Weld Epoxy Adhesive DP190 Grey; is a two-part epoxy adhesive with 1:1 by volume mix ratio. The two-part adhesive is pushed using a hand-operated device through an adhesive mixing nozzle. The adhesive has a working life of 120 min. the recommended curing cycle for the adhesive is discussed in the curing process section later.

5.3 Assembly, bonding, and curing

5.3.1 Assembly

After preparing all the components, the process of assembly and bonding can begin. The process is accomplished on a rectangular aluminium flat plate of dimensions' length 1000× width 650 × thickness 10 mm; that is large enough to accommodate six specimen side by side. The plate is covered with non-stick Teflon film for easy removal of spilled adhesive. Before beginning the process, the processing surface, i.e. the Teflon film, is cleaned using acetone.

First, six Fixture-A are arranged side by side and gage section of the main profile are carefully placed inside A (b). Then twelve Fixture-B are inserted from both sides (c), facing the adhesive front cavity outwards. Then 24 support profiles are positioned as per process (d). Finally, 12 Fixture-C are placed at both ends (e). To keep all the aforementioned entities, in their place, thermal tape is applied. After reaching the process step (e) the assembly looks as shown in Figure 5.10.

Figure 5.10 Assembly of main and support profile with Fixture- A, B & C

5.3.2 Bonding

The bonding process begins with ensuring the placement of the all the profiles. Before placement of tabs (f), a thin layer adhesive is applied to the tab laminates on the roughened side. On adhesive applied tab a thin net cloth also known as scream cloth placed, to ensure a constant thickness between the profile and the tab. After making the tabs with scream cloth ready, the two tabs are placed on the bottom (f). Following this adhesive filling in the cavity is carried out (g). This process takes 60-90 min as the adhesive filling required 600 ml of adhesive. Considering the working life of the adhesive it is recommended to perform this step in a single go and within the stipulated time. After ensuring the adhesive fill level minimum to profile levels, additional two tabs with scream cloth are placed (Figure 5.11-left). After placement of these tabs, in order to consolidate the joint additional pressure is applied through clamps (Figure 5.11-right). To apply the pressure uniformly all over the tab, two 15 mm thick aluminium plates of similar dimensions as the tabs are used. A layer of Teflon is placed between these plates and the tabs for easy removal.

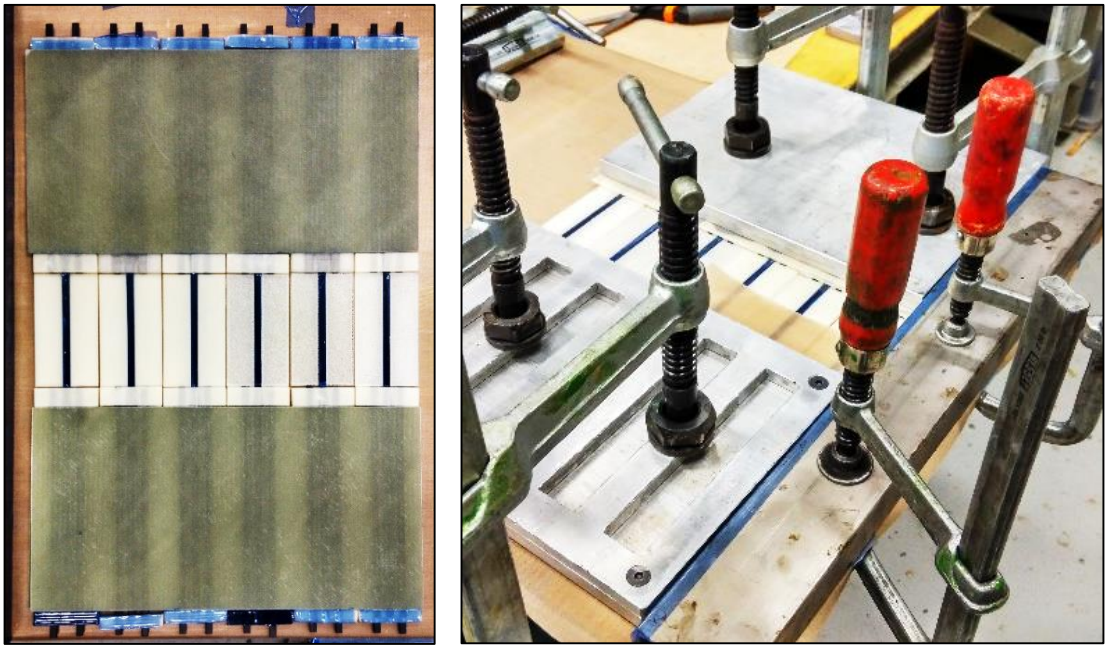

Figure 5.11 (left) Bonding of tabs to the assembly and (right) pressure application on the tabs with clamps

5.3.3 Curing

After ensuring proper application of pressure onto bonded area, the adhesive is left for curing. Curing is toughening or hardening by cross-linking of the adhesive polymer. Curing cycle opted for 3M DP190 is shown in Figure 5.12.

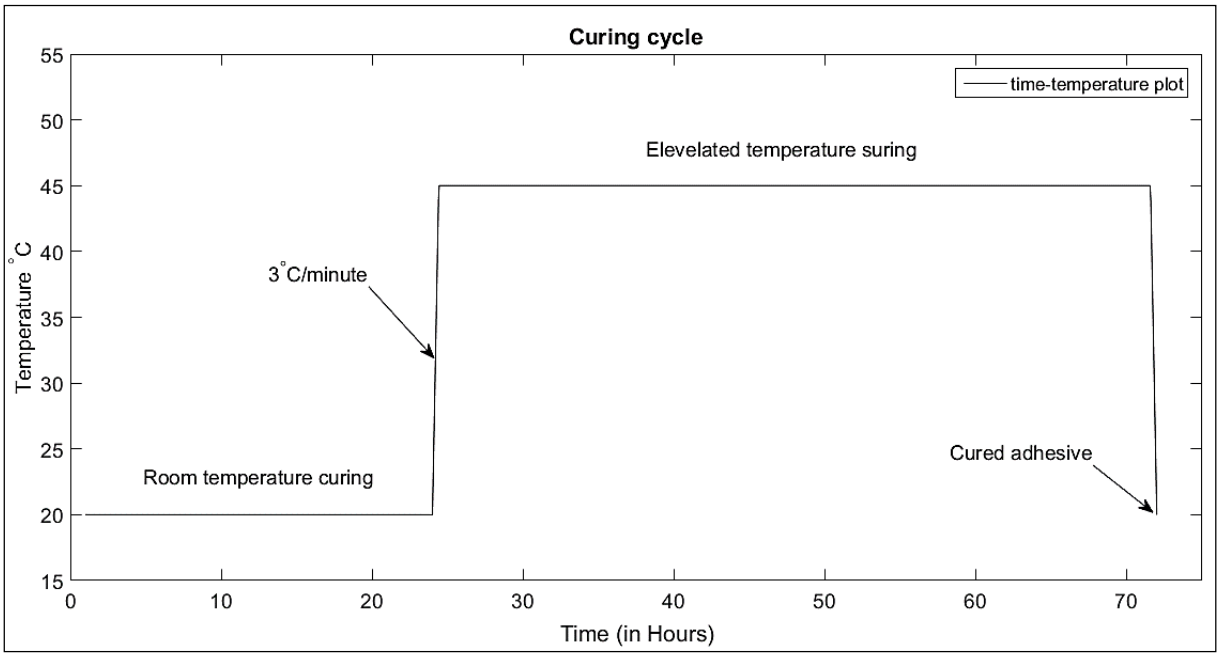

Figure 5.12 Curing cycle used for 3M DP190

For Room Temperature (RT) curing, the bonded tabs are kept under clamp pressure for 24 hours at room temperature. After RT curing, the specimen assembly is in semi-cured stage and requires post-curing at elevated temperature to gain complete strength. For post-curing, the RT cured assembly is unclamped from the plate. After removal from the plate, any adhesive spill on Fixture-A is removed ensuring no adhesive spill on gage section. Subsequently, Fixture-A is removed from the assembly as shown in Figure 5.13.

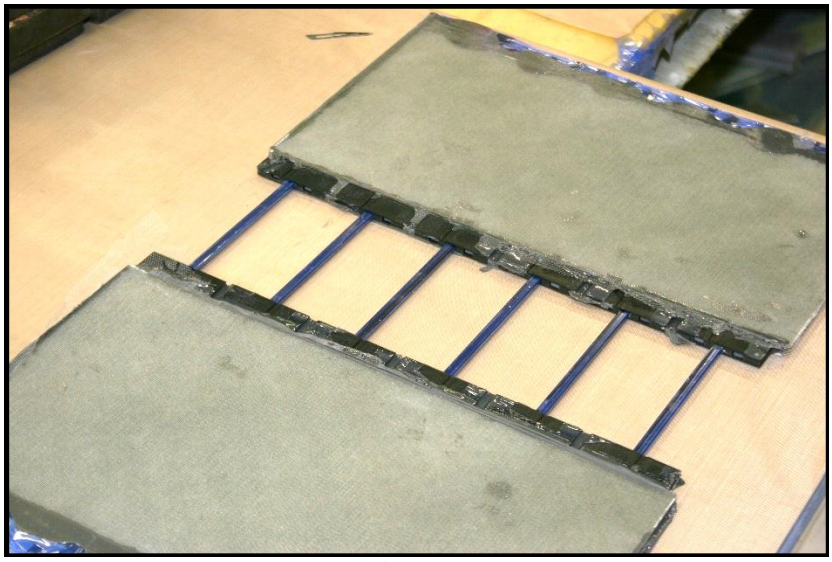

Figure 5.13 Specimen after room temperature curing

The assembly is now ready to be placed in an oven for post-curing. The assembly is post-cured at 45°C with a heating ramp rate of 3°C from room temperature (Figure 5.12). The temperature of 45°C is held for 48 hours before cooling it down at similar ramp rate.

5.4 Machining and finishing specimen

After post-curing, specimen assembly is now ready for machining. First, the individual specimens need to be separated from the assembly. For cutting the specimen from the assembly, 10 mm cutting allowance between each specimen was provided during process planning. A table saw with diamond coated blade circular blade of 4 mm thickness is used for cutting the specimen separate. Though this cutting does not ensure the alignment of the side edge of the specimen to main profile. This alignment is of critical importance while loading the specimen for testing as it ensures alignment of machine loading axis and the profile. In addition to this, the specimen is required to provide two tapers i.e. planar taper of 10° and a side taper of 1.6°. Hence, three cutting jigs for holding the specimen in the particular orientation while cutting are designed. These jigs are here onwards referred to as Straight jig, Planar jig, and Side jig.

5.4.1 Cutting Jig design

Straight jig (Figure 5.14 left) is designed to work with a table saw, and it has a slot for gage section holding and provides an offset from the reference guide of the table saw. The Planar jig (Figure 5.14 middle) is also designed to work with the table saw, it holds the gage section of the specimen at 10° angle from the guide of the table saw. The Side jig (Figure 5.14 right) is designed to work with a milling machine, as the material need to be removed is very small quantity. The Side jig rests on to milling machine bed, the specimen is then placed on the tab resting plane, thus providing an angle of 1.6° to the specimen with respect to machine flat.

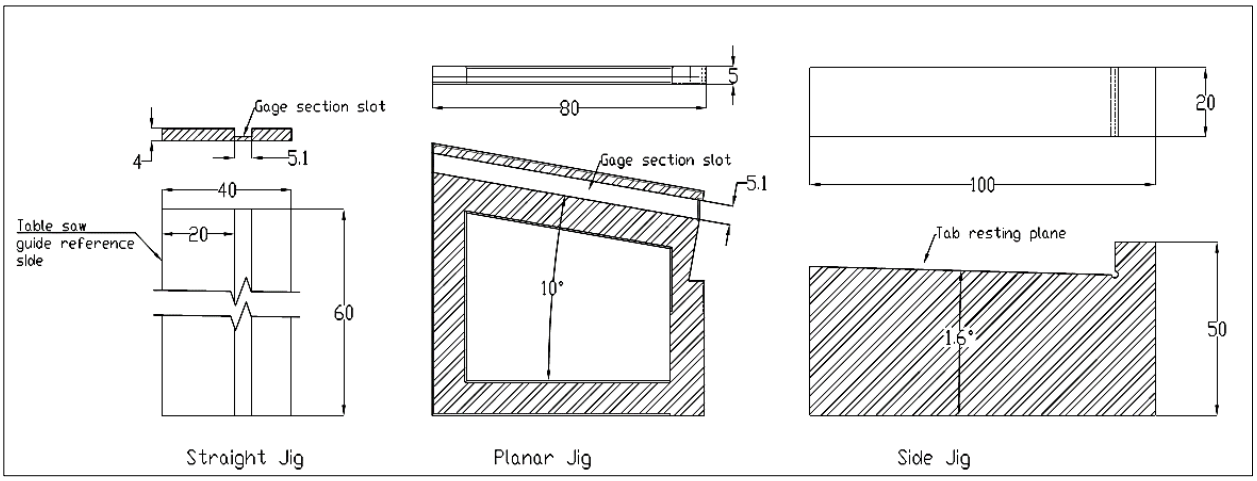

Figure 5.14 Straight Jig (left), Planar Jig (middle) and Side Jig (right)

Aforementioned jigs are manufactured using additive manufacturing using ABS plastic. The 3D printed zigs are shown in Figure 5.15.

Figure 5.15 Straight Jig (left), Planar Jig (middle) and Side Jig (right)

5.4.2 Straight edge machining

Straight side edge machining and holding is as shown in Figure 5.16, this figure indicates the placement of the straight zig in the specimen. The reference edge butting to the table saw guide, provides the reference for the circular table saw to make a cut at tab side edge parallel to the profile gage section.

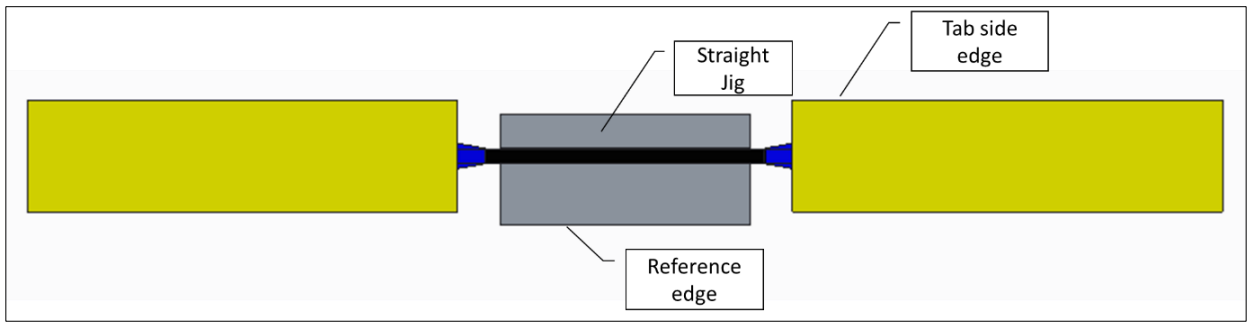

Figure 5.16 Placement of Straight jig for cutting the tab side edge parallel to profile

5.4.3 Planar taper machining

The Planar zig placement with respect to the specimen is displayed in Figure 5.17. The planar jig holds the profile at 10° with respect to reference edge. The cutting line indicates the circular blade position with respect to reference edge. As the specimen is moved along the reference line along the guiding edge of the table, the desired cut at 10° is achieved. The similar process needs to be repeated for all the four sides to achieve the planar taper angle on all sides.

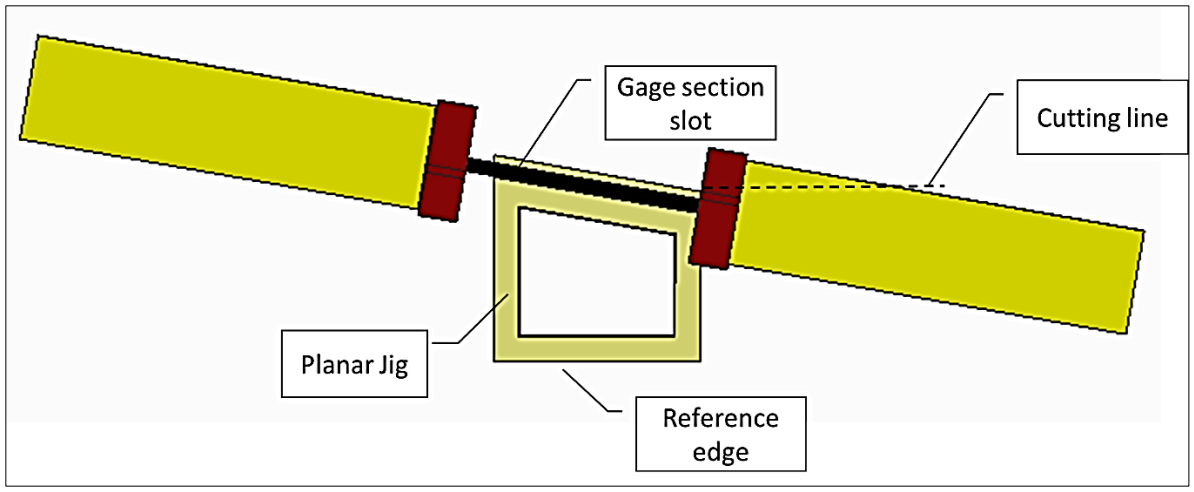

Figure 5.17 Placement of Planar jig for cutting planar angle of 10 ° with reference to profile

5.4.4 Side taper machining

The final taper to be machined is side taper, placement of side jig in the specimen is shown in the Figure 5.18. The specimen is held in place by clamping to the jig. The jig is then placed in the milling machine jaws, ensuring butting of reference edge to the machine bad. A flat diamond-coated grinding wheel is mounted in the milling machine chuck. The flat grinding tool is gradually moved down, removing material slowly providing a smooth taper. Descend of the grinding wheel is stopped as the tab tip grounded to matched with the adhesive front.

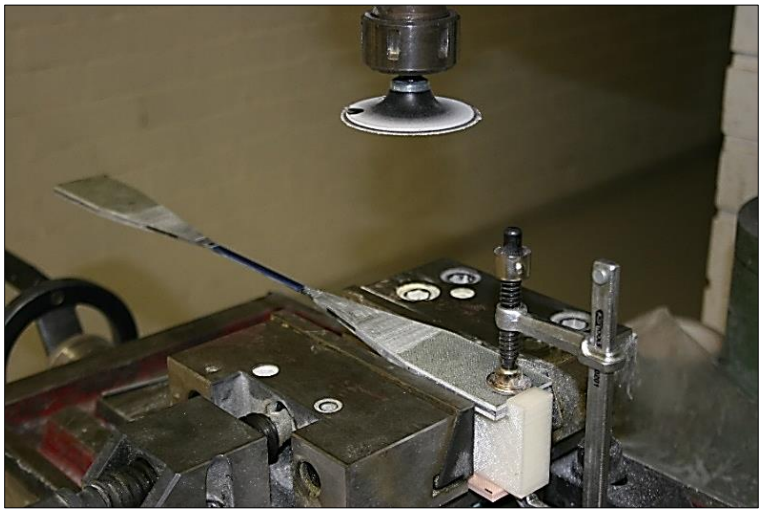

Figure 5.18 Grinding side angle setup in milling machine

5.4.5 Final finishing with sandpaper

After machining the specimen with aforementioned process, the specimen is very close to its final dimensions, however, the burs and unfinished edges remain. In order to remove the burs and providing smoothness to the tapered surfaces, the specimen is finished with fine sand paper with hand (Figure 5.19).

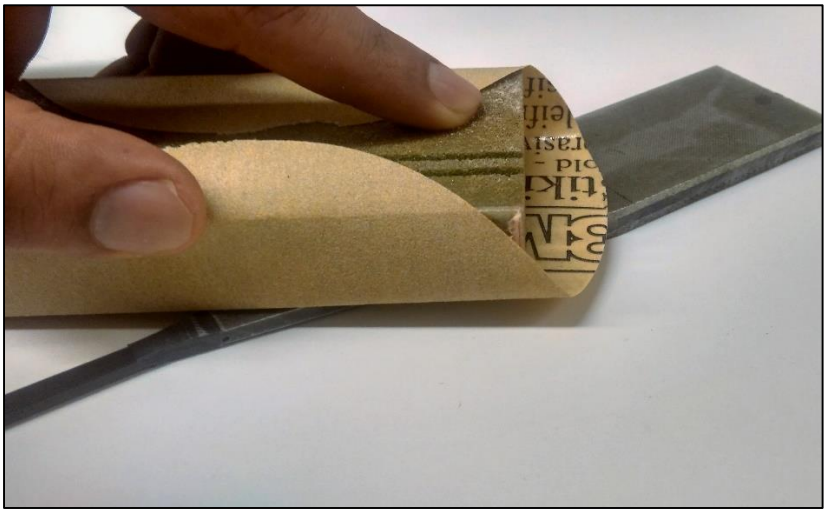

Figure 5.19 Final finishing with fine P80 sandpaper

5.5 Manufactured specimen

Each batch of manufacturing of six specimens (Figure 5.20) including the preparation of the individual components can take more than 2 weeks. Most of the manufacturing steps are done manually, thus require extra caution as a single mistake can cause damage to the specimen.

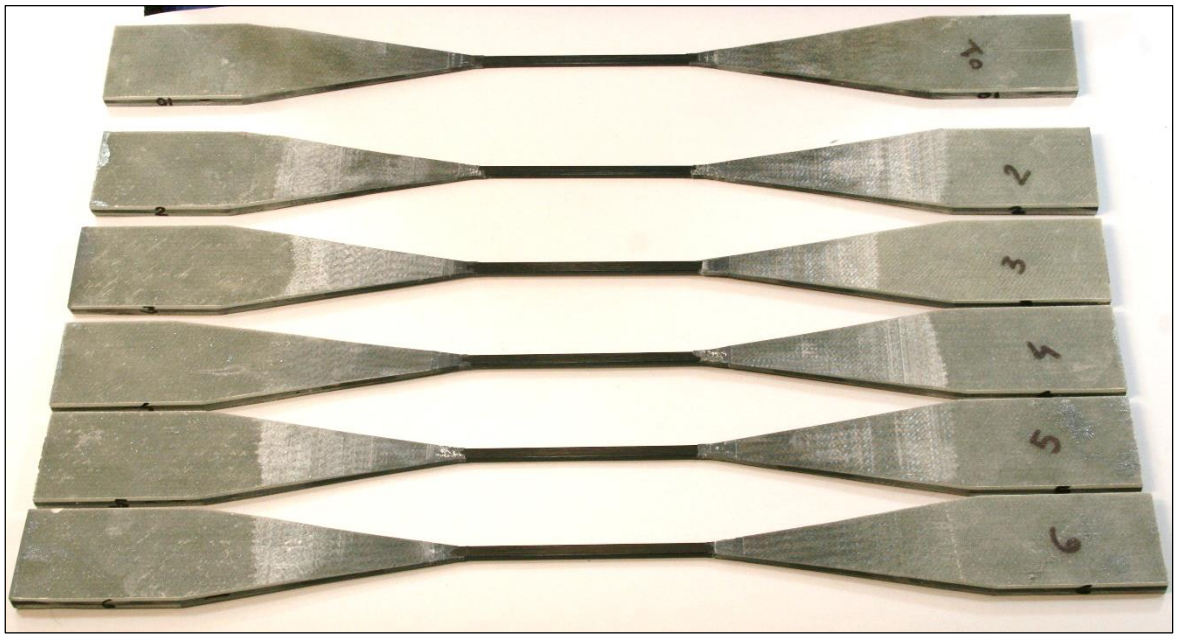

Figure 5.20 One batch of six D2 specimen

6 Static testing

The specimen design was carried out with a focus to reduce SCF in the specimen, assuming that it leads to improvement in the specimen performance. To evaluate the performance, i.e. the ultimate strength of the D2 specimen, a static tension test is carried out. In order to quantify the improvement in ultimate strength of the specimen, along with the testing of low SCF D2 specimen a similar testing of a high SCF specimen is also carried out. Evaluated ultimate strength for both the specimen compared against their SCF and the quantified improvements in the performance of the D2 specimen is discussed in this chapter.

In addition to the performance improvement, the static testing of the D2 specimen also provide the failure strain measurements. These failure strains will be used in the evaluation of the maximum load level for Fatigue testing as suggested by the ASTM standards (section ASTM Standards 3.1.1).

6.1 Specimens

Two specimens with different SCF are tested; the first specimen with lower SCF of 1.02 is the D2 specimen, and the second specimen called 30D Specimen with higher SCF of 1.39.

1) The D2 specimen design is as described in subchapter 4.4.
2) The 30D specimen configuration (Figure 6.1) is given its name due to the 30° taper angle. the specimen construction is very similar in construction of the D2 specimen configuration, as it also uses the support profiles and extended tabs. In order to keep the comparison simple, the tabbing parameters such as tab material, tab thickness, adhesive material and adhesive thickness are kept similar to the D2 specimen. The 30D specimen design differ only in terms of tab taper angle, as it has a large side angle of 30° and does not have any planar angle. Also, the tab length of the specimen is 99 mm.

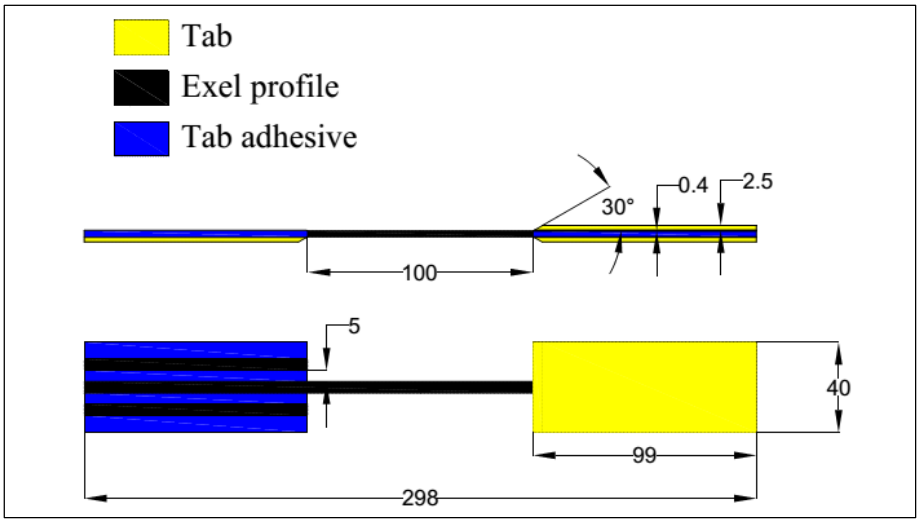

Figure 6.1 30D specimen configuration (All dimension in mm)

6.2 Test parameters and procedure

Static testing of the Exel and the 30D specimen is carried out as per the ASTM D 3039/D 3039M standards. The test is carried out on the Dartec test machine with MTS controller. The testing parameters are summarised in Table 6.1. A loading rate of 2 mm/minute is selected as recommended by the ASTM standards. During the test, the strain measurement is carried out using a 50 mm extensometer, mounted in the middle of gage section. Using the stresses measured at 0.1% and 0.3% strain, Young's modulus is evaluated. The gripping pressure of the jaws is controlled using a constant hydraulic pressure of 200 MPa.

Table 6.1 Static testing setup parameters

Test parameters	**Value**
Loading rate	2 mm /min
Strain measurement	50 mm extensometer
Number of specimens	6 - D2 specimens + 6 - 30D Specimens
Young's modulus evaluation range	Between strain value of 0.1% - 0.3%
Hydraulic pressure	200 MPa

Before testing, The specimens are inspected for the dimensions of the cross-section of gage area using micrometre (range 0-25 mm, least count 1 μm). After the dimensional inspection, the specimen is mounted in the testing equipment, ensuring the specimen alignment using digital angle metre (range 0-180°, least count 0.1°). Finally, the extensometer is mounted using rubber bands for the strain measurement.

6.3 D2 specimen test result

The test results for D2 specimen static testing are provided in Table 6.2, where D2_st is an identification number for a D2 specimen for static testing.

The average ultimate strength of the specimen is measured as 2603.05 with 3.5% CoV (Coefficient of variation). The cross-sectional area used for strength calculation is without correction for the corner radius of the Exel profile, i.e., 0.5 mm. Stress-strain curve for the D2 specimens is shown in Figure 6.2. The D2_st_01 & D2_st_02 plots in the stress-strain curve indicate different slopes. The same can be seen (Table 6.2) from the Young's modulus evaluated for D2_st_01 and D2_st_02 (i.e., 142.85 GPa and 132.41 GPa respectively), which varies by more than 10 GPa from the average Young's modulus, thus indicating an anomaly in the measured strain.

Table 6.2 D2 specimen Static testing result

Specimen number	Width average mm	Thickness average mm	Ultimate strength MPa	Modulus of elasticity GPa	Max. load KN	Max strain %
D2_St_01	5.07	2.56	2611.78	142.85	33.94	1.83
D2_St_02	5.08	2.56	2685.20	132.41	34.94	2.01
D2_St_03	5.08	2.57	2544.95	113.27	33.16	2.24
D2_St_04	5.07	2.56	2726.82	116.23	35.44	2.35
D2_St_05	5.07	2.56	2475.97	112.93	32.18	2.20
D2_St_06	5.07	2.56	2573.58	114.74	33.43	2.24
Average	5.07	2.56	2603.05	122.07	33.85	2.15
SD	0.00	0.00	92.23	12.55	1.20	0.19
CoV %	0.06	0.08	3.54	10.28	3.54	8.8

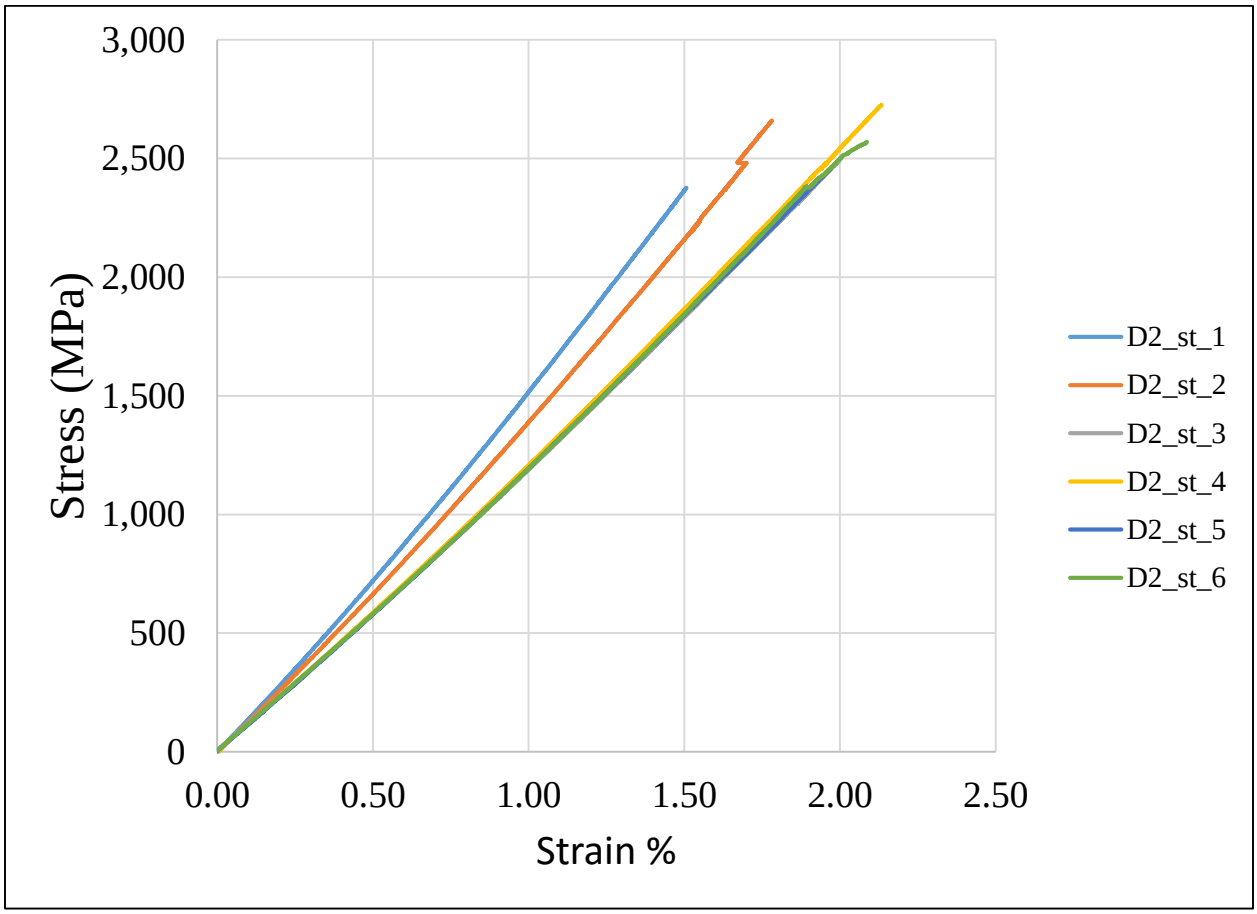

Figure 6.2 Stress-strain plot D2 specimen

At this point, it was obvious that the extensometer mounted onto the specimen was slipping or not holding stable, thus, the specimen was taped with plastic tape at the extensometer interface as shown in Figure 6.3, assuming that this would provide a better interface for the extensometer. The testing with taped interface was continued after from D2_st_03 to 06, the stress-strain curve observed consistent modulus values. However, the measured Young's modulus was well below expected modulus range of 160-165 GPa.

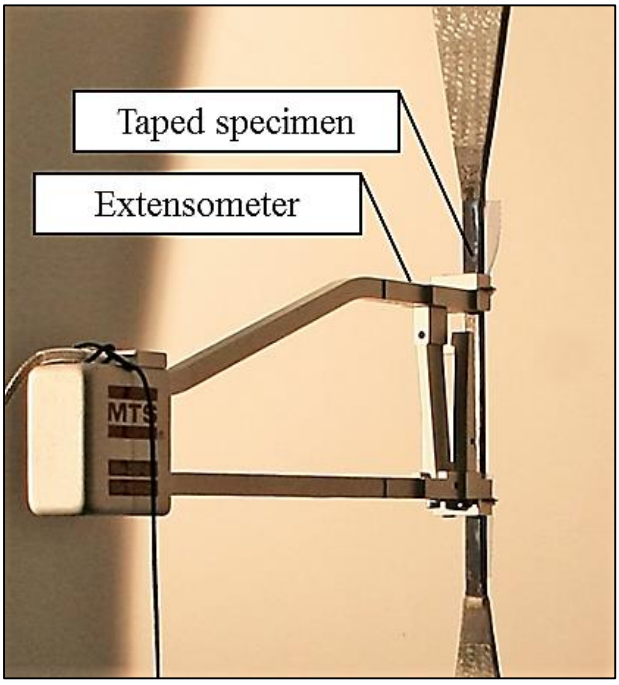

Figure 6.3 Extensometer mounted on the specimen gage section

6.4 D2 specimen failure mode

The specimen after the static testing are shown in Figure 6.4. The figure shows 6 D2 specimens where D2_st_01 to 06 are arranged from top to bottom. The following observations are made regarding failure of the specimen under tension loading

1. The failure in the specimen D2_st_01, 03, 05 & 06 is XGM (i.e. eXplosive Gage Middle) failure of the specimen.
2. D2_st_02 is failed due to tabs peel off from the edge of the specimen. The failure mode is provided with the ASTM standard code (GAT) Grips at tab Top.
3. The D2_st_04 failed in a non-standard way, which is not visible from the top view of the failed specimen. In the specimen, the fibre of the main profile from the middle of the profile got pulled and can be seen from the Figure 6.5.
4. In almost all the specimen, a debond along the main profile in the tabbing region is visible, and it appears as a white rectangular patch on the tab and is visible until the gripping starts.
5. In almost all the specimen, the adhesive front got crumbled in all the failed specimen and is not visible anymore in the failed specimen.

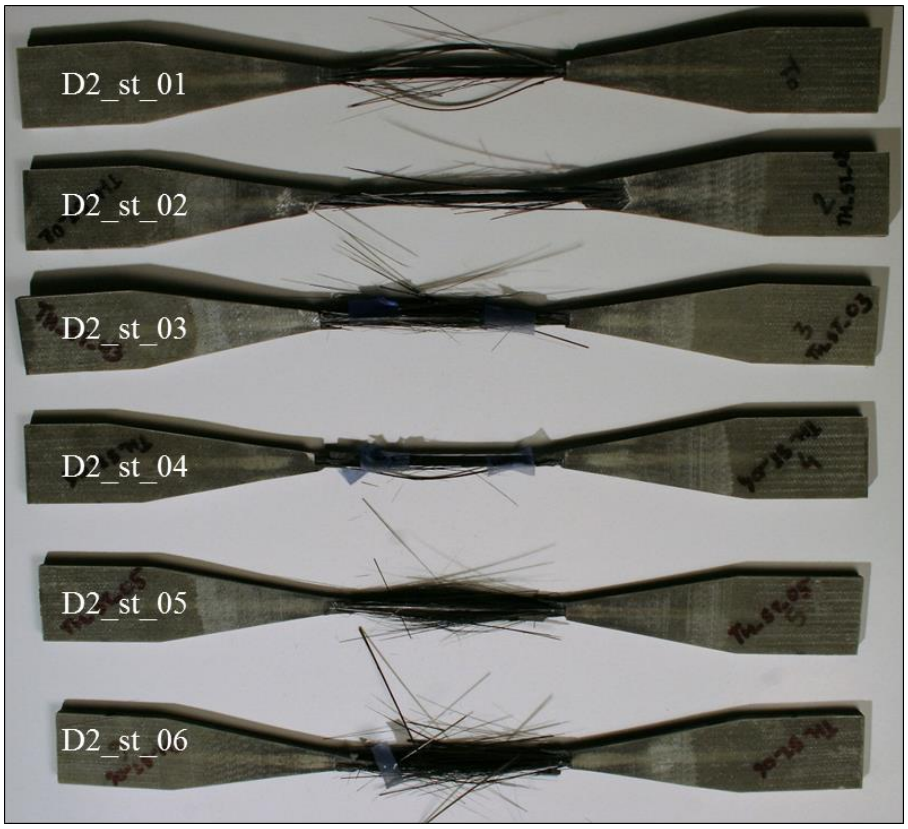

Figure 6.4 D2 specimen after static testing

Figure 6.5 D2_st_04 Fibre pulled from the middle of profile

6.5 30D specimen test result

The test result for the six 30D specimens for static tension testing is shown in Table 6.3, where 30D_st indicates the identification number of the specimen. Based on the D2 specimen testing, the interface of the specimen to extensometer is kept similar i.e. specimen is taped with plastic tape. The ultimate strength evaluated are 2519.11 MPa with a standard deviation of 107 MPa. The stress/strain plot for the 30D profile is shown in Figure 6.6. The Young's modulus evaluated for 30D_st_04 and 05 are marginally higher than the rest of the specimen.

The Young's modulus observed is consistently low compared to expected value of 160-165 GPa with high SD of ≅ 5 GPa. This result suggested that the measured value of the Young's modulus lower and erratic. Hence, the issue was probed and discussed later in the strain measurement section.

Table 6.3 30D specimen Static testing result

Specimen number	Width average mm	Thickness average mm	Ultimate strength MPa	Modulus of elasticity GPa	Max. load KN	Max. strain %
30D_St_01	5.06	2.56	2561.06	112.52	33.24	2.28
30D_St_02	5.07	2.56	2353.70	111.69	30.61	2.11
30D_St_03	5.07	2.57	2520.37	107.65	32.78	2.40
30D_St_04	5.07	2.56	2678.13	119.74	34.76	2.24
30D_St_05	5.08	2.56	2467.96	120.99	32.12	2.05
30D_St_06	5.06	2.56	2533.47	111.04	32.88	2.29
AVERAGE	5.07	2.56	2519.11	115.19	32.73	2.19
SD.	0.01	0.00	106.99	4.77	1.36	0.11
CoV %	0.11	0.08	4.25	4.14	4.16	4.87

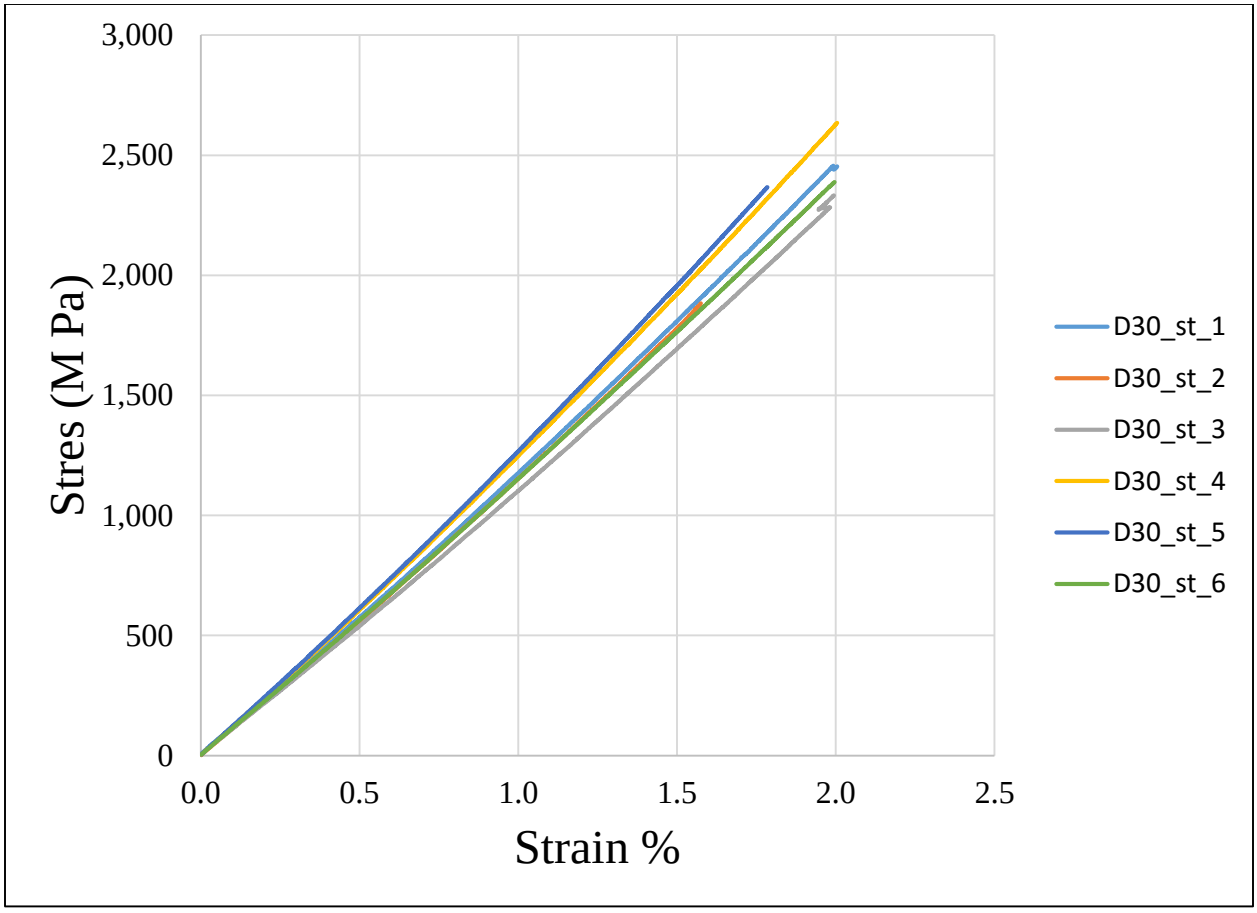

Figure 6.6 Stress-strain plot for 30D Specimen configuration

6.6 30D Specimen failure mode

After static testing, 30D specimens are shown in Figure 6.7, where the specimen is arranged from bottom to top 30D_st_01 to 06, respectively. Regarding failure of the 30D specimens following observation are made

1. All the 30D specimen failed in XGM (i.e. eXplosive Gage Middle) failure mode.
2. 30D specimen tabs have 99 mm tab length, leaving 35 mm of the tab outside the machine grips. In this area, tab debonds with the main profile is observed in a similar fashion as in D2 specimen with a white patch.

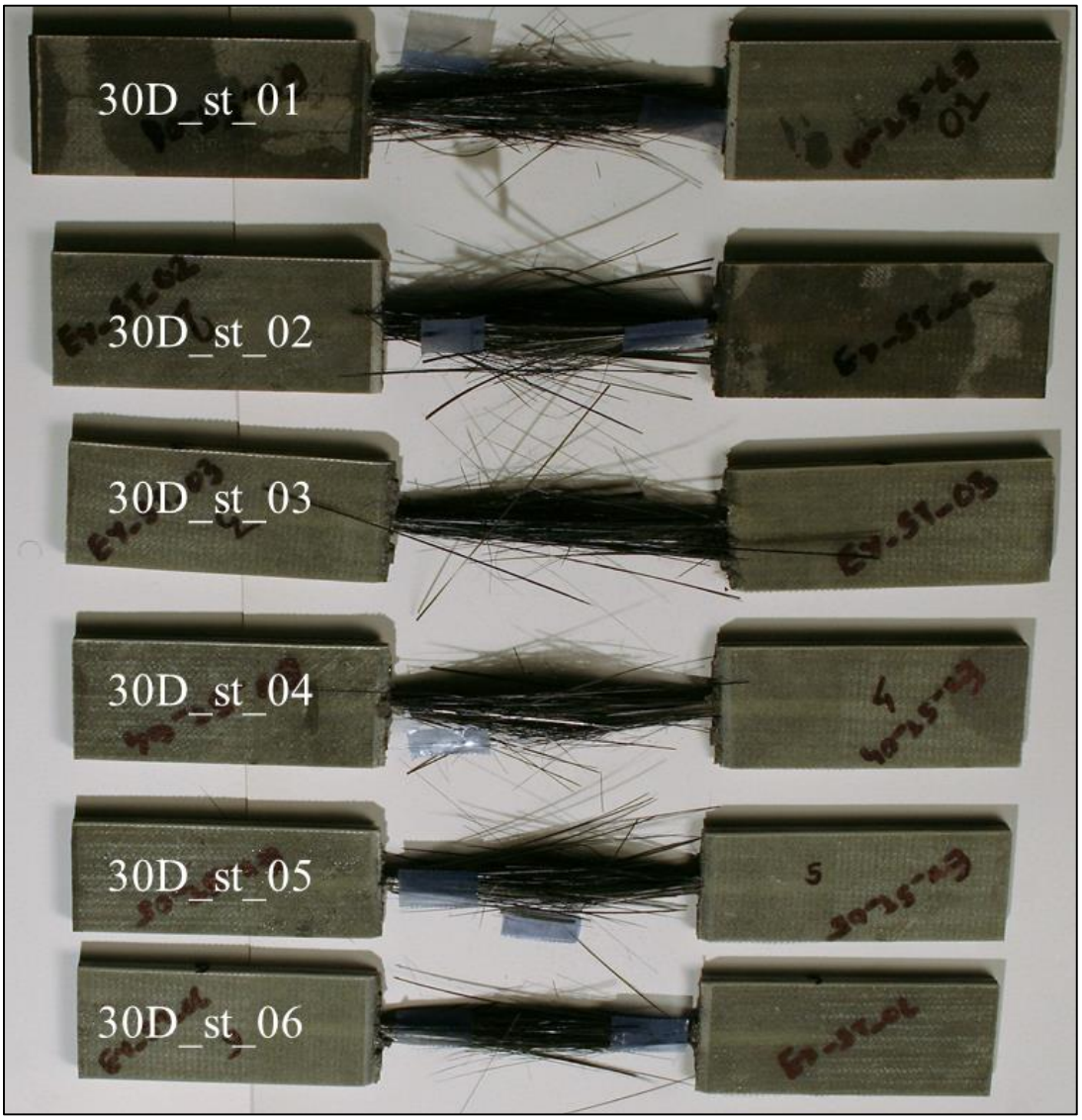

Figure 6.7 30D Specimen after static testing

6.7 Strain measurement

During the static testing of D2_st_01 and 02 specimens, the extensometer was mounted to the gage section directly using rubber bands. This resulted in high variation in the evaluated Young's modulus. Presuming that the mounted extensometer was slipping or not held properly, a plastic tape is applied to the specimen gage section, assuming it could avoid the slippage by providing a better gripping point. However, the stress-strain curve observed after 30D specimen testing were with even higher standard deviation, suggesting mounting anomaly of the extensometer onto the specimen.

To understand the effect of the plastic tape interface, additional tests were needed. One D2 specimen was equipped with 4 strain gages, i.e. two at the middle of gage section on either side of the specimen and two near the tabs on the same side of the specimen. In addition to the strain gage measurement, extensometer is mounted onto the specimen (Figure 6.8). The specimen was strained till 0.4% strain to evaluate Young's modulus from strain gage and extensometer simultaneously. Assuming the strain gage measurement as a reference, extensometer measurement is taken with three different interfaces i.e. bare specimen, taped specimen and painted specimen and result are compared in Table 6.4 where the interfaces are defined as follows

1) *Bare specimen*: the extensometer is directly mounted onto specimen (Figure 6.8)
2) *Taped specimen:* A blue plastic tape is applied at the gage section where the extensometer knife sits then the extensometer is mounted
3) *Painted specimen*: the gage section is painted with white paint (i.e. Staples correction fluid), with single brush stroke creating a thin uniform layer of paint at the interface where the extensometer knife sits and then the extensometer is mounted

Table 6.4 Young's modulus measurement by Extensometer and strain gage

Extensometer mounting on	Young's modulus from (average)		Difference
	Strain gage	Extensometer	
1) Bare specimen	151.5435	155.2276	-3.68411
2) Taped specimen	151.3387	124.1097	27.22902
3) Painted specimen	151.2939	152.4579	**1.16402**

The higher young's modulus shown in the result should not be taken at face value, as it belongs to a profile with different fibre volume fraction. Nevertheless, the changes indicated with different interface provide is very useful as it clearly shows the anomaly which was observed for the taped specimen. The difference column in the table indicates the lowest variation for the painted interface. The taped specimen evaluated Young's modulus is low by ≅28 GPa. Thus, a painted specimen interface with the extensometer will be used during the fatigue testing for Young's modulus evaluation.

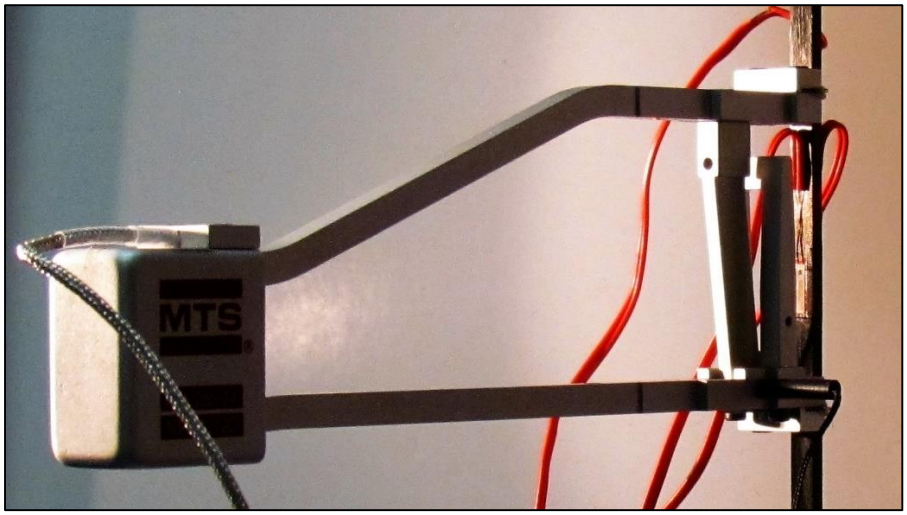

Figure 6.8 Strain gage bonded and extensometer mounted onto bare specimen gage section for simultaneous measurement of strain

The Ultimate strength and SCF for the D2 and 30D specimen is compared in Table 6.5. the reduction of SCF by 36% in SCF improves the ultimate strength by 3.6 % in the specimen. The improvement although not very significant, suggests that the D2 specimen is better and hence will be taken for further fatigue testing.

Table 6.5 The D2 vs 30D specimen comparison of Ultimate strength against SCF

	SCF	Ultimate strength (MPa)
The D2 specimen	1.02	2603.05
The 30D specimen	1.39	2519.11
% change	36.3 %	3.6 %

The failure strain measurement from the static testing of the D2 specimen is unreliable due to the extensometer mounting anomaly. In addition, it was later informed that the Exel profile used for static testing has different fibre volume fraction than the one to be tested under fatigue testing. Considering the aforementioned trail of events together with the time constraint of the project, re-measurement of the failure strain is avoided. Therefore, for further work a failure strain of 1.7% is assumed that represents an average value of failure strain for typical carbon fibres within the range of 1.4% -2%. However, this value can be updated in future works to achieve correct load levels.

7 Fatigue testing

7.1 Fatigue test arrangements

The fatigue testing is carried using the ASTM standards (section 3.1.1). Total 12 D2 specimens are tested with two different load levels, i.e., six specimens with each load level. The maximum load level F for each specimen is calculated using Equation 7.1. Where, the failure strain ε_f = 1.7% and the Young's modulus E and cross section area A are measured individually for each specimen.

$$F = \varepsilon_f \times L \times E \times A \qquad \ldots\ldots\ldots \{7.1\}$$

Where,
ε_f=failure strain, L=% load level, E=Young's modulus and A=cross section area

The fatigue testing carried out on a Dartec test machine with MTS controller; the summary of fatigue test parameters areas shown in Table 7.1. The selection of loading frequency is done based on the observed temperature in the tabbing area using Fluke thermographic camera. The frequency trial started on a dummy specimen with test frequency 10 Hz resulting in max temperature measured 52°C. Hence, the test frequency reduced gradually to a minimum of 3Hz which brought the max temperature observed to 37°C. A lower frequency than 3 Hz would require very long time to complete the desired number of cycles within the time frame of this work. Thus, despite the higher temperature than recommended, loading frequency of 3Hz is selected. The hydraulic pressure for the testing kept at the constant 200 MPa to avoid slipping of the specimen.

Table 7.1 Test parameters for tension-tension fatigue testing

Test parameters	**Value/instrument**
Loading frequency	3 Hz
Minimum load	0.5 KN
Maximum load	Equation 7.1
L (% load level)	60% and 65 %
Number of Specimen	6 specimens with 65% load + 6 Specimens with 60% load
Young's modulus evaluation range	Between strain value of 0.1% - 0.3%
Gripping pressure	200 MPa
Stop testing at	Failure or 1,000,000 cycles whichever is first

Minimum load of 0.5 KN is selected to avoid any compression loading in the specimen. The load level L is selected based on trial-and-error method; starting with load level of 75%, gradually reducing it with steps of 5% on a dummy test specimen. The dummy specimen survived 1000 cycle at 65% load level, with no visible damage in the specimen. Thus, load levels of 65% and the next lower step of 60% are chosen, assuming that, these load levels would be sufficient to

observe the fatigue in the specimen. The test was carried out until 1 million cycles or failure whichever comes first. The primary objective of fatigue test is to observe the suitability of the D2 specimen for tension-tension fatigue loading.

The fatigue testing procedure can be divided into two major stages; 1) To measure the Young's modulus of the specimen 2) Activate fatigue test run. During the first stage, the specimen cross section dimensions are measured using a micrometre. The specimen is then mounted in the machine grips, aligning the specimen profile to the machine loading axis using digital angle metre within 0.1°. The mounted specimen is then painted with white paint, with single brush stroke creating a uniform layer of paint at the interface. The Extensometer is then mounted on the painted specimen using rubber bands (Figure 7.1 left). The test is stopped at the 0.4% strain, to gather data in the machine system for Young's modulus evaluation. The load level for the fatigue testing is then obtained from equation 7.1.

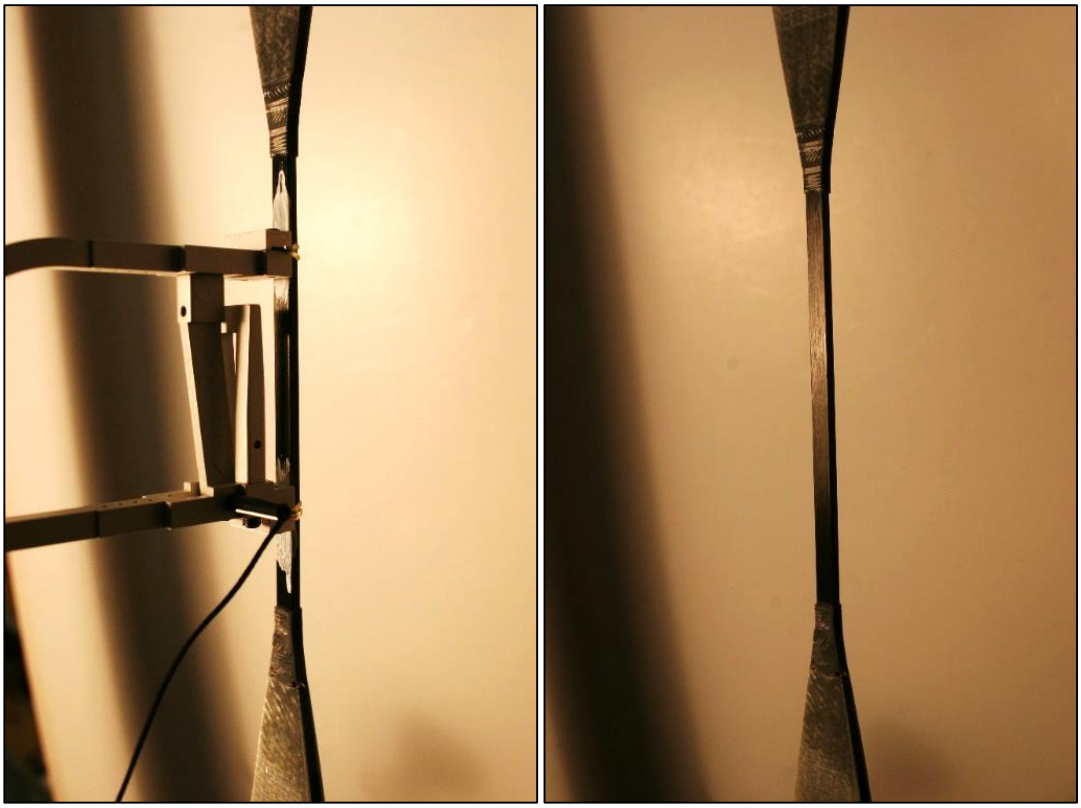

Figure 7.1 Extensometer mounted with paint interface (left) cleaned specimen ready for fatigue testing (right)

In the second stage, the specimen is unloaded by the system. Then, the extensometer is removed and the gage section is cleaned for the testing (Figure 6.5 right) subsequently, the test is run. During the fatigue testing, pictures of the specimen are taken at certain cycle intervals, additionally, thermal plots are also recorded using Fluke thermal camera.

7.2 Fatigue test result

For 65% load level (i.e. 1.105% initial strain), fatigue test results and tested specimens are shown in Table 7.2 and Figure 7.2 respectively, where D2_ft indicates the specimen identification number. As can be observed from Table 7.2 with 65% load level, all the specimens could complete 1 E+05 cycles except D2_ft_03. The D2_ft_03 failed prematurely after less than 1000 cycles due to unknown reasons. Based on the observation of the failed specimen, three specimens, i.e. D2_ft_01, 02 and 05 specimens failed in XGM (eXplosive Gage Middle) mode, and other three specimens, i.e. D2_ft_03, 04 and 06 failed in SGM (long Splitting Gage Middle) mode.

The additional observation regarding The Young's modulus from the test result of 65% load level, that the young's modulus measured with white paint interface is very consistent with CoV of less than 1%.

Table 7.2 Fatigue test at 65% load level

Specimen	**(S) Stress**	**Modulus**	**(N) Number of**	**Force**
number	MPa	GPa	Cycle	KN
D2_ft_01	1563.37	141.48	2.12E+05	20.03
D2_ft_02	1579.67	142.96	2.74E+05	20.23
D2_ft_03	1559.84	141.16	7.24E+02	20.00
D2_ft_04	1598.98	144.70	1.39E+05	20.47
D2_ft_05	1560.61	141.23	9.34E+05	19.98
D2_ft_06	1581.22	143.10	1.71E+05	20.24
Average	1573.95	142.44	-	20.16
SDT	15.50	1.40	-	0.19
CoV %	0.98	0.98	-	0.95

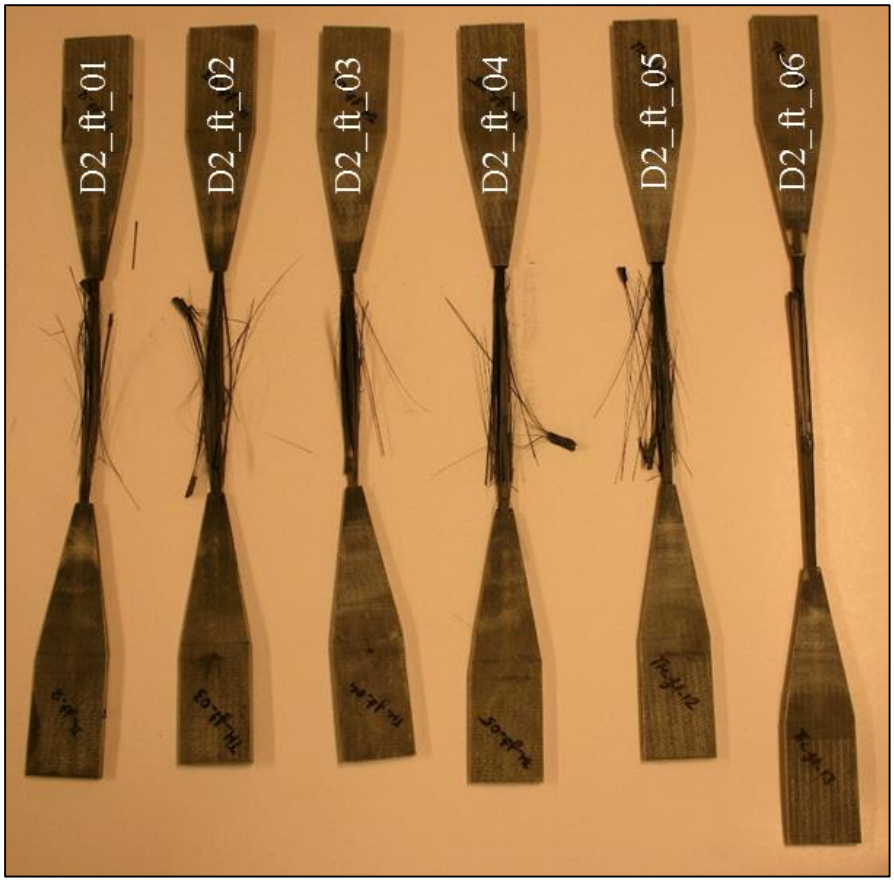

Figure 7.2 Specimens after fatigue testing with 65% load level

For 60% load level (i.e. 1.02% initial strain), fatigue test results and tested specimens are shown in Table 7.3 and Figure 7.3 respectively. As can be observed from Table 7.3, with 60% load level, D2_ft_08 & 11 failed prematurely after a few thousand cycles due to unknown reason. Observing the failed specimen, D2_ft_07 and 11 specimens failed in XGM (eXplosive Gage Middle) mode, whereas D2_ft_08 failed in SGM (long Splitting Gage Middle) mode.

Table 7.3 Fatigue test at 60% load level

Specimen number	**(S) Stress MPa**	**Modulus GPa**	**(N) Number of Cycle**	**Force KN**
D2_ft_07	1444.91	141.66	1.18E+05	18.50
D2_ft_08	1451.75	142.33	1.44E+03	18.58
D2_ft_09	1456.63	142.81	1.00E+06	18.64
D2_ft_10	1454.34	142.58	1.00E+06	18.62
D2_ft_11	1463.56	143.49	1.74E+03	18.74
D2_ft_12	1452.51	142.40	1.00E+06	18.59
Average	1453.95	142.54	-	18.61
SDT	6.14	0.60	-	0.08
CoV %	0.42	0.42	-	0.42

Three specimens D2_ft_09, 10 & 12 completes 1.00E6 cycles; After completing the cycles, the Exel profile surface fibres at the tab edge are cut and are fibres are bristling out in almost each specimen.

Figure 7.3 Specimens after fatigue testing with 60% load level

7.3 Fatigue damage progression

Three D2 specimens D2_ft_09,10 & 12 completed 1.00 E+6 cycles specimens, out of this specimen D2_ft_09 is taken to show typical damage progression in the specimen under fatigue loading. The Figure 7.4 and 7.5 shows the damage progression after a certain number of cycles where 1K stands for 1000 cycle. Typical damage progression is explained as follows

- After loading the specimen and starting the fatigue loading (Figure 7.4-1), between 0-1K cycles the debond between the tab and the main profile can be observed.

- After 1K cycles, the detachment of adhesive front from the tab, while it is still bonded to the profile can be observed from both the ends. The detachment is visible when the specimen is in a loaded condition, hence, it is not visible in Figure 7.4-1.
- Detached adhesive front oscillates freely along the profile, causing the initial fibre peel off at the tab tip, as can be seen at 30K as shown in Figure 7.4-2. Similar peel off can also be observed at the other end of the specimen at 60K in Figure 7.4-3.

- The peel off observed in Figure 7.4-3 is progressing in the top fibre layers of the main profile. This peel off grows as more cycles are applied, the peel off growth are limited to surface fibres of the profile, as can be seen at 80K cycles in Figure 7.4-4.

- A saturation of peel off can be seen as the bottom adhesive front detaches completely at 140K cycles (Figure 7.4-5). Along with adhesive front, it takes surface fibre of the profile, leaving the core of the profile intact.

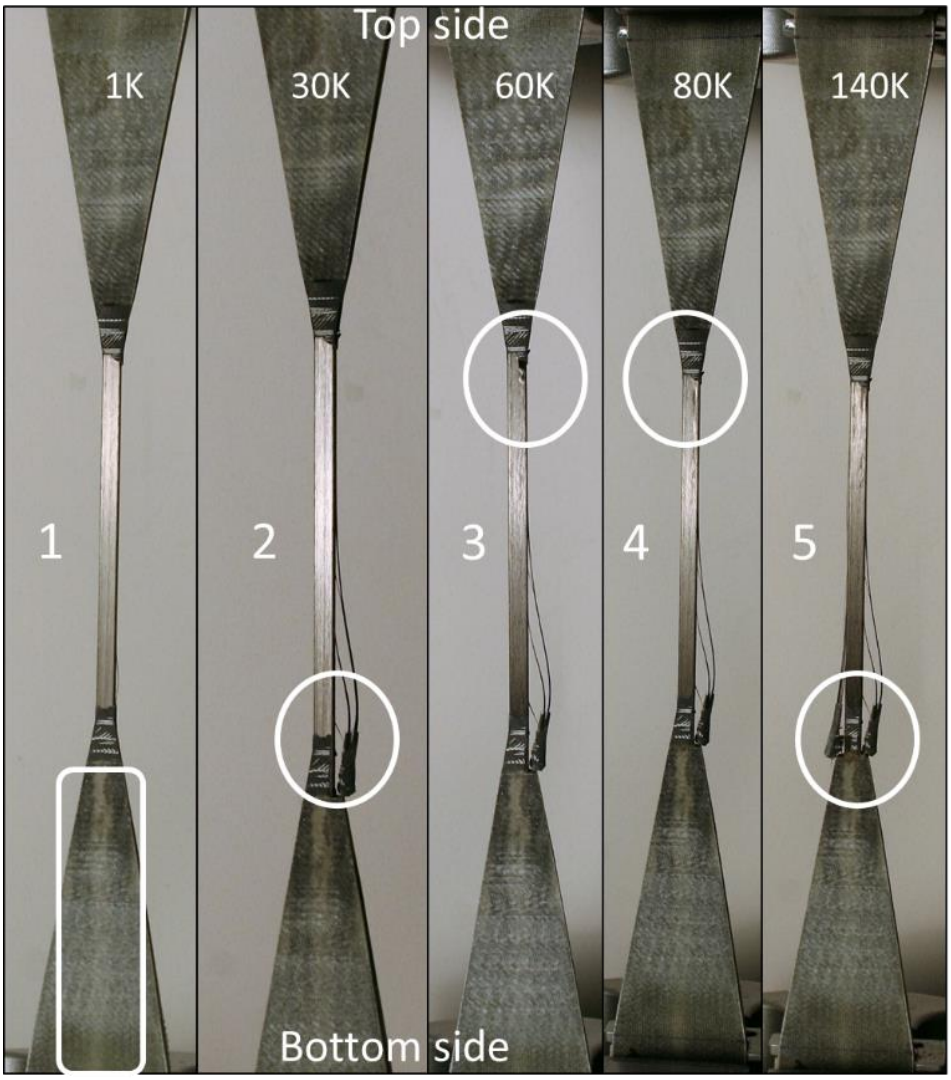

Figure 7.4 Damage progression in D2 specimen under Fatigue loading (1/2)

- After 150K cycles the peel offs looks stabilised though 200K the top peel off start growing (Figure 7.5-6) and resulting in cracking of adhesive front top at 400K cycles (Figure 7.5-7).

- At 600K cycles the peel off from the top adhesive front seems to be growing and from all sides of the profile (Figure 7.5-8). Further, this peel offs are merging at the mid of gage section at 800K cycle, thus peeling most of the surface fibre of the profile (Figure 7.5-9).

- At 1000K cycles, the testing is stopped, and the peel offs from the top and bottom sides are almost detached with surface fibre from the main profile, leaving the main profile otherwise intact.

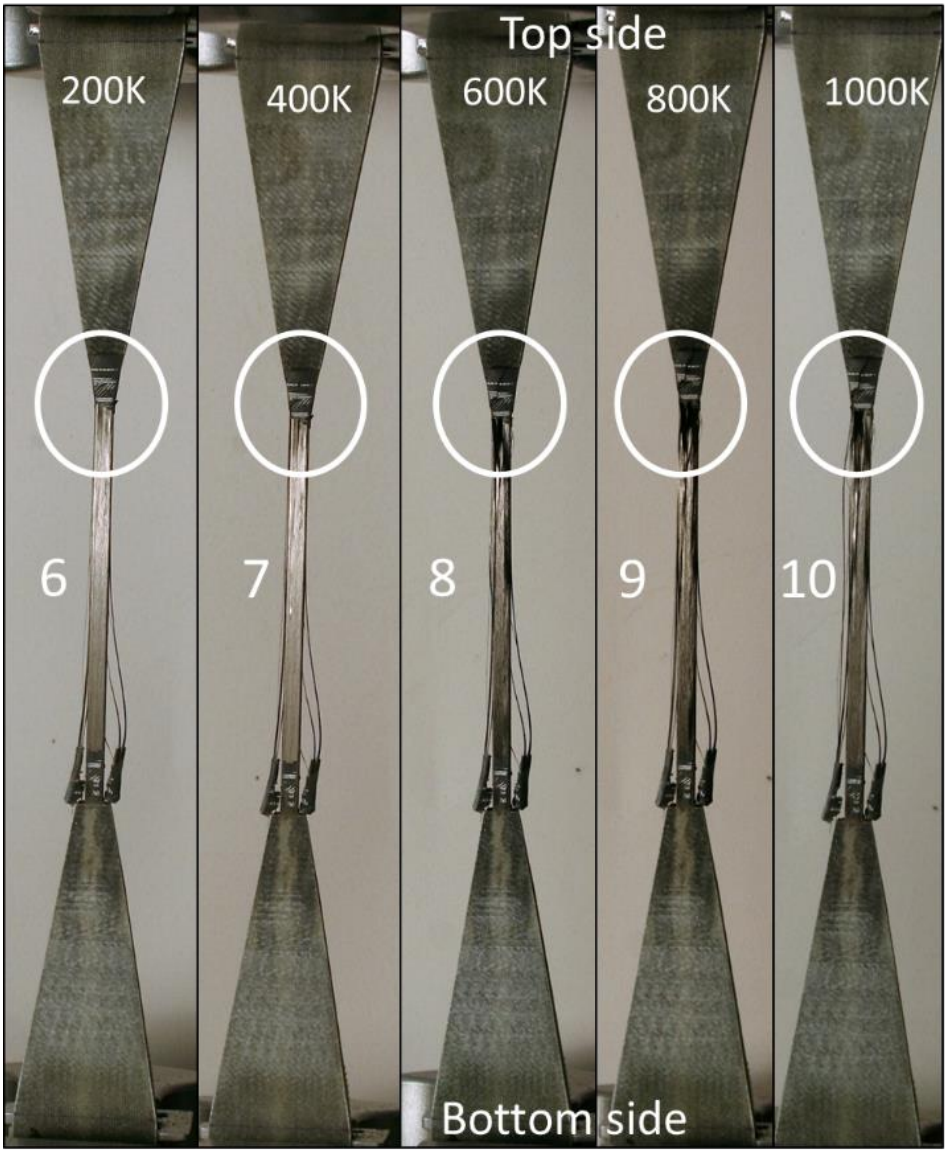

Figure 7.5 Damage progression in D2 specimen under Fatigue loading (2/2)

The damage in the tested D2 specimen initiates with the tab-profile debond and progresses with peeling of the fibre at the tab tip. So, the failure does not initiate in the gage section, instead it initiates in the tab tip. In order to display the graphically fatigue life of the UD CFRP specimen,

Talreja et al.(7) Figure 2.8 plotted the results in three separate regions. Utilizing the similar approach, the resultant fatigue-life diagram is shown in Figure 7.6. Ten out twelve specimens are in line with the results presented by Talreja et al.(7)

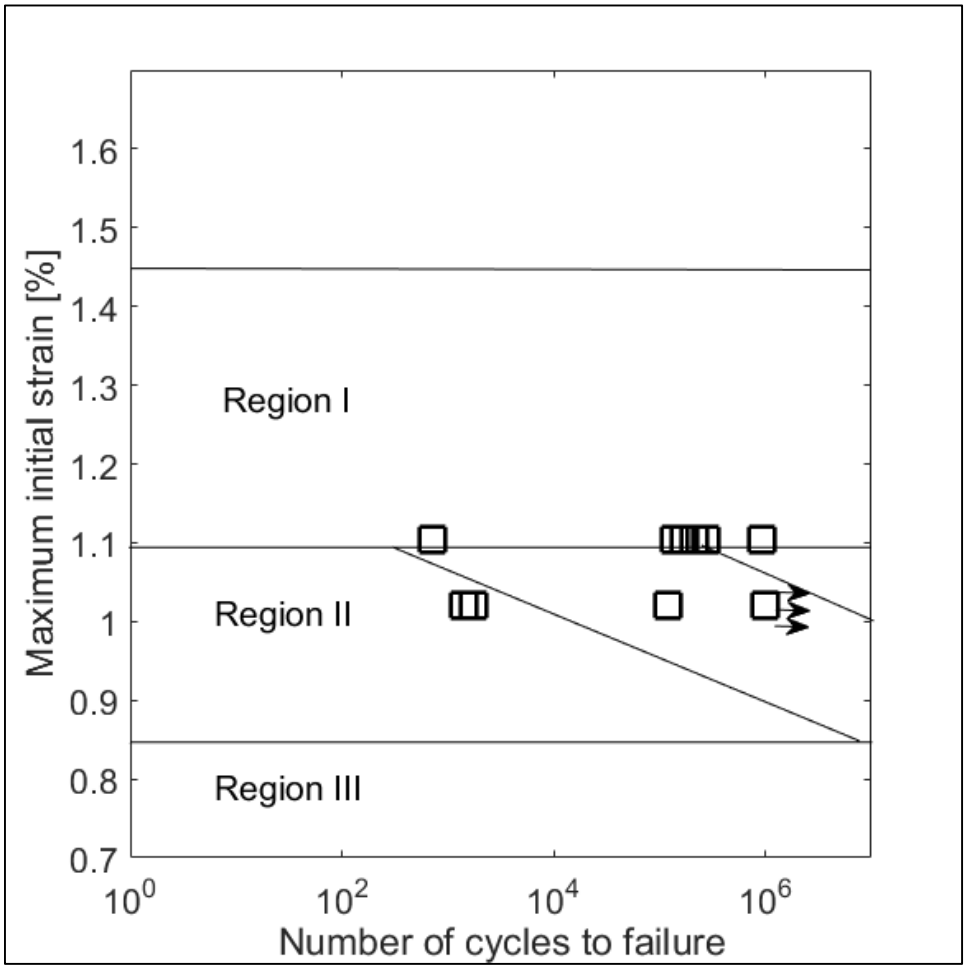

Figure 7.6 Fatigue life diagram for D2 Specimen

Other than the aforementioned damage progression, following observation are made regarding the fatigue tested specimen

- Most of the damage to in the failed specimens are visible and are located in the gage area
- Tabs are intact in most of the tested specimen (Figure 7.7)
- During the fatigue testing after the tab has deboned in the initial phase of the cycle, the profile rubs against the tab creating an adhesive dust at the juncture of the adhesive front and tab and is shown in Figure 7.8.

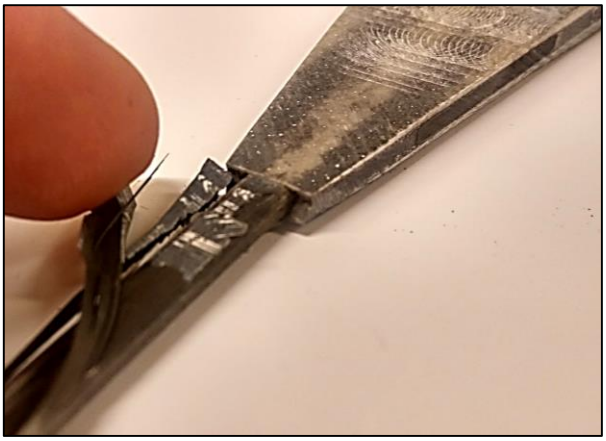

Figure 7.7 Intact tab in the tested specimen

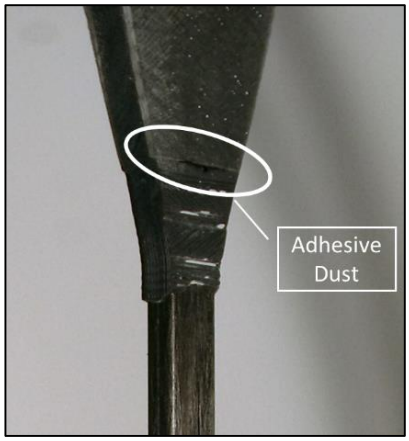

Figure 7.8 Adhesive dust due to profile rubbing to the debonded tab

- During the fatigue cycle, after the failure of Top & Bottom (T&B) adhesive (Figure 7.9), the profile was able to move slightly relative to the tab, i.e. the Exel profile was sliding between the tab in the T&B debonded area. Suggesting that the Side Adhesive (SA) is either deforming too much or is debonded from the profile and allowing the profile to move relative to the tab.

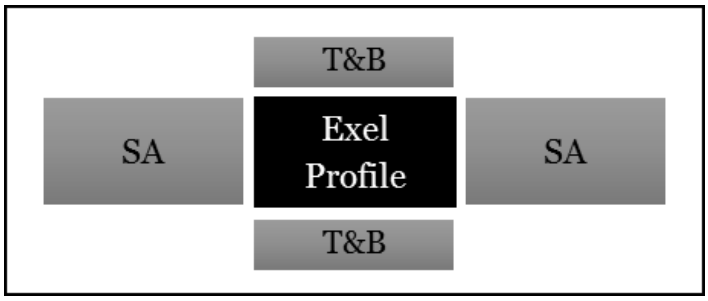

Figure 7.9 Schematic view of the adhesive around profile in the D2 specimen

- As the thermal image shows (Figure 7.10) the temperature during the fatigue loading with 3 Hz frequency was close to 37°C. The debond in the tabbing area (Figure 7.4-1) and the heating in the tabbing area are at the same location.

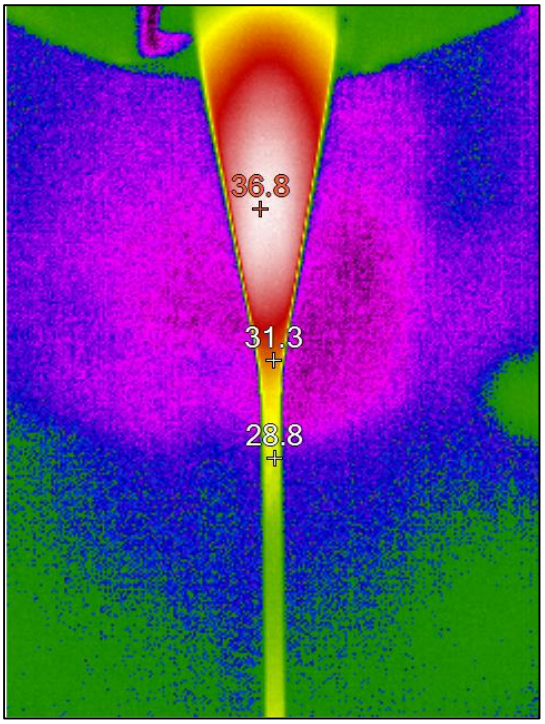

Figure 7.10 Thermal images of the specimen Tabbing area indicating temperature in °C during fatigue testing

8 Discussion

The adhesive with lower modulus was chosen while designing the specimen based on the FEA results for reducing SCF in the specimen. As subjected to fatigue loading, the adhesive fails during initial cycles, resulting in a debond between tab and the profile. This debond increases SCF in the tabbing area, causing damage initiation in the profile at the tab tip. However, despite the unexpected damage initiation, the fatigue results of the D2 specimen are in line with the results presented by Talreja et al.(7) The failure of the tab adhesive at the debond can be attributed to three main reasons

- High shear stresses in the adhesive
- Due to high temperature in the tabbing area, degradation in the adhesive strength
- High deformation or debond in the side adhesive, thus increasing the stresses in the T&B adhesive

The increase in the temperature in the tabbing area have been reported by Frédéric Lani (36), Bailey et al. (34), Baere et al. (31), G D Sims (42) and Vassilopoulos et al (35). None of the literature specifically correlates the rise in temperature with the debond in the tabbing area, although, Baere et al. (31) reported that the CFRP cross-ply laminate under tension-tension fatigue inside failed prematurely due to temperature rise in the tabbing area.

The lack of correlation between the temperature rise and tab debond can be due non-visibility of the tabbing area during testing. As most the specimen design studied have the tab length equal to the machine jaw, thus concealing the tabs making it difficult to identify any visible debond. Whereas, visible tab length in the D2 specimen is about 100 mm lying outside the machine jaw, making the debonded area visible. Additionally, the debond is occurring at a location where the tab thickness is gradually reducing to a minimum, hence, improving the visibility even more.

The second stage of failure starts with fibre peeling off and bristling out, due to higher SCF caused by detachment of the adhesive front resulting in an abrupt tab ending. The high SCF caused the surface fibre peel off in the profile resulting in fibre bristling. The detachment of the adhesive front can be attributed to high stresses caused in the adhesive front after T&B adhesive fails.

As the addition of the adhesive front for reducing SCF has been proposed by Portnov et al. (26), although, there have not been any reported test on the proposed concept. Considering the analytical finding, an adhesive front was incorporated in the D2 specimen design. The increase in the ultimate strength of the D2 specimen over the 30D specimen can partially be attributed to the adhesive front. However, under the fatigue loading the adhesive front detaches after a few thousand cycles, causing a sudden increase in SCF in the tab termination zone. Hence, it is difficult to confirm the effect of reduced SCF in the D2 specimen under fatigue loading.

9 Conclusion

The main goal of the thesis work is to design, develop and validate a tension-tension fatigue test setup for the pultruded profile provided by Exel Composites Oyj. Due to the anisotropic nature of UD CFRP material, the testing requires careful selection of tabbing and gripping parameters to minimise the stress concentration. Additionally, the specific shape of the Exel profile, i.e. t/w ratio = ½ requires higher force transfer with the limited gripping area.

To overcome the aforementioned challenges, the primary design of the specimen is achieved based on the literature. The specimen design approach found in most literature has been with a focus on reducing stress concentration in the tabbing area. Hence, the primary designed is refined with a similar approach using FEA, consequently reaching at the D2 specimen configuration with an SCF of 1.02. For experimental validation, The D2 specimen was manufactured using described manufacturing process and tooling.

To test the improvements in the strength due to reduced SCF, D2 specimen with its two sided tab taper angle was tested along with a 30D specimen (SCF 1.39) with single taper of 30°, under the static tension loading. The D2 specimen with 36% lower SCF provided 3.6% increase in the ultimate strength. During the static tension test, due to Young's modulus measurement anomaly, the extensometer mounting interface was also probed. By testing three different interfaces, a white paint thin layer interface arrived and is recommended for the consistent Young's modulus measurement.

Tension-tension fatigue testing maximum load level is evaluated with average failure strain of 1.7%. The fatigue testing is carried out for two load levels of 60% and 65%. During the testing, 3 of the 12 specimen failed prematurely due to unknown reasons. Nine of the twelve specimens completed more than 10^5 cycles. The final failure of the specimens occurs in the gage section. However, the damage initiates at the tab tip due to the adhesive debond. Despite the unexpected mode of damage initiation, the test results obtained are in line with the results found from the literature. Based on the observations made during the fatigue testing, fatigue damage progression begins with adhesive failing at the profile tab interface, this debond at the tab profile interface can be mainly attributed to the following

1) Low adhesive modulus
2) Degradation in adhesive strength due to high temperatures at the interface
3) High deformations or debonded side adhesive

In addition to the debond, the adhesive front detaches after a few thousand cycles causing an increase in SCF at the TTZ, causing peeling off of the fibre. Hence, The D2 specimen configuration needs to be further improved to avoid the debonding and peeling off, before it can be used for evaluating fatigue life of the Exel profile.

10 Recommendation for future work

The improvements need in the D2 specimen are based on the failure observed during the fatigue loading. However, the changes should be made keeping an eye on their effect on stress concentration in the specimen. Following suggestions are proposed for progressing towards future work with similar specimen design

Tab adhesive with high strength at elevated temperature: The adhesive fails during the first few thousand cycles at the elevated temperature in the tabbing area, indicating the low strength of the adhesive at that temperature. Hence finding an adhesive with higher strength at elevated temperature can help in avoid debonding.

Reducing adhesive between main and side profiles: During the initial debonding, the Exel profile is able to slide between the tabs. This suggests higher deformation of side adhesive or debonding between the profile and the side adhesive. The deformation should be reduced to deformation levels of T&B adhesive for achieving equal distribution of the stress around the profile. This can be achieved by reducing the thickness of the adhesive between the main and support profile.

Increasing the bond line between the adhesive front and the tab: The adhesive front detaches from the tab between 1-1000 cycles. This indicates a weaker bond strength between the adhesive front and the tab. In order to keep the adhesive front attached, the bond-line between the adhesive front and tab needs to be increased. This can be achieved by modifying the existing manufacturing of adhesive front and allowing additional adhesive spilling onto the tab, thus increasing the bond area of the adhesive front to the tab.

References

1. Bortolotti P. Carbon glass hybrid materials for wind turbine rotor blades. Delft: Delft University of Technology; 2012.

2. Iqbal MA. Fatigue Life of Pultruded and Hand Lay-Up GFRP Exposed to Different Environmental Conditions: The University of Maine; 2002.

3. Lee J, Harris B, Almond DP, Hammett F. Fibre composite fatigue-life determination. Composites Part A: Applied Science and Manufacturing. 1997;28(1):5-15.

4. Harris B. Fatigue behaviour of polymer-based composites and life prediction methods. Durability Analysis of Structural Composite Systems, AH Cardon (Ed), Balkema, Rotterdam. 1996:49-84.

5. Reifsnider KL. Chapter 1 - Introduction. In: Reifsnider KL, editor. Composite Materials Series. Volume 4: Elsevier; 1991. p. 1-9.

6. Talreja R. 1 - A conceptual framework for studies of durability in composite materials. In: Carvelli V, Lomov SV, editors. Fatigue of Textile Composites: Woodhead Publishing; 2015. p. 3-27.

7. Gamstedt E, Talreja R. Fatigue damage mechanisms in unidirectional carbon-fibre-reinforced plastics. Journal of materials science. 1999;34(11):2535-46.

8. Huston RJ. Fatigue life prediction in composites. International Journal of Pressure Vessels and Piping. 1994;59(1–3):131-40.

9. Nguyen T, Tang H, Chuang T, Chin J, Wu F, Lesko J. A fatigue model for fiber-reinforced polymeric composites for offshore applications: US Department of Commerce, Technology Administration, National Institute of Standards and Technology; 2000.

10. Talreja R, Singh CV. Damage and failure of composite materials: Cambridge University Press; 2012.

11. Talreja R. Internal variable damage mechanics of composite materials. Yielding, damage, and failure of anisotropic solids. 1987:509-33.

12. Talreja R, editor Fatigue of composite materials: damage mechanisms and fatigue-life diagrams. Proceedings of the Royal Society of London A: Mathematical, Physical and Engineering Sciences; 1981: The Royal Society.

13. Jones C, Dickson R, Adam T, Reiter H, Harris B, editors. The environmental fatigue behaviour of reinforced plastics. Proceedings of the Royal Society of London A: Mathematical, Physical and Engineering Sciences; 1984: The Royal Society.

14. Sturgeon J. Fatigue and creep testing of unidirectional carbon fibre reinforced plastics. Reinforced plastics- Ever new. 1973.

15. ASTM D3479 / D3479M - 12 Standard Test Method for Tension-Tension Fatigue of Polymer Matrix Composite Materials. American Society for Testing and Materials; 2015.

16. ASTM E122 - 09e1 Standard Practice for Calculating Sample Size to Estimate, With Specified Precision, the Average for a Characteristic of a Lot or Process. American Society for Testing and Materials; 2009.

17. ASTM D3039 / D3039M - 14 Standard Test Method for Tensile Properties of Polymer Matrix Composite Materials. American Society for Testing and Materials; 2014.

18. ISO 13003:2003 - Fibre-reinforced plastics -- Determination of fatigue properties under cyclic loading conditions. International Organization for Standardization; 2013. p. 17.

19. ISO 527-1:2012 - Plastics -- Determination of tensile properties -- Part 1: General principles. International Organization for Standardization; 2012.

20. Sturgeon JB. Fatigue Testing of Carbon Fibre Reinforced Plastics. 1975.

21. Curtis PT. Tensile fatigue mechanisms in unidirectional polymer matrix composite materials. International Journal of Fatigue. 1991;13(5):377-82.

22. Curtis PT, Moore BB. A Comparison of Plain and Double Waisted Coupons for Static and Fatigue Tensile Testing of Unidirectional GRP and CFRP. In: Marshall IH, editor. Composite Structures 2: Springer Netherlands; 1983. p. 383-98.

23. Cunningham ME, Schoultz SV, Toth J. Effect of end-tab design on tension specimen stress concentrations. Recent advances in composites in the United States and Japan, ASTM STP. 1985;864:253-62.

24. Wisnom M, Maheri M, editors. Tensile strength of unidirectional carbon fibre-epoxy from tapered specimens. Second European Conference on Composites Testing and Standardization, Hamburg; 1994.

25. Kulakov VL, Tarnopol'skii YM, Arnautov AK, Rytter J. Stress-Strain State in the Zone of Load Transfer in a Composite Specimen under Uniaxial Tension. Mechanics of Composite Materials. 2004;40(2):91-100.

26. Portnov GG, Kulakov VL, Arnautov AK. A refined stress-strain analysis in the load transfer zone of flat specimens of high-strength unidirectional composites in uniaxial tension 2. Finite-element parametric analysis. Mechanics of Composite Materials. 2007;43(1):29-40.

27. Portnov GG, Kulakov VL, Arnautov AK. A refined stress-strain analysis in the load transfer zone of flat specimens of high-strength unidirectional composites in uniaxial tension 1. Theoretical analysis. Mechanics of Composite Materials. 2006;42(6):547-54.

28. Portnov GG, Kulakov VL, Arnautov AK. A refined stress-strain analysis in the load transfer zone of flat specimens of high-strength unidirectional composites in uniaxial tension 3. Effect of grip misalignment. Mechanics of Composite Materials. 2007;43(6):503-12.

29. Adams DO, Adams DF. Tabbing guide for composite test specimens. DTIC Document, 2002.

30. De Baere I, Van Paepegem W, Degrieck J. On the design of end tabs for quasi-static and fatigue testing of fibre-reinforced composites. Polymer Composites. 2009;30(4):381-90.

31. De Baere I, Van Paepegem W, Quaresimin M, Degrieck J. On the tension–tension fatigue behaviour of a carbon reinforced thermoplastic part I: Limitations of the ASTM D3039/D3479 standard. Polymer Testing. 2011;30(6):625-32.

32. Vassilopoulos A, Keller T. Introduction to the Fatigue of Fiber-Reinforced Polymer Composites. Fatigue of Fiber-reinforced Composites. Engineering Materials and Processes: Springer London; 2011. p. 1-23.

33. GODWIN EW. Mechanical testing of advanced fibre composites: Elsevier; 2000. 378 p.

34. Bailey P, Lafferty A. Specimen gripping effects in composites fatigue testing–Concerns from initial investigation. Express Polymer Letters. 2015;9(5).

35. Vassilopoulos AP, Keller T. Fatigue of fiber-reinforced composites: Springer Science & Business Media; 2011.

36. Lani F, editor " Effect of load ratio, testing frequency, temperature, moisture, notch and stacking sequence on the fatigue resistance of woven CFRP laminates. 6th International Conference on Fatigue of Composite ICFC2015; 2015.

37. Maheri M. An improved method for testing unidirectional FRP composites in tension. Composite structures. 1995;33(1):27-34.

38. ESAcomp. Material library. In: Agency ES, editor.

39. N/A. Military Handbook - MIL-HDBK-17-3F: Composite Materials Handbook, Volume 3 - Polymer Matrix Composites Materials Usage, Design, and Analysis. U.S. Department of Defense.

40. Korkiakoski S, Brøndsted P, Sarlin E, Saarela O. Influence of specimen type and reinforcement on measured tension–tension fatigue life of unidirectional GFRP laminates. International Journal of Fatigue. 2016;85:114-29.

41. Mittelstedt C, Becker W. Free-edge effects in composite laminates. Applied Mechanics Reviews. 2007;60(5):217-45.

42. Sims GD. 2 - Fatigue test methods, problems and standards. In: Harris B, editor. Fatigue in Composites: Woodhead Publishing; 2003. p. 36-62.